



**Kaunas University of Technology**  
Faculty of Mechanical Engineering and Design

**Evaluation of Thermal and Hydraulic Effects of Conformal  
Cooling Channel Profiles and Process Parameters in Injection  
Moulding**

Master's Final Degree Project

---

**Rahul Siddharth Wase**

Project author

**Assoc. Prof. Dr. Inga Skiedraitė**

Supervisor

---

**Kaunas, 2026**



**Kaunas University of Technology**  
Faculty of Mechanical Engineering and Design

# **Evaluation of Thermal and Hydraulic Effects of Conformal Cooling Channel Profiles and Process Parameters in Injection Moulding**

Master's Final Degree Project  
Industrial Engineering and Management (6211EX018)

---

**Rahul Siddharth Wase**

Project author

**Assoc. Prof. Dr. Inga Skiedraitė**

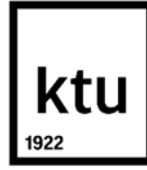
Supervisor

**Assoc. Prof. Dr. Saulius Diliūnas**

Reviewer

---

**Kaunas, 2026**



**Kaunas University of Technology**  
Faculty of Mechanical Engineering and Design  
Rahul Siddharth Wase

# **Evaluation of Thermal and Hydraulic Effects of Conformal Cooling Channel Profiles and Process Parameters in Injection Moulding**

## **Declaration of Academic Integrity**

I confirm the following:

1. I have prepared the final degree project independently and honestly without any violations of the copyrights or other rights of others, following the provisions of the Law on Copyrights and Related Rights of the Republic of Lithuania, the Regulations on the Management and Transfer of Intellectual Property of Kaunas University of Technology (hereinafter – University) and the ethical requirements stipulated by the Code of Academic Ethics of the University;
2. All the data and research results provided in the final degree project are correct and obtained legally; none of the parts of this project are plagiarised from any printed or electronic sources; all the quotations and references provided in the text of the final degree project are indicated in the list of references;
3. I have not paid anyone any monetary funds for the final degree project or the parts thereof unless required by the law;
4. I understand that in the case of any discovery of the fact of dishonesty or violation of any rights of others, the academic penalties will be imposed on me under the procedure applied at the University; I will be expelled from the University and my final degree project can be submitted to the Office of the Ombudsperson for Academic Ethics and Procedures in the examination of a possible violation of academic ethics.

Rahul Siddharth Wase  
*Confirmed electronically*



**Kaunas University of Technology**

Faculty of Mechanical Engineering and Design

**Task of the Master's Final Degree Project**

**Given to the student – Rahul Siddharth Wase**

**1. Title of the Project**

Evaluation of Thermal and Hydraulic Effects of Conformal Cooling Channel Profiles and Process Parameters in Injection Moulding

*(In English)*

Terminio ir hidraulinio poveikio konforminių aušinimo kanalų profiliams ir proceso parametrams liejimo formose tyrimas

*(In Lithuanian)*

**2. Aim and Tasks of the Project**

Aim: to evaluate the effect of cooling channel cross-section profiles and process parameters on the thermal and hydraulic performance of injection moulding through parametric simulation

Tasks:

1. to study existing injection mould cooling strategies;
2. to identify channel profiles, process parameters, thermal and hydraulic performance indicators for injection moulding simulation;
3. to simulate the thermal performance of traditional straight channels and conformal cooling channels with circular, teardrop and elliptical profiles using conjugate heat transfer analysis;
4. to compare cooling time, warpage, pressure drop, and other thermal and hydraulic relations for all configurations using RSM analysis;
5. to assess the impact of RSM-predicted optimal cooling configuration with potential cycle time and energy savings for industrial applications.

**3. Main Requirements and Conditions**

Simplified battery casing inspired CAD geometry prepared in SolidWorks; Full Transient cooling analysis in Moldex3D; Circular, elliptical and teardrop conformal cooling channel profiles with under fixed parameters; Coolant flow rates: 2, 5, and 10 L/min; Coolant inlet temperature: 15°C, 25°C, and 35°C; Extracted outputs: average part temperature, maximum part temperature, time to reach ejection temperature, pressure drop, average Reynolds number and warpage; RSM analysis and fitted model

**4. Additional Requirements for the Project, Report and its Annexes**

Moldex3D Simulation Data and Results, RSM outputs from JASP, CAD screenshots

Project author	Rahul Siddharth Wase	02-03-2026
	<i>(Name, Surname)</i>	<i>(Date)</i>
Supervisor	Inga Skiedraitė	02-03-2026
	<i>(Name, Surname)</i>	<i>(Date)</i>
Head of study field programs	Regita Bendikienė	02-03-2026
	<i>(Name, Surname)</i>	<i>(Date)</i>

Wase Rahul Siddharth. Evaluation of Thermal and Hydraulic Effects of Conformal Cooling Channel Profiles and Process Parameters in Injection Moulding. Master's Final Degree Project, supervisor assoc.prof.dr. Inga Skiedraitė; Faculty of Mechanical Engineering and Design, Kaunas University of Technology.

Study field and area (study field group): Production and Manufacturing Engineering (E10), Engineering Sciences (E).

Keywords: Injection moulding; conformal cooling channels; cooling channel cross-section; Moldex3D simulation; cooling time optimisation.

Kaunas, 2026. 88 p.

### **Summary**

This study examines the comparative performance of three cross-section profiles of conformal cooling channels, circular, elliptical and teardrop, for injection-moulding on a simulation basis. The work is based on the need to understand whether the profile geometry of the cooling channels itself can influence cooling behaviour when the conformal channel route, mould geometry, material, process parameters and standoff distance are kept constant, while coolant inlet temperature and coolant flow rate are varied. The straight-line cooling channel has been added as a reference baseline to put the conformal cooling benefit into perspective; the primary comparison should be that of the profile-level inside the conformal cooling group. A simplified battery casing inspired part geometry was modelled in SolidWorks; the simulations were done in Moldex3D with 20% talc-filled polypropylene and a P20 tool-steel as mould material. A design of experiments matrix comprised of the circular, elliptical and teardrop profiles, with flow rates of the coolant at 2, 5, and 10 L/min and coolant inlet temperatures of 15°C, 25°C and 35°C, a total of 27 conformal cooling simulations and 3 straight-line reference simulations were analysed. The responses extracted from the simulation results were average part temperature, maximum part temperature, time to reach ejection temperature, pressure drop, average Reynolds number and warpage displacement. The effect of the factors and the predicted optimum operating region were determined using response surface methodology. Results indicated that the average part temperature was not significantly affected by the profile geometry, but the maximum part temperature and cooling time were significantly affected by the profile geometry. The lowest maximum part temperature and cooling time was obtained with the teardrop profile, and the lowest pressure-drop tendency was obtained with the elliptical profile. The differences of the warpages between the profiles were small. It is concluded that the conformal channel cross-section profile is a sensible design parameter, and that the teardrop profile has the best thermal performance within the simulation domain explored.

Wase Rahul Siddharth. Terminio ir hidraulinio poveikio konforminių aušinimo kanalų profiliams ir proceso parametrų liejimo formose tyrimas. Magistro baigiamasis projektas, vadovė doc. dr. Inga Skiedraitė; Kauno technologijos universitetas, Mechanikos inžinerijos ir dizaino fakultetas.

Studijų kryptis ir sritis (studijų krypčių grupė): Gamybos inžinerija (E10), Inžinerijos mokslai (E).

Reikšminiai žodžiai: Įpurškiamasis liejimas; konforminiai aušinimo kanalai; aušinimo kanalo skerspjūvis; „Moldex3D“ modeliavimas; aušinimo laiko optimizavimas.

Kaunas, 2026. 88 p.

### **Santrauka**

Šiame tyrime modeliavimo pagrindu nagrinėjamas trijų konforminių aušinimo kanalų – apskritų, elipsinių ir lašo formos – skerspjūvių profilių lyginamasis našumas liejant įpurškimu. Darbas grindžiamas poreikiu suprasti, ar pačių aušinimo kanalų profilio geometrija gali turėti įtakos aušinimo elgsenai, kai konforminio kanalo maršrutas, liejimo formos geometrija, medžiaga, proceso parametrai ir atstumas tarp jų yra pastovūs, o aušinimo skysčio įleidimo temperatūra ir srauto greitis kinta. Tiesiosios linijos aušinimo kanalas buvo pridėtas kaip atskaitos taškas, siekiant įvertinti konforminio aušinimo naudą; pagrindinis palyginimas turėtų būti profilio lygis konforminio aušinimo grupėje. Supaprastinta akumulatoriaus korpuso įkvėpta detalės geometrija buvo sumodeliuota naudojant „SolidWorks“ programą; modeliavimas atliktas naudojant „Moldex3D“ programą, naudojant 20 % talko užpildytą polipropilena ir P20 įrankinį plieną kaip liejimo medžiagą. Eksperimentų matricos dizainas sudarytas iš apskrito, elipsinio ir lašo formos profilių, kurių aušinimo skysčio srauto greičiai buvo 2, 5 ir 10 L/min., o aušinimo skysčio įleidimo temperatūros buvo 15 °C, 25 °C ir 35 °C. Iš viso buvo išanalizuotos 27 konforminio aušinimo simuliacijos ir 3 tiesiosios linijos etaloninės simuliacijos. Iš modeliavimo rezultatų gauti atsakai buvo vidutinė detalės temperatūra, maksimali detalės temperatūra, laikas pasiekti išstūmimo temperatūrą, slėgio kritimas, vidutinis Reinoldso skaičius ir deformacijos poslinkis. Veiksnių poveikis ir numatomas optimalus veikimo regionas buvo nustatyti naudojant atsako paviršiaus metodiką. Rezultatai parodė, kad vidutinei detalės temperatūrai profilio geometrija reikšmingos įtakos neturėjo, tačiau maksimaliai detalės temperatūrai ir aušinimo laikui reikšmingą įtaką turėjo profilio geometrija. Mažiausia maksimali detalės temperatūra ir aušinimo laikas gauti naudojant lašo formos profilį, o mažiausia slėgio kritimo tendencija – naudojant elipsinį profilį. Profilių deformacijų skirtumai buvo nedideli. Išvada: konforminis kanalo skerspjūvio profilis yra protingas projektavimo parametras ir kad lašo formos profilis pasižymi geriausiomis šiluminėmis savybėmis nagrinėjamoje modeliavimo srityje.

## Table of Contents

<b>List of Figures</b> .....	<b>9</b>
<b>List of Tables</b> .....	<b>10</b>
<b>List of Abbreviations and Terms</b> .....	<b>11</b>
<b>Introduction</b> .....	<b>12</b>
<b>1. Injection Moulding: Overview and Challenges</b> .....	<b>14</b>
1.1. Injection Moulding Process and the Role of Cooling .....	14
1.2. Traditional Straight-Channel Cooling System in Injection Moulding .....	15
1.3. Conformal Cooling Channels in Injection Moulding .....	16
1.4. Effect of Cooling Channel Cross-Section Profile on Thermal Performance .....	18
1.5. Effects of Process Parameters on Cooling Performance .....	19
1.5.1. Coolant Flow Rate and Flow Regime .....	20
1.5.2. Coolant Inlet Temperature .....	20
1.6. Thermofluidic Performance Characterisation of Cooling Channels .....	21
1.7. Research Gap and Justification .....	22
1.8. Chapter Summary .....	23
<b>2. Simulation Framework and Comparative Evaluation Methodology</b> .....	<b>24</b>
2.1. Simulation-Based Study Approach .....	24
2.2. Simulation Design and Factor Selection .....	25
2.3. Fixed Process Parameters .....	26
2.4. Part Geometry, Mould Model and Cooling Channel Profiles .....	28
2.4.1. Part Geometry .....	28
2.4.2. Virtual Mould Configuration .....	30
2.4.3. Conformal Cooling Channel Routing .....	31
2.4.4. Cooling Channel Cross-Section Profile .....	31
2.5. Simulation Setup .....	34
2.5.1. Process Analysis Type .....	35
2.5.2. Mesh Generation .....	35
2.5.3. Cooling Analysis Computation Setup .....	36
2.6. Output Extraction and Thermofluidic Characterisation .....	36
2.6.1. Extracted Simulation Response Variables .....	36
2.6.2. Hydraulic Diameter ( $D_h$ ) .....	37
2.6.3. Flow Velocity ( $V$ ) .....	38
2.6.4. Reynolds Number ( $Re$ ) .....	38
2.7. Response Surface Methodology .....	39
2.7.1. RSM Input Factors and Response Variables .....	40
2.7.2. Second-Order Polynomial Model .....	40
2.7.3. RSM Design Structure and Model Adequacy .....	41
2.7.4. RSM Implementation in JASP .....	42
2.8. Methodological Scope, Assumptions and Limitations .....	43
2.9. Chapter Summary .....	44
<b>3. Results and Discussion</b> .....	<b>45</b>
3.1. Simulation Response Data .....	45
3.2. RSM Model Adequacy and Validation .....	47
3.2.1. Coefficient of Determination and Predictive Fit .....	47

3.2.2. Residual Diagnostics .....	48
3.3. Effect of Process Parameters on Thermal Responses.....	49
3.3.1. Average part Temperature ( $T_{avg}$ ) .....	49
3.3.2. Maximum Part temperature ( $T_{max}$ ).....	51
3.3.3. Cooling Time ( $t_{cool}$ ) .....	53
3.4. Effect of Process Parameters on Hydraulic and Dimensional Responses.....	56
3.4.1. Pressure Drop ( $\Delta P$ ).....	57
3.4.2. Average Reynolds Number ( $Re_{avg}$ ).....	59
3.4.3. Warpage Displacement ( $Warp$ ) .....	61
3.5. Factor Significance Analysis .....	63
3.5.1. Linear Effects of Coolant Temperature and Flow Rate.....	63
3.5.2. Quadratic and Interaction Effects .....	65
3.5.3. Overall Factor Ranking and Interpretation.....	66
3.6. Multi-Response Optimisation Results .....	66
3.6.1. Optimisation Results by Cooling Channel Profile .....	67
3.6.2. Interpretation of the Optimised Operating Region.....	68
3.7. Cross-Profile Performance Comparison.....	69
3.8. Conformal Cooling Channel and Baseline Straight Cooling Channel Comparison.....	70
3.9. Results Interpretation and Limitations .....	72
3.10. Chapter Summary .....	72
<b>4. Economic and Environmental Impact Analysis .....</b>	<b>74</b>
4.1. Basis and Assumptions of the Profile-Based Impact Model .....	74
4.2. Productivity Impact of Cooling Channel Profile Selection .....	76
4.3. Energy Usage and Hydraulic Operating Trade-Off.....	78
4.4. Environmental and Economic Impact of Profile Selection .....	79
4.5. Practical Implementation and Conformal Profile Selection.....	81
4.6. Chapter Summary .....	81
<b>Conclusions .....</b>	<b>83</b>
<b>Recommendations.....</b>	<b>84</b>
<b>List of References.....</b>	<b>85</b>
<b>Appendices .....</b>	<b>89</b>

## List of Figures

<b>Fig. 1.</b> (A) Injection moulding cycle and (B) relative cycle time for each stage (in %) [2] .....	15
<b>Fig. 2.</b> Conventional cooling channels in (A) Cavity and (B) Core of a Mould [9] .....	15
<b>Fig. 3.</b> Conformal cooling channels in injection moulding core and cavity [9].....	16
<b>Fig. 4.</b> Modelled reference used as part geometry a) Top view; b) Front view; c) Isometric view; d) Side view .....	29
<b>Fig. 5.</b> Virtual mould with dimensions a) 296L × 246W and b) 350H .....	30
<b>Fig. 6.</b> Conformal Cooling Channel with Circular Profile .....	32
<b>Fig. 7.</b> Elliptical Conformal Cooling Channel .....	33
<b>Fig. 8.</b> Teardrop Conformal Cooling Channel .....	34
<b>Fig. 9.</b> RSM response surface plots for Average part temperature ( $T_{avg}$ ) as a function of flow rate and coolant temperature: a) circular profile, b) elliptical profile, c) teardrop profile .....	50
<b>Fig. 10.</b> RSM response surface plots for Maximum part temperature ( $T_{max}$ ) as a function of flow rate and coolant temperature: a) Circular Profile, b) Elliptical Profile, c) Teardrop Profile.....	52
<b>Fig. 11.</b> RSM response surface plots for Cooling Time ( $t_{cool}$ ) as a function of flow rate and coolant temperature: a) Circular Profile, b) Elliptical Profile, c) Teardrop Profile .....	54
<b>Fig. 12.</b> Comparison of cooling time ( $t_{cool}$ ) for circular, elliptical and teardrop CCC profiles under matched coolant flow rate and coolant temperature conditions .....	56
<b>Fig. 13.</b> Response surface plots of coolant pressure drop ( $\Delta P$ ) as a function of coolant inlet temperature and coolant flow rate: a) circular profile, b) elliptical profile, and c) teardrop profile .	57
<b>Fig. 14.</b> Response surface plots for average Reynolds number ( $Re_{avg}$ ) as a function of coolant inlet temperature and coolant flow rate: a) circular profile, b) elliptical profile, and c) teardrop profile .	59
<b>Fig. 15.</b> Response surface plots of warpage displacement ( $Warp$ ) as a function of coolant inlet temperature and coolant flow rate: a) circular profile, b) elliptical profile, and c) teardrop profile .	61

## List of Tables

<b>Table 1.</b> Full-Factorial DOE Matrix .....	25
<b>Table 2.</b> Fixed process and material parameters used in the simulation runs.....	28
<b>Table 3.</b> Geometric Properties of Channel Profiles .....	32
<b>Table 4.</b> Mesh Convergence Study .....	35
<b>Table 5.</b> Calculated Hydraulic Diameter .....	38
<b>Table 6.</b> RSM input factors, and physical levels, and coded equation symbols.....	40
<b>Table 7.</b> Physical interpretation of the second-order polynomial terms for this study.....	41
<b>Table 8.</b> Degrees of freedom for each profile-response RSM model.....	41
<b>Table 9.</b> Model evaluation metrics for fitted RSM models .....	42
<b>Table 10.</b> Software tools used in the methodological workflow .....	43
<b>Table 11.</b> Full Simulation Run Data from Moldex3D and additional 3 Straight cooling channel baseline runs .....	46
<b>Table 12.</b> RSM Model Fit Statistics.....	47
<b>Table 13.</b> $T_{avg}$ comparison across all three profiles at all operating conditions.....	51
<b>Table 14.</b> $T_{max}$ comparison across conformal cooling channel profiles.....	53
<b>Table 15.</b> $t_{cool}$ comparison across profiles.....	55
<b>Table 16.</b> Coolant pressure drop ( $\Delta P$ , kPa) across all three channel profiles.....	58
<b>Table 17.</b> $Re_{avg}$ for all three profiles .....	60
<b>Table 18.</b> Warpage Displacement (mm) across all three profiles.....	62
<b>Table 19.</b> Linear regression coefficients for coolant temperature (A) and flow rate (B) in the fitted RSM models .....	63
<b>Table 20.</b> Quadratic ( $A^2$ , $B^2$ ) and interaction (AB) coefficients in the fitted RSM model.....	65
<b>Table 21.</b> Overall factor influence based on fitted RSM coefficient behaviour.....	66
<b>Table 22.</b> RSM-predicted optimum conditions as response values for each CCC profile .....	67
<b>Table 23.</b> Overall performance comparison of conformal cooling channels profiles.....	69
<b>Table 24.</b> Thermal response comparison (conformal cooling channels vs straight line cooling channels baseline).....	70
<b>Table 25.</b> Assumption basis for profile-based economic and environmental model.....	75
<b>Table 26.</b> Estimated productivity impact of conformal cooling channel profile selection at 5L/min and 25 °C range .....	77
<b>Table 27.</b> Estimated machine-energy and hydraulic-power comparison of the CCC profiles at 5L/min and 25°C .....	78
<b>Table 28.</b> Calculated impact of elliptical and teardrop profiles on energy savings and CO2 reduction at matched process conditions selected .....	80
<b>Table 29.</b> Per-profile strength, implementation concern and practical interpretation .....	81

## List of Abbreviations and Terms

### Abbreviations:

AM – Additive Manufacturing  
ANOVA – Analysis of Variance  
CAD – Computer Aided Design;  
CCC – Conformal Cooling Channels  
CHT – Conjugate Heat Transfer  
DED – Direct Energy Deposition  
DOE – Design of Experiments  
JASP – Jeffery’s Amazing Statistics Program  
PBF – Powder Bed Fusion  
RSM – Response Surface Methodology  
TCU – Temperature Control Unit.

### Terms:

CL – Circular  
EL – Elliptical  
TD - Teardrop  
 $T_{avg}/T_{avg}$  – Average Part Temperature  
 $T_{max}/T_{max}$  – Maximum Part Temperature  
 $t_{cool}/T_{cool}$  – Time to reach ejection temperature  
 $\Delta P/dP$  – Coolant pressure drop  
 $Re_{avg}/Re_{avg}$  – Average Reynolds Number  
Q – Coolant flow rate  
Tc – Coolant inlet temperature  
Dh – Hydraulic Diameter  
Warp – Warpage displacement  
 $P_{hyd}$  – Ideal hydraulic power  
 $R^2$  – Coefficient of determination  
Adj  $R^2$  – Adjusted coefficient of determination  
Pred  $R^2$  – Predicted coefficient of determination  
S – Standard error of regression

## Introduction

Injection moulding is one of the most popular manufacturing processes for producing high-volume polymer components. In this process, plastic parts are produced by melting thermoplastics or thermosetting plastics as a polymer melt. The polymer melt is forced into a mould cavity and then is cooled down to solidify the plastic into the desired shape of the mould. Once the melted plastic is cooled down enough, it turns hard and sets into the shape of the mould, and afterwards it is ejected. This process is called demoulding, and the temperature at which this happens is called the ejection temperature. In this entire process, the mould cooling time accounts for approximately 60-70% of the total cycle time. In complex parts such as battery casings, having thin walls, mounting bosses, internal rib structures, etc, due to non-uniform heat distribution during the cooling stage causes overheating at specific regions called hot spots. This results in extended cycle times, part warpage and dimensional inaccuracy in the parts. These defects have a direct impact on production output, material utilisation, and energy consumption, which makes the optimisation of the mould cooling problem of significant industrial and economic relevance. To speed up the cooling process in injection moulding, the core is equipped with cooling channels through which coolant flows. The coolant captures the heat of the molten plastic, which gets dissipated into the inner walls of the core. Traditionally, these cooling channels are drilled into the core in straight lines and usually have a fixed linear geometry. It is difficult to maintain a consistent distance of the cooling channels from curved or complex mould surfaces. This results in uneven extraction of heat, leading to the formation of thermal hotspots, i.e. regions where heat builds up and delays the solidification of the plastic. This limitation of traditional cooling channels is partially mitigated by using conformal cooling channels (CCCs). Conformal cooling channels (CCCs) are similar to traditional cooling channels in terms of fixed-diameter channel networks, but the cooling channels follow the mould surface contour instead of having a fixed linear geometry. Fabrication of complex conformal cooling channels is enabled by additive manufacturing, and the channels distribute the coolant uniformly across the mould core. Despite the great improvement that conformal cooling channels offer over straight-drilled cooling channels, most of the research concentrated on circular cross-sections of the cooling channels. Partly this is a carry-over from traditional drilling methods, which yield a subtractive manufacturing process resulting in circular channels. But, with metal additive manufacturing, more complicated cross-sectional internal cooling channels are now possible. This provides a chance to explore the potential of non-circular conformal cooling channels to provide a better performance (cooling or hydraulic behaviour) than the circular conformal baseline. This study compares the three conformal cooling channel cross-section profiles (circular, elliptical and teardrop) with Moldex3D simulation. The same mould geometry, polymer material, mould material and conformal channel route are used in the evaluation of the profiles. Coolant flow rate and the inlet temperature of the coolant is varied as process parameters. There are 27 conformal cooling simulations and three straight-line baseline simulations. The primary responses obtained are average part temperature, maximum part temperature, time to reach ejection temperature, pressure drop of coolant, average Reynolds number and warpage displacement. The effects of the factors, interaction behaviour and performance in profile levels throughout the tested range are then evaluated by response surface methodology.

**Aim:** to evaluate the effect of cooling channel cross-section profiles and process parameters on the thermal and hydraulic performance of injection moulding through parametric simulation.

**Tasks:**

1. to study existing injection Mould cooling strategies;
2. to identify channel profiles, process parameters, thermal and hydraulic performance indicators for injection Moulding simulation;
3. to simulate the thermal performance of traditional straight channels and conformal cooling channel with circular, teardrop and elliptical profiles using conjugate heat transfer analysis;
4. to compare cooling time, warpage, pressure drop, and other thermal and hydraulic relations for all configurations using RSM analysis;
5. to assess the impact of optimal cooling configuration with potential cycle time and energy savings for industrial applications.

**Hypothesis:** Variation in thermal and hydraulic performance of cooling channels can be different across different channel profiles, such as elliptical and teardrop profiles, and process parameters. Quantifying these differences can help identify the optimal profile and process parameter combination to improve cooling time in injection moulding process.

## **1. Injection Moulding: Overview and Challenges**

### **1.1. Injection Moulding Process and the Role of Cooling**

Injection moulding is one of the most commonly used manufacturing processes used to manufacture polymer components at a large scale. The injection moulding process consists of several steps: plasticating, filling, packing, cooling, and ejection [1]. Each stage directly affects the dimensional accuracy, mechanical properties and surface quality of the final part. At the plasticating stage, which initiates the cycle, solid polymer granules called pellets are fed from a hopper into a heated barrel. Here, a screw-feeding system compresses and further melts the material to the required viscosity, creating a metered shot volume ready for injection [2]. The quality of plasticating, melt temperature, consistent shot volume, viscosity of the melt shot, etc., directly affects the quality of the remaining stages. At the next stage, which is the filling stage, the feed screw moves at a fast rate. This forces the polymer melt through the sprue, runner system, and the gate into the mould cavity in a high-pressure manner. The melt advances along the cavity, where the flow pattern is controlled by the geometry of the part and the mould core, position of the gate, viscosity of the melt and the injection rate. If the filling parameters are not controlled properly, it can lead to incomplete filling, premature solidification at the gate, or air traps can all occur resulting in part failure. The packing stage initiates immediately after the filling stage. Additional material is pressed into the cavity under constant holding pressure to offset the volumetric contraction that takes place as the polymer cools down and starts to solidify. The gate is left open when packing, and the material flows inwards. Once the gate freezes, hardened and closed, it is impossible to add any additional material, and the cooling stage begins with a fixed volume of material in the mould cavity [3].

The cooling stage is the longest and the most thermally intensive stage of the cycle. This stage takes up to 60-70% of the total cycle time in the injection moulding process. The polymer is solidified by removing the heat via a series of cooling channels embedded in the mould itself. A coolant, usually water, constantly circulates through these channels. The part should not be removed from the mould until it is hardened enough that even the thickest parts can resist the force of ejection without deformation. Thick sections like mounting bosses and rib intersections solidify much more slowly than thin walls. In geometrically complex components, the cooling stage is intentionally longer than the time taken by the fastest cooling feature to solidify [4]. Lastly, during the ejection stage, the mould is opened, and the solidified part is forced out of the cavity by ejector pins. Where the part is not cooled enough, surface marking, warpage or structural damage is caused by ejection forces. The cycle is then repeated as the mould closes and a new melt shot is injected again. Following Fig. 1 illustrates the injection moulding cycle and relative cycle times of each stage. Poor or uneven cooling not only increases the cycle time, but it also directly results in quality flaws of many types. Warpage happens when various areas of the part cool and shrink at different rates. This creates internal stresses which disfigure the final geometry after the ejection [5]. Sink marks are seen on the external surfaces due to the thick sections where the packing pressure is insufficient, and the cooling process is slow, such that the material sinks back inwards. Residual stresses that remain trapped in the part during the uneven cooling process also lower the mechanical strength and fatigue resistance. Due to the shrinkage of the part in a non-uniform manner, defects such as dimensional inaccuracies are also formed. Therefore, essential features like mounting bosses, holes, and mating or coupling interfaces are sometimes inaccurately formed due to differences in tolerances. Such imperfections are highly critical in components such as battery cases. In such parts, high-dimensional accuracy is important for assembly fit, structure and sealing of components. Due to the combination of various thin and

thick-walled features in complex parts, it creates a similar non-uniform thermal load on the mould as well. This cooling problem remains unattended even when traditional cooling systems are employed [6].

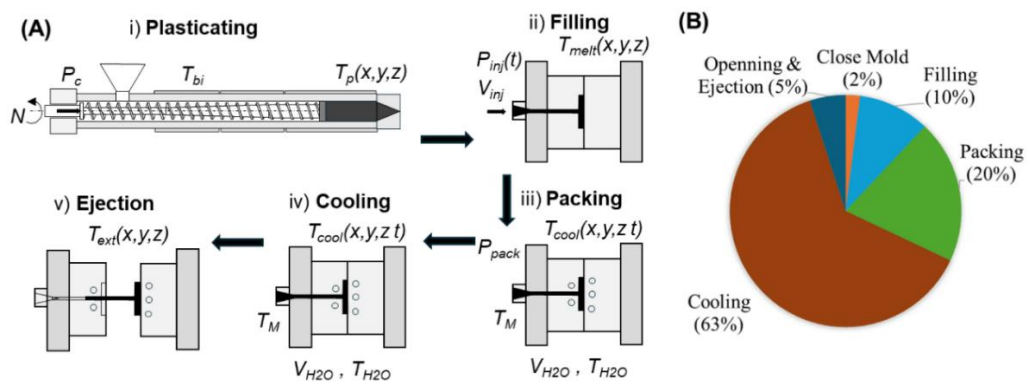


Fig. 1. (A) Injection moulding cycle and (B) relative cycle time for each stage (in %) [2]

## 1.2. Traditional Straight-Channel Cooling System in Injection Moulding

The straight-channel cooling system is the most common type of mould cooling used in the industrial practise. In this, cooling channels are provided through straight holes that are drilled through the mould plates, through which the coolant, usually water, is circulated to remove the heat out of the mould walls and the polymer undergoing curing [7]. This approach is simple and has been the industry standard over decades, and it is still the standard on which all more sophisticated cooling strategies are assessed. Straight cooling channels are usually cross-sectional circular with a diameter of 6mm down to 14mm, depending on the size of the mould and the thermal demands. They are designed in a series of parallel or interdependent linear tracks which constitute a closed cooling circuit in the mould plate. The structure is limited completely by the drilling system, the channels are always straight, should not cross structural systems like ejector pin holes or parting lines and should have a minimum of wall thickness between the channel and mould cavity surface to maintain structural integrity [8, 9]. Following Fig. 2. illustrates standard or drilled cooling channels in cavity and mould core.

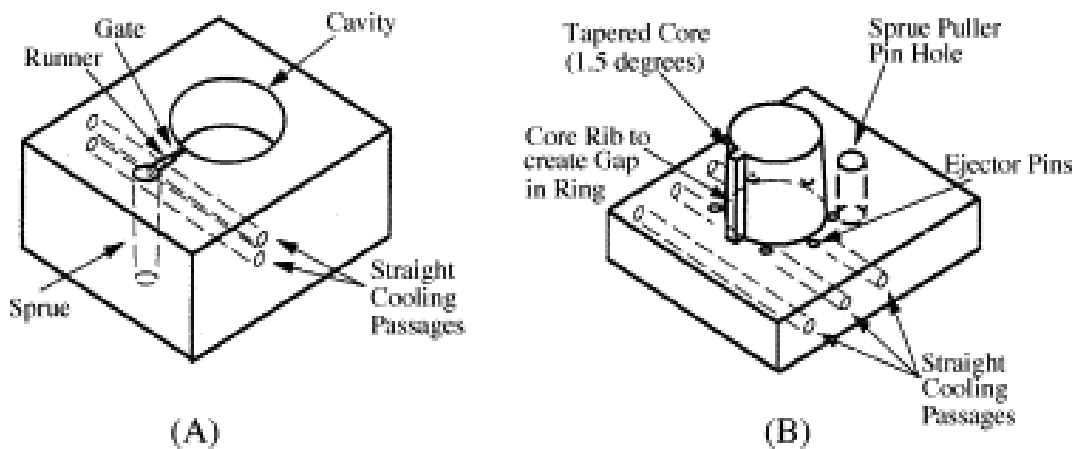


Fig. 2. Conventional cooling channels in (A) Cavity and (B) Core of a Mould [9]

Practically, this implies that the cooling circuit is optimised with reference to the mechanical limits of the mould and not with reference to the thermal requirements of the part itself. This inherent

limitation leads to the greatest limitation of straight-channel cooling, namely the impossibility to maintain a constant distance between the cooling channel and the surface of the mould cavity. In simple or flat geometries, a straight channel may operate with a relatively constant depth underneath the cavity surface, which gives fairly constant heat removal. Non-linear, curved, geometrically complex components, e.g., battery casings with bosses, ribs, and corner details, are, however, the subjects of the straight channel having to alter its distance to the cavity surface with the change in surface geometry. Cooling is done aggressively to the regions which are near the surface of the channel, whereas minimal cooling is done to regions far away. The consequence is an uneven temperature distribution on the mould surface that is a direct cause of warpage, residual stress and dimensional inaccuracy [10].

Another drawback is the total lack of a localised cooling capacity. Since drilling limits routes to straight lines, it is geometrically impossible to make a traditional channel directly below a mounting boss, into a deep rib pocket, or around a sharp corner - the very things that are known to create the highest thermal loads. These hot-spot areas are then reliant on conductive heat transfer using the bulk mould material to reach the nearest channel, which is slow and ineffective and stretches out the cooling process, leaving residual heat in the part at ejection. The nature of the pressure drop in straight channels is usually low, and the flow rates of coolants can be easily controlled. This makes the traditional cooling systems simple to run and maintain, along with a low cost of manufacturing. These operational benefits, however, fail to counter the thermal performance of multifaceted part geometries [11].

### 1.3. Conformal Cooling Channels in Injection Moulding

In order to mitigate the imperfections of straight-cooling channels, conformal cooling channels (CCCs) were developed. This is enabled by additive manufacturing (AM) technologies, where the mould core can be fabricated layer by layer. Due to this unique ability of additive manufacturing, it became possible to create complex routing for cooling channels, unique to the part being processed. Conformal cooling channels, unlike straight-drilled channels, are made to be directed or conform to the surface of the mould cavity, at a constant distance, resulting in more uniform heat removal in the part geometry [12]. This design philosophy is a significant change in design: instead of drilling coolant where it can be drilled, conformal cooling routes drill coolant where it is needed [5]. Following Fig. 3. illustrates schematics of conformal cooling channels CCCs in the mould core.

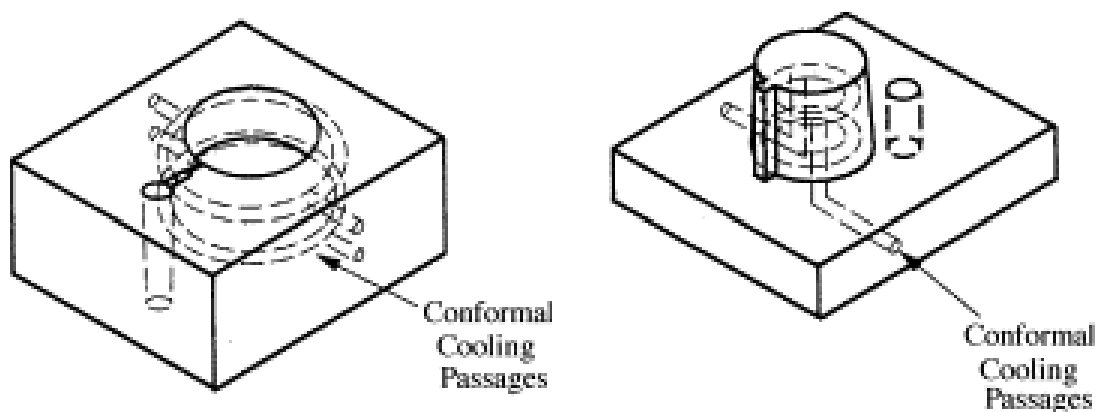


Fig. 3. Conformal cooling channels in injection moulding core and cavity [9]

The development of metal additive manufacturing, known as Powder Bed Fusion (PBF) and Directed Energy Deposition (DED) processes, made the realisation of conformal cooling channels possible [13]. These technologies free the design of the cooling channel to the geometrical limitations of subtractive machining, whereby channels can conform to curved surfaces, and curve around cylindrical cores and circumnavigate internal mould features that cannot be accessed by drilling. The mould insert, or core with the conformal channels, is designed as a structure of layers made directly of metal powder - usually tool steel or aluminium alloy - with the cooling channels formed as internal voids in the solid structure [14]. Conformal channels provide much more even temperature on the mould surface by keeping the standoff a constant distance, which usually ranges between 1.5 to 2.5 times the channel diameter. This directly minimises the temperature difference between hot and cold areas of the mould, thus minimising the difference in the shrinkage and resulting warpage of the ejected part. Cycle time has been reported to be reduced by 20-40% and large improvements in warpage when straight-channel cooling is substituted with conformal cooling designs on complex part geometries. Nonetheless, conformal cooling channels do not eliminate all limitations. The most basic is that they are still channel-based, i.e. the coolant is directed along discrete tubular paths of fixed cross-sectional diameter, and the cooling effect at any point in the mould surface is determined by the closeness and velocity of flow of the closest channel. In components of very localised thermal hot spots, e.g. thick mounting bosses with thin walls surrounding them, a conformal channel with a constant distance to the surface is still unable to distinguish the cooling rate of the high load boss area and the low load flat wall area. The two are given the same channel diameter, flow velocity and the same coolant temperature, although they have vastly different thermal requirements [15].

The performance advantage of conformal cooling versus conventional straight-drilled channels has been shown to be consistently measured in both a wide range of part geometries and in simulation experiments. Conformal cooling layouts have been reported to reduce cooling time by 20-40%, compared to straight-drilled channels in geometrically complex parts, and greater reductions of up to 66% have been reported in slender or high-aspect-ratio geometries where straight channels are the most severely limited by the impossibility of maintaining a constant standoff distance. Experimental work on conformal cooling moulds have also reported reductions in cooling time and part quality when compared with straight-line cooling moulds [16].

The design of a conformal cooling channel system is based on a specification of a set of geometric parameters that collectively determine the thermal behaviour of the circuit. The three primary parameters are the channel diameter, the distance between the centerline of the channels and the surface of the mould (standoff distance) and the pitch (distance between centers of two channels). The standoff distance should not exceed 1.5 to 2.5 times of the channel diameter as a means of guaranteeing an appropriate uniformity in the heat removal at the cavity surface without making the mould wall structurally weak. Channel pitch determines how much thermal overlap there is between adjacent channels: excessively large channel pitches result in localised hot spots, which interfere with temperature uniformity, and excessively small channel pitches make the hydraulics of the circuit difficult, and can lead to structural failure of the mould. The commonly quoted ratio of 3:1 between the pitch and the diameter of the channels is a typical starting point in conformal channel layout, although the optimum ratio is dependent on the geometry and material, and is typically determined via simulation. Position of the channels with the mould surface and channel diameter as the two most important geometric design factors which dictated the thermal outcome were also identified by sensitivity analysis of conformal cooling system performance, which further contributed to the

opinion that these parameters should be handled systematically, as opposed to relying on arbitrary rules [17].

#### **1.4. Effect of Cooling Channel Cross-Section Profile on Thermal Performance**

One of the design variables that are fundamental to the design of a cooling channel is the cross-sectional geometry of the cooling channel that defines the amount of internal surface area exposed to heat transfer, the hydraulic resistance that is placed on the flow of the coolant, and the distribution of thermal energy inside the mould wall [18]. Historically, circular cross-sections have been the norm in the industry in both straight-drilled and conformal cooling channels, largely because it is easy to make circular holes using drilling. Nevertheless, the development of additive manufacturing methods has removed the limitations of manufacturing of complex cooling channel geometries [19]. This has prompted the question, whether there can be an alternative cross-section profile that can provide quantifiable benefits in thermal or hydraulic performance compared with the traditional circular baseline. The operating principle of how cross-section geometry influences the performance of heat transfer is based on the principle of hydraulic diameter ( $D_h$ ). For channels of equal or nearly equal cross-sectional areas, the hydraulic diameter, wetted perimeter and local flow distributions may differ, for the same volumetric flow rate, even though the nominal mean velocity of the two profiles is the same. These differences have an influence on Reynolds number, pressure drop and local heat transfer behaviour. Hence, the effect of the cross-section profile cannot be explained by area alone, but it should be expressed by the combined effect with flow area, wetted perimeter, hydraulic diameter and the operating flow condition. [20].

Initial studies of the non-circular profiles of cooling channels used in injection moulding indicated that significant differences in thermal behaviour were observed between circular and rectangular cross-sections. It was discovered that rectangular channels of identical cross-sectional area as circular channels would reach a shorter time to part solidification and this was explained by the higher ratio of wetted perimeter to flow area in rectangular geometry, which has more wall surface area to the same volume of coolant. This discovery formed an early foundation of considering cross-section geometry as a design variable that is thermally important, independent of the path geometry of the channel. A more recent design of experiments study was a simulation-based design of experiment study to assess the thermal and warpage performance of conformal cooling channels with circular and square cross-sections during injection moulding of a cup-shaped polypropylene part. Response variables were assessed as three geometric parameters, including cross-section geometry, channel-to-part distance and channel dimension were varied. Mould temperature distribution and part warpage were assessed as response variables. The findings proved that the cross-section geometry as well as channel-to-part distance, had statistically significant effects on responses measured. Moreover, a 9.26% decrease in final warpage was proven with conformal channels as opposed to conventional straight channels in steel moulds, rising to 32.4% with geometrically flexible parts. This research can be considered the closest directly applicable precedent to the current work because it explicitly considers cross-section profile as a design variable, in a DOE framework. Nonetheless, it was only conducted on two profile geometries and the interaction between profile shape and coolant flow conditions was not examined so the relative performance of profiles across various operating conditions remains undetermined [21].

Simulation of thermal effects of different cross-section profiles on the conformal cooling channel performance has also been studied using trapezoidal and rectangular profile in addition to the standard

circular geometry [7]. The findings affirmed that profile shape changes the temperature distribution of the surface of the mould in a profile-dependent fashion, generating clear thermal gradients compared to the circular base. Nevertheless, the experiment was performed at one fixed combination of process conditions and there was no study of the variation of thermal ranking of profiles with flow rate or coolant temperature. This is a major drawback, as the interdependence between hydraulic diameter, wetted perimeter and flow velocity implies that relative convective performance of profiles is necessarily flow-condition dependent. An extensive survey of conformal cooling channel technology has validated that cross-section shape is a growingly accepted performance parameter, with cross-sectional profiles such as rectangular and profiled geometries able to enhance the effective cooling surface area over circular channels of the same cross-sectional area and simulation studies have shown that profiled conformal channels can be cooled more quickly than circular channels of the same cross-sectional area. Nevertheless, the same review notes a persistent gap in the literature: systematic multi-factor studies that isolate the influence of cross-section profile and at the same time vary flow conditions have not been performed, especially in asymmetric profiles like elliptical and teardrop geometries, which create an asymmetry in directional heat transfer not found in circular or rectangular channels [8].

It is further observed that the influence of channel diameter as a geometric channel on the warpage of parts has been investigated using Moldex3D simulation software over four circular channel diameters (6-12 mm). The findings showed that the channel diameter and warpage had a non-monotonic dependence, with intermediate sizes of 8 and 10 mm yielding lower warpage as compared to smaller and larger sizes. Such non-linearity makes thermal optimisation in injection mould cooling a complex issue, and it is important to note that parametric evaluation should be done in a systematic manner and not on an individual basis [19]. Notably, this work held the profile shape to be circular everywhere, and the geometry of the interaction between cross-section and channel size was not addressed at all. A combination of the evidence presented above shows that cooling channel cross-section profile is a thermally important design factor, whose effects on mould temperature distribution, cooling uniformity, and part warpage can be measured. The literature is, however, restricted to comparisons of circular channels with at most one other profile, at fixed process conditions, and without thermofluidic characterisation of the flow behaviour in the channel. Asymmetric non-circular profiles (e.g., elliptical, teardrop cross-sections) behaviour under a variety of flow conditions has not been characterised, and the interaction between the shape of the profile and process parameters (e.g., flow rate, coolant temperature) is an open gap.

### **1.5. Effects of Process Parameters on Cooling Performance**

In addition to the geometrical arrangement of the cooling channel, the thermohydraulic behaviour of the cooling system is highly controlled by the circumstances within which the coolant is fed. The volumetric flow rate of the coolant and its temperature at the inlet of the channel are the two operationally important process-side parameters [14]. A combination of these parameters determines the convective conditions in the channel and the thermal driving force to remove heat in the mould wall. Importantly, the two parameters both depend on the geometric characteristics of the channel - and in particular on its hydraulic diameter - so that their impact on cooling performance cannot be considered separately of channel cross-section geometry.

### 1.5.1. Coolant Flow Rate and Flow Regime

The most important operational variable is the volumetric flow rate of the coolant that controls the strength of forced convection in the channel of cooling. Convection heat transfer takes place between the mould wall and the coolant, and the speed at which this heat transfer takes place per unit area of the wall is defined by the convective heat transfer coefficient  $h$ . This coefficient is highly sensitive to the flow regime in the channel, that is, in laminar flow ( $Re < 2300$ ), in transitional flow ( $2300 < Re < 4000$ ), or in turbulent flow ( $Re > 4000$ ) [22]. The turbulent flow dramatically increases the exchange of thermal energy between the hot wall and the bulk coolant by the chaotic mixing of fluid layers across the channel cross-section, the values of  $h$  are much higher than those obtained in laminar flow at the same volumetric flow rate. As has been determined, injection mould cooling applications prefer turbulent flow. The heat transfer benefits of increasing Reynolds number beyond about 10,000 are greatly offset by the associated increase in pressure drop and pumping power needed to sustain the higher flow rate [23]. Thus, a practical operating range of  $Re$  is often quoted as 4,000 to 10,000. The implications of this trade-off between heat transfer enhancement and hydraulic cost directly impact the choice of flow rate levels in a DOE study: levels that cut across the laminar-to-turbulent transition will give the most diverse range of thermal responses in channel configurations, allowing the response surface model to represent the non-linear behaviour of the system. A numerical study which involved a parametric study of the combined effects of coolant channel layout, flow rate and coolant temperature on the performance of mould cooling identified that compliance with the set of channel design guidelines led to a 70% difference in the cooling time between the most and least favourable designs. The same study has shown that a decrease in the coolant temperature by 5°C enabled the flow rate to decrease by over half but with the same cooling time, which shows how much the two parameters are interacting. It is physically based: as the rate at which heat is extracted is determined by the driving temperature change (mould-to-coolant) and the convective coefficient (which varies with flow rate), a trade-off between the two is thermodynamically possible within constraints. The practical implication is that flow rate and coolant temperature cannot be studied individually but instead they should be studied together, which is the rationale behind their combined consideration as DOE factors in the current study [5].

Also, it should be noted that the hydraulic diameter of a channel of non-circular cross section is not the same as that of a circular channel having an equivalent open cross section. At a constant cross-sectional area, a constant volumetric flow rate will generate a flow velocity in the middle of the flow that is broadly similar. But profile differences may still exist in terms of wetted perimeter, hydr. diameter and local velocity distribution. For this reason, two profiles of the same channel, running at the same nominal flow rate, do not necessarily give the same Reynolds number, pressure-drop characteristic or local wall-flow interaction. This implies that cross-sectional area is not a good indicator of the influence of profile geometry. It needs to be interpreted along with hydraulic diameter, coolant flow rate and coolant temperature. This relationship between channel geometry and the conditions on the process side is one of the reasons why there is a limited understanding of the thermal and hydraulic behaviour of non-circular conformal cooling channels with fixed-condition profile comparisons.

### 1.5.2. Coolant Inlet Temperature

The temperature of the coolant inlet is used to define the thermal driving force required to remove heat out of the mould. The velocity of heat transfer across the wall of the mould is proportional to the

temperature difference between the bulk coolant and the wall (which is the temperature difference in the heat exchanger analysis) and the log mean temperature difference. The lower the coolant inlet temperature thus enhances this driving force, so that the rate of heat removal is accelerated, and the time taken to cool the polymer melt down to the ejection temperature is decreased [22].

In industry, the inlet temperature of coolant depends on the kind of temperature control unit (TCU) employed. Standard TCUs circulate coolant at close to ambient temperatures of about 15 to 25°C whereas chilled water units can deliver coolant as low as 5 to 10°C to the demanding applications. High coolant temperatures (30 to 50°C) can be intentionally used in processes where surface finish or crystallisation behaviour demands a warmer mould surface at the expense of lower cooling efficiency. The temperature span of 15 to 35°C thus covers a practically useful and relevant operating range for many thermoplastic mould-cooling studies. It was confirmed in a simulation study of eight different types of coolant media in a fixed flow rate and fixed inlet temperature that the thermal and physical properties of the coolant directly correspond to the cooling time and uniform temperature in the moulded part with water exhibiting the best cooling behaviour of all the coolant media tested because of its high thermal conductivity and heat capacity. Although this research maintained inlet temperature fixed, the findings support the idea that the parameters of the coolant side are the main determinants of the thermal performance of the cooling phase. A predictive study of the behavior of conformal cooling systems using machine learning further found that only coolant inlet temperature of two important coolant-side variables, in addition to the inlet pressure, are non-linearly predictive of cooling efficiency, and that their combined effects with the channel geometry cannot be explained by a single-factor study [5, 22].

The coolant inlet temperature in this context presents a differential thermal driving force across the 27 simulation runs which, together with the difference in the convective coefficient due to varying channel profiles and flow rates, provides a rich multi-factor response surface. This is especially important since the advantage of a lower coolant temperature is not uniformly distributed across channel profiles, profiles with a larger convective coefficient take up more heat per unit of temperature driving force, and therefore the performance advantage of a lower coolant temperature can be enhanced or diminished by the channel geometry. This is one of the main physical processes that inspired the multi-factor design of this study.

## **1.6. Thermofluidic Performance Characterisation of Cooling Channels**

The thermal and hydraulic behaviour of a cooling-channel system cannot be completely defined using part-level injection moulding outputs only. Practical factors like part temperature, warpage and cooling time characterise the final moulding response, but do not address the mechanisms behind the response from the coolant side. To this end, thermofluidic characterisation is often employed to aid with the interpretation of cooling channel performance. Reynolds number and pressure drop are especially convenient, since they characterise the coolant-flow regime and the hydraulic resistance of the cooling circuit. For non-circular profiles, a hydraulic diameter is used instead of a physical diameter of the channel to compare different cross-sections on a common hydraulic basis. The Reynolds number tells if the flow of the coolant is laminar, transitional or turbulent. This is of critical importance since the flow regime will affect the convective heat transfer between the channel wall and the coolant. Pressure drop is also significant because the greater the flow of coolant, the more cooling can be achieved but the more the flow resistance of the cooling circuit and the more the pumping requirement could increase. Thus, it is important to think about the thermal performance of

non-circular cooling channels in conjunction with coolant-flow behaviour, as well as the temperature or cooling-time results at the part level.[14, 24].

### **1.7. Research Gap and Justification**

The reviewed literature in the above sections provides a strong body of evidence to support the fact that conformal cooling channels are always superior to the traditional straight-drilled channels in terms of uniform temperature, cycle time minimisation and part warpage control. The conformal channel performance benefit is achieved through the fact that the distance between the channel and the surface of the mould and, therefore, between the channel and the complex part geometry can be controlled and kept constant, which provides more consistent heat removal in the complex part geometries. Nevertheless, in spite of this and the increasing amount of research in this field, there are several key areas of research gaps that have not been filled in the published literature. The largest disconnect is related to the conformal cooling channel cross-section profile. The vast majority of published work only analyses circular cross-sections, and where non-circular profiles are analysed, only compare to a single alternative geometry analysed at a constant set of process conditions. Based on the literature reviewed, there is limited systematic research on asymmetric non-circular profiles (elliptical and teardrop cross-sections) under a multi-factor framework that also considers changing coolant operating conditions. The various cross-section or profile changes have been studied so far, but most of the studies are confined to a comparison of selected families of polygonal or conventional profiles and not a direct comparison of circular, elliptical and teardrop conformal channels [18]. This has led to the interaction between cross-section profile and process parameters like flow rate, coolant temperature, not being characterised often, yet the interaction is physically necessary because the hydraulic diameter varies due to the profile, leading to differences in Reynolds number at the same flow rate.

Another area of gap is on the analytical model used in evaluation of cooling channel performance. Most DOE studies in injection mould cooling report a single macro-level response variable, usually cooling time or part warpage, without describing the thermofluidic behaviour of the coolant in the channel. This not only restricts the physical interpretability of measured results but also makes it impossible to generalise to alternative channel geometries, part materials or process conditions. The recent review literature has explicitly stated that the field has no extensive multi-objective characterisation methods and future research ought to be carried out with a temperature profile metrics in addition to the conventional outcome-based responses. Also, there is a knowledge gap in the experimentally validated 3D solid body CFD-mode simulation of non-circular conformal cooling channels. On several occasions, independent studies have shown that the Moldex3D simulation software can give accurate predictions on the thermal behaviour of mould when it is compared with experimental measurements. In addition, Moldex3D directly accepts non-circular solid body cooling channels, and the 3D CFD analysis of non-circular channels since version R11.0, which allows the complete three-dimensional solution of velocity and temperature fields in arbitrary cross-sections of the channels without the simplifying assumptions of network analysis. This feature renders a parametric study of non-circular profiles, using simulation, both methodologically and practically viable, without having to manufacture a prototype [25].

These gaps allow for a simulation-based design matrix with a systematic variation of the conformal cooling channel cross-section profile, coolant flow rate and coolant inlet temperature. A profile comparison for one operating condition would be inadequate, as the effect of geometry of the cross

section is intertwined with hydraulic diameter, wetted perimeter, the behaviour of the Reynolds number and the pressure drop. Hence, a multi-factor simulation and response surface approach is a proper framework to make the comparison of circular, elliptical and teardrop conformal cooling channel profiles. In this kind of system, straight-line cooling can provide the reference baseline to compare the overall advantage of conformal routing, and the profile-level behaviour of conformal channels is the primary concern.

## **1.8. Chapter Summary**

This chapter covered the importance of cooling in injection moulding and the significance of the design of cooling channels for cycle time, thermal uniformity and dimensional quality. Cooling is a large component in the injection moulding process, and if the heat is not removed evenly, hot spots can occur, resulting in extended cooling times, warpage and dimensional inaccuracies. The traditional straight-line cooling channels are simple and hydraulically efficient, but have a problem with the linear path and inability to be kept at a constant distance from complex mould surfaces. This restriction can be overcome by conformal cooling channels, which can match the mould cavity more closely and lead to more uniform removal of heat. The literature reviewed however, indicates that the research on conformal cooling is still mainly focused on circular channel profiles. The non-circular internal channels are made possible by the principle of additive manufacturing, but the impact of the cross-section profile on the thermal, hydraulic and dimensional performance is not fully developed, particularly for asymmetric cross-sections like elliptical and tear-drop channels. The chapter also discussed the significance of the flow rate and inlet temperature of coolant as operating parameters. Flow rate affects the coolant velocity, and Reynolds number and pressure drop, and coolant inlet temperature affects the thermal driving force for heat removal. These effects are compounded by geometry of the channel and therefore, the performance of the profile cannot be assessed at one operating condition. Thus, a multi-factor simulation approach is needed. The identified research gap is the absence of systematic comparison of circular, elliptical and teardrop conformal cooling channel profiles with different coolant flow rates and inlet temperatures. The present study fills this gap by employing Moldex3D simulation and six response variables along with the response surface methodology (RSM). The main focus is the profile level comparison of the three conformal cooling channel cross-sections, the straight-line channel is used as a reference baseline.

## **2. Simulation Framework and Comparative Evaluation Methodology**

This chapter presents the methodology used to compare the thermal, hydraulic and dimensional performance of three conformal cooling channel cross-section profiles. The study is a controlled simulation-based comparison in which the circular, elliptical and teardrop profiles are compared for the same mould geometry, material system, route to the cooling channel and process conditions. This method enables the effect of profile geometry, coolant flow rate and inlet coolant temperature to be studied whilst minimising the effect of any other variations associated with different mould layouts and part design. In this kind of comparative study, simulation-based thermal analysis is appropriate due to the fact that the conformal cooling is highly dependent on the geometry of the channels, the flow behaviour and the heat transfer characteristics of the coolant within the mould [26]. The three conformal cross-section profiles are the main comparative area, and the straight-line cooling channel is provided as a reference baseline.

### **2.1. Simulation-Based Study Approach**

It is technically challenging and expensive to carry out a physical experiment to compare the different conformal cooling channel profiles in injection moulding. There would be a need for a different mould insert or an interchangeable insert system for each profile variant, and for the comparison to be meaningful, the part temperature, cooling time, pressure drop of the coolant and warpage would need to be measured and controlled under the same process conditions. This is more challenging for non-circular conformal channels as these are usually produced by additive manufacturing or custom tooling, rather than drilling. This prompted a simulation-based approach to be chosen for this study. The aim of the simulation framework is to simulate the relative behaviour of circular, elliptical and teardrop conformal cooling channel profiles under controlled conditions. All of the part geometry, mould material, polymer material, channel routing and processing parameters are kept constant, and the flow rate, inlet coolant temperature, and channel cross-section shape are changed. This allows for a more targeted comparison of the observed differences in thermal, hydraulic and dimensional response, as it will be possible to attribute the differences primarily to the chosen design variables. In the past few years, there have been studies involving comparison using simulation that can now help in the assessment of the cooling-channel performance prior to the actual moulding [27].

Moldex3D was used to perform the injection moulding and cooling simulations. The geometry of the cooling channel was imported into the software, which was then used to analyse the cooling-channel geometry as part of the moulding system and extract the response variables necessary for the study. These responses are the average part temperature, maximum part temperature, time to ejection temperature, coolant pressure drop, average Reynolds number and total warpage displacement. To ensure the same profile comparison throughout the design matrix, the same simulation set-up was used for all three conformal profiles. The methodology is designed as a structured comparative methodology. First, the circular, elliptical and teardrop shapes are characterised by having cross-sectional areas that are close to the same size. Secondly, the flow rate of the coolants is changed, and the temperature of the coolants inlet is changed based on the chosen simulation matrix. Thirdly, the thermal, hydraulic and dimensional responses are obtained from Moldex3D. Lastly, the influence of the coolant operating conditions is interpreted using response surface methodology and multi-response optimisation to determine the profile giving the best performance in the range of the simulations performed. The straight-line cooling channel has been implemented solely as a reference point for the context of the benefits of conformal routing.

## 2.2. Simulation Design and Factor Selection

The simulation design was created to evaluate the conformal cooling channel profiles (circular, elliptical, teardrop) under controlled operating conditions and compare them. The following three factors: channel cross-section profile (circular - CL, elliptical - EL, and teardrop - TD), volumetric flow rate of the coolant (Q), and coolant inlet temperature (T<sub>c</sub>) were considered in the full conformal-cooling simulation matrix. There are three profile factors: circular, elliptical and teardrop. The coolant flow-rate levels are 2, 5 and 10 L/min, while the coolant inlet-temperature levels are 15, 25 and 35°C. This provides a full conformal-cooling simulation matrix, 3×3×3, with 27 simulation runs. The range of flow rates selected is considered to represent the low, medium and high flow ranges of coolant associated in an acceptable mould-cooling environment. The 2 L/min condition corresponds to lower flow, in which the coolant flow will be transitional or near the lower turbulent threshold for the flow, depending on the profile and coolant temperature. The 5 L/min condition is a medium operating condition and is selected as the comparison condition in the middle. The 10 L/min condition is considered as a high flow condition, with greater convective cooling but at the expense of increased pressure drop. Conformal cooling, recent studies have also employed simulation to analyse cooling channel variables and to determine cooling time enhancements before or in conjunction with physical tooling efforts to implement conformal cooling [28].

Three different inlet coolant temperatures (15°C, 25°C and 35°C) were used to investigate the effect of thermal driving force on part cooling. The lower the coolant inlet temp the greater the temp difference between the hot polymer/mould area and the coolant, and the higher the coolant inlet temperature, the less the difference. The three chosen temperature levels, therefore, provide the ability to assess the response to each channel profile under cold, medium and warm coolant conditions. Three straight-line baseline simulations were performed, along with the 27 conformal cooling simulations. The following baseline simulations were performed at the centre flow rate of 5 L/min and at coolant inlet temperatures of 15, 25 and 35 °C. The straight-line baseline simulations are not part of the conformal profile comparison and RSM model fitting. They have been added as reference cases only for the purpose of context when discussing the thermal effect of conformal routing under matched coolant-flow and coolant-temperature conditions. Following Table 1. Shows the complete simulation matrix, including all 27 conformal cooling configurations with 3 Straight-line (SL) baseline runs.

**Table 1.** Full-Factorial DOE Matrix

Run	Profile	Flow Rate (L/min)	Coolant Temp. (°C)	Run ID
1.	Circular	2	15	CL-2-15
2.	Circular	2	25	CL-2-25
3.	Circular	2	35	CL-2-35
4.	Circular	5	15	CL-5-15
5.	Circular	5	25	CL-5-25
6.	Circular	5	35	CL-5-35
7.	Circular	10	15	CL-10-15
8.	Circular	10	25	CL-10-25
9.	Circular	10	35	CL-10-35
10.	Elliptical	2	15	EL-2-15
11.	Elliptical	2	25	EL-2-25

Run	Profile	Flow Rate (L/min)	Coolant Temp. (°C)	Run ID
12.	Elliptical	2	35	EL-2-35
13.	Elliptical	5	15	EL-5-15
14.	Elliptical	5	25	EL-5-25
15.	Elliptical	5	35	EL-5-35
16.	Elliptical	10	15	EL-10-15
17.	Elliptical	10	25	EL-10-25
18.	Elliptical	10	35	EL-10-35
19.	Teardrop	2	15	TD-2-15
20.	Teardrop	2	25	TD-2-25
21.	Teardrop	2	35	TD-2-35
22.	Teardrop	5	15	TD-5-15
23.	Teardrop	5	25	TD-5-25
24.	Teardrop	5	35	TD-5-35
25.	Teardrop	10	15	TD-10-15
26.	Teardrop	10	25	TD-10-25
27.	Teardrop	10	35	TD-10-35
28.	Straight Line	5	15	SL-5-15
29.	Straight Line	5	25	SL-5-25
30.	Straight Line	5	35	SL-5-35

The design structure allows a controlled comparison between geometry of the profile and operating conditions of the coolant. In the test of conformal cooling runs, the tests are performed for nine different flows and inlet coolant temperatures. This translates to allowing for comparison of the difference in the responses extracted at matched operating conditions. The straight line baseline is processed separately since it is not a different conformal cross-section profile, it is a different route of cooling channel.

### 2.3. Fixed Process Parameters

The input conditions should be exactly the same for all runs in a comparative simulation study, so that any differences in the results are due to the design variables that are chosen. The factors in the present study vary are the conformal cooling channel profile, the volumetric flow rate of the coolant ( $Q$ ) and the inlet temperature of the coolant ( $T_c$ ). The other 27 conformal cooling simulations and 3 straight-line baseline simulations have all other process, material and geometric settings as shown below fixed. This method enables comparison of the thermal, hydraulic and dimensional responses with a controlled setting. In injection moulding, it is important to control the fixed process parameters as the final properties of the parts and their mechanical characteristics can be influenced by the mould temperature, material properties, packing conditions, cooling time and melt temperature [29].

*Part Material:* The same part material, PP\_POLYFORTFPP20T, which is a 20% talc-filled polypropylene grade available in the Moldex3D material library, is used in all the simulations. The material used for all the simulation runs is the same, and therefore the polymer thermal properties, viscosity behaviour, PVT relationship and ejection-temperature condition are all the same throughout

the study. This is crucial, as the heat load, cooling rate and warpage response would change if the polymer material were changed, and the profile comparison would become less controlled. The material chosen was polypropylene because it is the most popular material used in injection moulding technical parts and recent studies have demonstrated that the moulded part properties are sensitive to injection moulding parameters and polypropylene grade properties [29].

*Mould Material:* For all simulations, the mould material is set to be P20 tool steel. With the use of the same mould material, the thermal boundary condition around the cooling channel is the same for all three profiles, circular, elliptical and teardrop. The same data for the thermal properties of the mould is transferred to all the cases during the simulation set-up, meaning that any difference in the cooling response cannot be attributed to a change in the thermal properties of the mould: conduction and heat capacity. This is important since the study does not aim at comparison of the mould material but at the profile level [2].

*Melt Temperature:* The melt temperature is set at 230°C, and the initial mould temperature is set at 50°C. This is the initial thermal condition of polymer and mould prior to assessing the cooling response. If the melt temperature is kept constant, the initial heat load into the mould cavity will be the same for each simulation. By maintaining the mould temperature constant, the initial mould condition will be the same, and this allows for the comparison of cooling channel profiles. Melt temperature and mould temperature are also important controlled variables in the injection-moulding process, especially for the filling, cooling and part quality during process-development studies [30].

*Mould Temperature:* The temperature of the initial mould is pre-set at 50°C. This is a typical processing range of polypropylene, and is consistent with values in similar injection moulding simulation research of this material type. The temperature of the mould is the initial unheated temperature of the mould insert at the beginning of the cooling process in the Moldex3D transient analysis. It serves as the initial temperature over which the cooling system is required to initiate the cooling of the cold cavity to a thermally stable cyclic state. A temperature of 50°C is used instead of a lower temperature like 40°C to more closely approximate the real-life steady-state mould temperature of 50°C after several production cycles, and is always higher than the temperature of the coolant because of the constant heat input at each of successive shots.

*Filling, Packing, Cooling and Mould Opening Time:* The input of the filling time, packing time, cooling time and the mould opening time are also maintained constant for all the runs. The filling-time is set to 2.75 s, packing-time is set to 9.56 s, cooling-time is set to 30 s, and mould-opening time is 5 s, so the total cycle-time value is 47.31 s. These values are considered to represent constant simulation conditions, which allow the effect of the cooling-channel profile and coolant operating condition to be isolated. The response, Max Time to reach Ejection Temperature ( $t_{cool}$ ), is then extracted from Moldex3D, which is the time at which the hottest region of the part reaches the desired ejection temperature. The  $t_{cool}$  response is different from the input cooling time set as 30 s, and is not a fixed parameter.

*Coolant Medium:* All simulations are carried out with water as coolant. The coolant material is kept constant to ensure that any change in pressure drop, Reynolds number and thermal response are only due to the change in conditions of the coolant and not the coolant material itself. The inlet temperature of the coolant is only changed as a DOE variable at 15°C, 25°C and 35°C, but the medium of the coolant itself is still the same for all tests, water. This offers a controlled method for studying the

effect of thermal driving force, but with the thermophysical behaviour of the coolant constant in the Moldex3D material definition.

*Channel Standoff Distance:* Channel standoff is 15 mm away from the part surface. This distance remains constant for the circular, elliptical and teardrop conformal profiles to ensure the comparison is based on profile geometry, not channel location. The distance between the channel and the cavity surface might affect the cooling response in addition to the profile shape, if the standoff distance is changed between profiles. Thus, for a fair comparison of the profiles, the standoff distance needs to be fixed.

The following Table 2 summarises the fixed parameters applied across all simulation runs.

**Table 2.** Fixed process and material parameters used in the simulation runs

Parameter	Fixed Value
Part Material	PP_POLYFORTFPP20T (20% talc-filled PP)
Mould Material	P20 Tool Steel
Melt Temperature	230°C
Mould Temperature	50°C
Ejection Temperature	102.93°C
Packing Time	9.56 s
Filling Time	2.75 s
Cooling Time (Input)	30 s
Mould Opening Time	5 s
Total Cycle Time	47.31s
Coolant Medium	Water
Channel Standoff Distance (From Part Surface)	15 mm

## 2.4. Part Geometry, Mould Model and Cooling Channel Profiles

The simulation setup comprises the geometry of the moulded pieces, the virtual mould insert and the cooling-channel system. To ensure that the comparison between the circular, elliptical and teardrop profiles is controlled, the part geometry and mould model is the same for all the simulation runs. The cross-section profile of the cooling channel as well as the coolant flow rate and coolant inlet temperature, are the only parameters that are different for the three conformal profiles, while the cooling channel route is the same for all three. This means that response differences observed are primarily associated with the channel profile and the operation of the coolant. The geometry of the cooling channels should be designed according to the geometry of the part and the local cooling needs, particularly for complex conformal sections [14].

### 2.4.1. Part Geometry

The chosen part geometry is a simplified representative casing geometry, similar to that of battery housings. A model was created to give a controlled geometry of an injection-moulding simulation for comparing the various conformal cooling channel profiles. The idea of the part is not therefore to make a replica of the commercial part having exact dimensions, but to model a casing type geometry with relevant thermal and geometrical features for the cooling analysis. The overall length of the

CAD model is 115 mm, its width is 92 mm, and its height is 107.5 mm. The thickness of the main outer walls is 2.5mm, and the internal rib-like partitions is 1.5mm. These internal partitions help to subdivide the open casing volume into several compartments and cause some local variation in the heat flow during the cooling. Furthermore, the bottom of the part features larger mounting elements which extend outwards by around 12.5 mm and have a height of 10.45 mm.

To ensure a fair comparison, the same part geometry was used for all cooling-channel configurations. This implies that the same moulded part, wall thickness distribution and thermal loading conditions were used for all the circular, elliptical and teardrop channel cases. So the variation of the average part temperature, maximum part temperature, cooling time, pressure drop, Reynolds number and warpage response can be primarily attributed to the cooling-channel profile and the coolant operating conditions, and not to the variation in the geometry of the moulded part. Therefore, the part should be interpreted as representative geometry for a casing-type part to use for simulation comparison. Thus, the results of the study are viewed as a comparison of the performance of the cooling channels for the chosen casing geometry and not a prediction of the performance for a commercial battery casing. The geometry of the part that has been used for the simulation study is shown in Fig. 4.

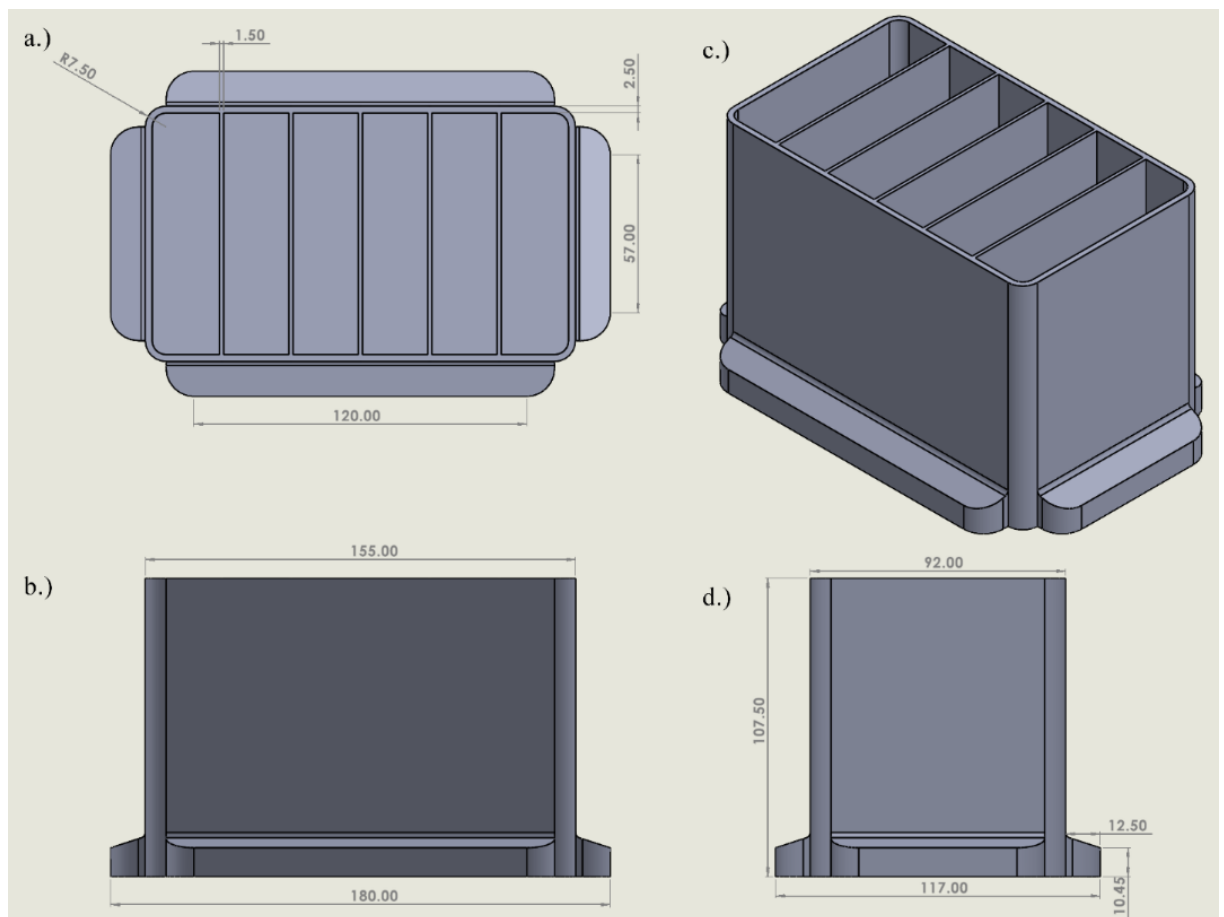


**Fig. 4.** Modelled reference used as part geometry a) Top view; b) Front view; c) Isometric view; d) Side view

The geometry was chosen because it includes a number of features that are important to assess the mould cooling performance. These include large flat areas, vertical side walls, rounded corner areas, internal rib sections and area thickness changes near the base. These features, which provide different cooling situations within the part, are more thermally significant than a plain flat plate. Corners,

thicker base and deeper areas and ribs can hold heat for longer periods of time while thin walls and ribs cool more quickly. The part geometry thus makes it possible to see how the average temperature, maximum temperature, cooling uniformity and potential warpage response varies based on different cooling-channel designs. The geometry was chosen to be as simple as possible to allow a better investigation of the effect of the cooling-channel profile. Specific details of products were not included, as this would make the modelling and meshing more complicated, with no direct benefit to the comparison of the different channel shapes. This simplification helps to have a more controlled simulation study, whose primary goal is to compare the behaviour of circular, elliptical and teardrop cooling channels under the same conditions.

#### 2.4.2. Virtual Mould Configuration

The mould geometry was virtually modelled as P20 steel insert, including mould cavity and the geometry of cooling channels. The same mould block size (296 mm × 246 mm × 350 mm) was employed for all the simulation cases. Mould block dimensions should not be changed because the quantity of steel in and around the cavity directly impacts on the heat storage and heat transfer in the cooling phase. If the mould size is different between simulations, the surrounding thermal mass would also differ, and the difference in temperature or cooling-time could no longer be attributed to the cooling-channel profile alone. As such, the same mould volume has been adopted in the circular, elliptical and teardrop conformal cooling-channel comparison. The use of P20 tool steel was also kept constant for all simulations. This will ensure that the thermal conductivity, heat capacity and heat-transfer behaviour of the mould insert is the same in all cases. In this study, the influence of the cross-section of the cooling channel on the mould should be compared, so any change in the size of the mould block and the material of the mould would add another variable to the analysis. The virtual model of the mould is shown in Fig. 5, and the key dimensions of the virtual model.

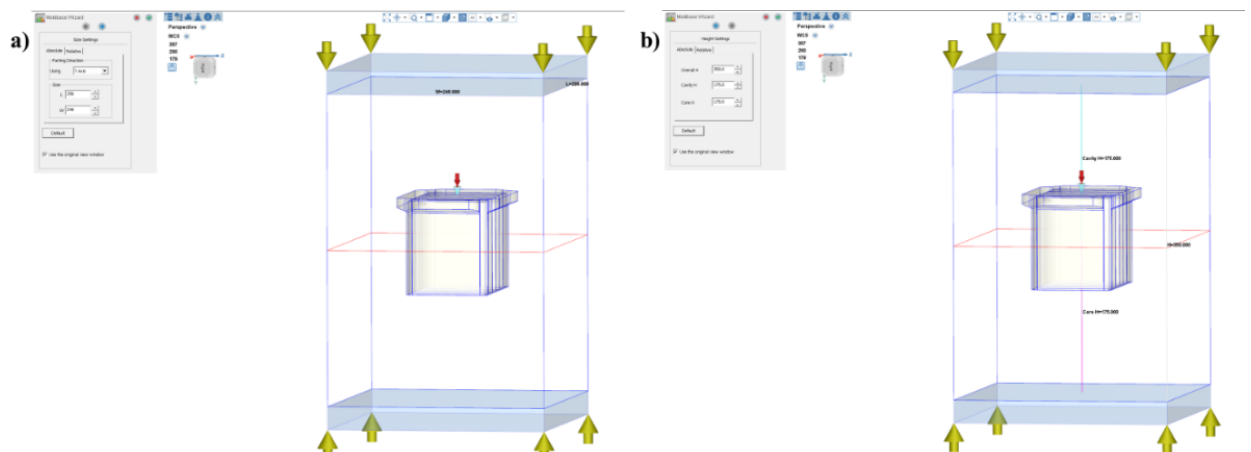


**Fig. 5.** Virtual mould with dimensions a) 296L × 246W and b) 350H

The comparison will be more controlled, maintaining the same mould material and the same mould geometry, and the changes observed for the average part temperature, maximum part temperature, cooling time, pressure drop, Reynolds number and warpage will be directly related to the cooling-channel geometry and the operating conditions of the coolant. The virtual mould configuration was specially created for the cooling stage comparison and not for the production mould design. For this reason, auxiliary mould features like the runner system, ejector system, clamping detail, fastening components and detailed mould-base hardware were not modelled. In a genuine production mould

the following would be essential for the manufacture and working of the mould, but are not considered the primary items of the present comparison. With their removal, the CAD model is simplified, and the meshing of the other parts is easier, while the simulation can focus on the cavity region, the surrounding mould material and the cooling-channel volume. These are the most relevant regions for the assessment of the thermal and hydraulic behaviour of the cooling system. This is also a modelling simplification that makes the comparative study more consistent. All profiles are exposed to the same boundary condition and the same surrounding thermal mass, as the same simplified mould block is used for each simulation. This means that the cooling channels are compared on the basis of the same geometric and material conditions. This renders the virtual mould appropriate for the isolation of the effect of profile geometry without any unnecessary changes caused by variation of external mould features.

### **2.4.3. Conformal Cooling Channel Routing**

The conformal cooling channel is not a straight-line drilled route but has the general shape of the part geometry. This helps to ensure that the cooling path is closer to the part surface and is more able to follow the thermal regions of the part. In this study, the same conformal route is used for the circular, elliptical and teardrop profiles. This is essential because the goal is to compare the behaviour of a cross-section profile and not different channel layouts. Any change of route between profiles would impact the results, due to the location of the channel as well as the geometry of the profiles, so the comparison would not be direct. The study is designed to maintain the same route, thus keeping the influence of profile shape, wetted perimeter, hydraulic diameter and coolant-flow behaviour isolated. The channel standoff distance to the part surface is constant for all conformal profiles, and the distance is 15 mm. This distance determines the proximity of the coolant path to the mould cavity and hence, the cooling effectiveness has a direct impact on this. A different standoff distance between profiles could alter the thermal response due to a change in channel location, but not to a change in channel cross-section geometry. Therefore, the standoff is set to 15 mm in all the conformal cooling simulations. This provides an equal comparison of the circular, elliptical and teardrop profiles and eliminates the potential for biasing results due to different distances of the channel from the cavity surface (See Appendix 1).

### **2.4.4. Cooling Channel Cross-Section Profile**

In this study, the main geometric parameter is the conformal cooling channel cross-section profile. Three different profiles are being compared: circular, elliptical and teardrop. These profiles have been chosen for the geometric complexity they increase by without changing the nominal flow area. The circular profile is taken as reference conformal profile, the elliptical profile is a widened profile having a larger contact width on the cavity side, while the teardrop profile is designed as an asymmetric profile for localised better thermal behaviour. All three profiles have a similar cross-sectional area, that of a 10 mm diameter circular channel. This equal-area condition is very important as it will ensure the same nominal coolant-flow capacity between profiles. So, the same volumetric flow rate is a similar coolant-throughput condition for each profile. Previous mould-cooling research has explored profiled conformal cooling channels as these non-circular sections can alter the cooling performance, pressure drop and temperature uniformity from that of simply traditional circular conformal channels [31]. Following Table 3. Summarises the geometric properties of all three channel profiles.

**Table 3.** Geometric Properties of Channel Profiles

Profile	Dimensions	Cross-Sectional Area (mm <sup>2</sup> )	Perimeter, P (mm)
Circular	d = 10mm	78.54	31.42
Elliptical	12.24mm x 8.17mm	78.55	32.38
Teardrop	9.59mm W x 7.19mm H, 0.5mm tip	78.52	32.50

*Circular Cross-Section Profile:* The conformal cross-section with a circular profile has a diameter of 10.00 mm, a cross-sectional area of 78.54 mm<sup>2</sup> and a wetted perimeter of 31.42 mm. The circular profile is simple in geometry and has a wide understanding in terms of heat transfer and fluid flow. Furthermore, the distance from the centre to the wall is the same in every radial direction, which is a 15mm Standoff distance, giving the circular section a stable reference geometry for comparison of the effect of changing the channel shape. In this study, simply the circular profile doesn't correspond to the straight-line baseline, but to the easiest cooling profile in the conformal cooling group. Thus, its performance is taken as the benchmark to determine if the elliptical/teardrop profiles offer any improvement in performance. All three profiles have been formed with a very similar cross-sectional area, and thus, for the same value of volumetric flow rate, the mean coolant velocity is nearly the same. But the circular profile results in a slightly larger hydraulic diameter and, consequently, a larger response to the Reynolds number. From a methodological perspective, it is important to include the circular profile since it permits the study of the two effects: conformal routing and the effect of modifying the profile from the circular shape. There would be no simple conformal reference profile if it were only elliptical or teardrop profiles that were compared. Thus, the circular conformal channel can be used as a baseline profile to evaluate the thermal, hydraulic and dimensional impact of profile shaping. The model of the circular conformal cooling channel is illustrated in Fig. 6.

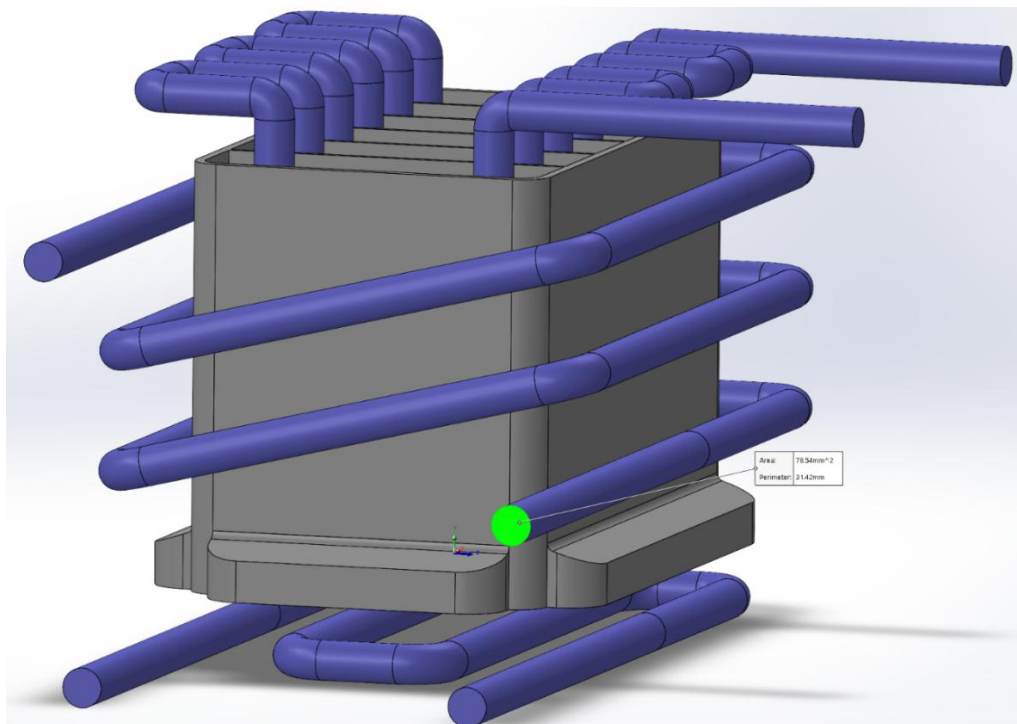


**Fig. 6.** Conformal Cooling Channel with Circular Profile

*Elliptical Cross-Section Profile:* The elliptical profile is included as the first modified conformal cross-section. It has dimensions of 12.24 mm × 8.17 mm, a cross-sectional area of 78.55 mm<sup>2</sup>, and a wetted perimeter of 32.38 mm. The cross-sectional area is maintained very similar to the circular profile so that a large difference in the capacity of the coolant to flow does not dominate the comparison. Rather, the elliptical shape changes the shape of the channel, but the flow area is approximately the same. The major axis is parallel to the cavity wall, with a large channel surface being nearer to the thermally active portion of the mould. This orientation aims at the optimisation of the contact relationship between the cooling channel and the cavity-facing mould part, not to alter the conformal route. The elliptical profile has a slightly greater wetted perimeter and less hydraulic diameter than the circular profile from a hydraulic perspective. However, as the cross-sectional area is close to the same, the mean coolant velocity at a specific volume flow rate is approximately similar as that of the circular channel. Thus, any variation in cooling or pressure drop response is primarily related to the varying perimeter, hydraulic diameter and flow distribution in the region, rather than to a significant area change. The elliptical profile is of particular interest to the study since it is a non-circular shape that is smoother than the circular shape. It enables the analysis to assess if widening the channel in the area facing the cavity side improves the thermal behaviour with a still favourable hydraulic resistance. This profile is particularly helpful in the results, when comparing the thermal performance and pressure drop. The model of conformal cooling channel is elliptical, like shown in Fig. 7.

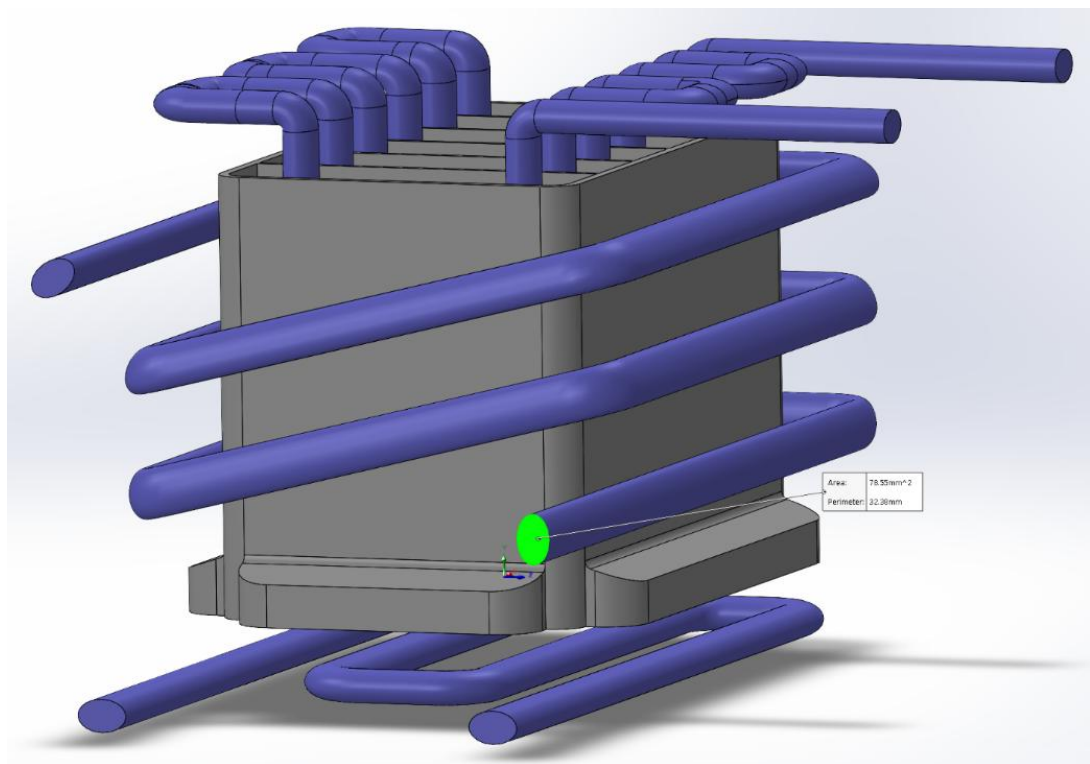


**Fig. 7.** Elliptical Conformal Cooling Channel

*Teardrop Cross-Section Profile:* The shape of the teardrop profile is the most geometrically distinctive profile of conformal cooling channels that are studied. Its radius of the tip is 0.50 mm, the centreline to tip length is 7.19 mm and the diameter of its lobe is 9.59 mm and is rounded. Measured cross-sectional area: 78.52 mm<sup>2</sup> Wetted Perimeter: 32.50 mm It is maintained close to the circular and the elliptical profile so as to have a similar nominal coolant-flow capacity. But the teardrop-

shaped section is not symmetrical like the circular and elliptical sections. The rounded side of the profile faces towards the cavity region, the tapered side faces away from the cavity. This orientation is chosen to be facing the area of most important heat removal, the wider rounded area. The teardrop profile is added to study the possibility of having a better local thermal behaviour using an asymmetric profile as opposed to the symmetric channel profiles. The flow area is similar for all the other profiles, and therefore, the expected difference in performance is not due to greater flow area or greater mean velocity of the coolants. Rather, the difference is a function of wetted perimeter, hydraulic diameter and the orientation of the profile and local heat-removal behaviour in the vicinity of the cavity-facing side. The wetted perimeter is the biggest for the teardrop profile and the smallest for the hydraulic diameter. This can cause it to exhibit different characteristics with regard to pressure drop and Reynolds number, and may have potential thermal benefits in the area closest to the part. For this reason, it is important to assess the teardrop profile to determine if profile shaping can be performed to achieve better hot-spot control and cooling time with an acceptable hydraulic or dimensional penalty. The CAD model of teardrop conformal cooling channel is shown in Fig. 8.

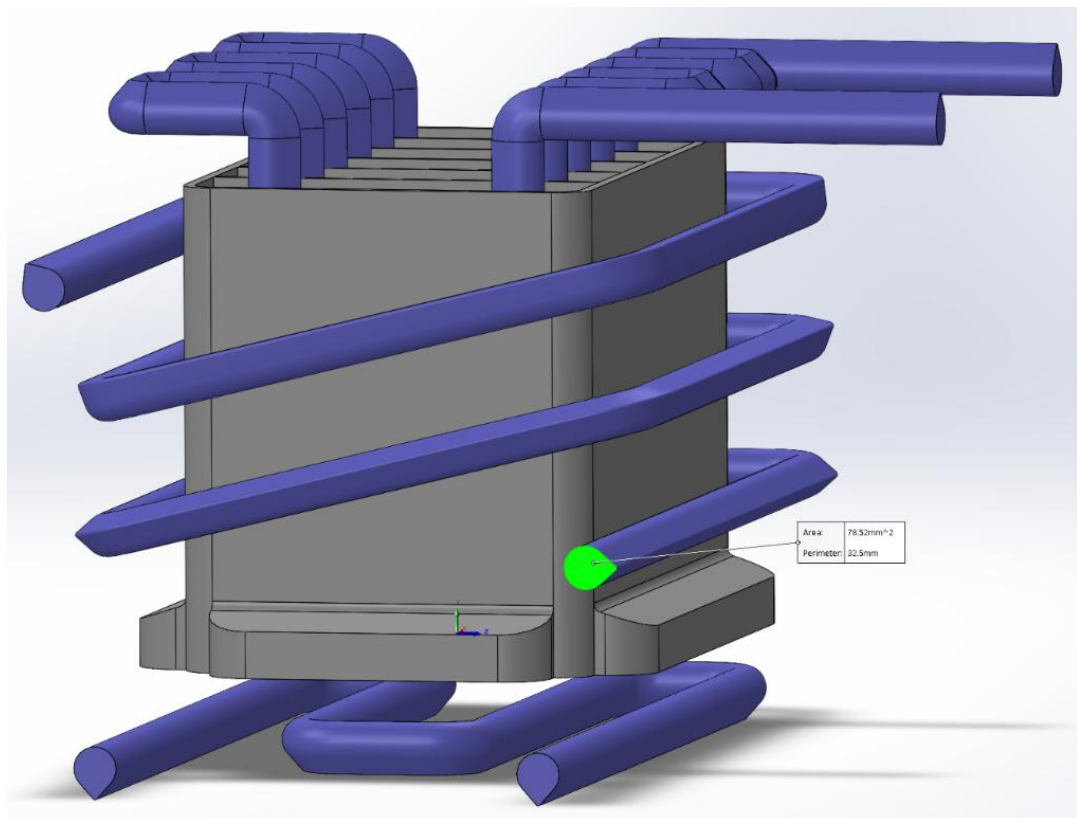


**Fig. 8.** Teardrop Conformal Cooling Channel

## 2.5. Simulation Setup

Each of the simulations was carried out with the Moldex3D transient analysis sequence. Analysis sequence comprises the cyclic cooling, filling, packing, transient cooling and warpage stages. This sequence is indicated as Ct-F-P-Ct-W, and the cooling and mould-temperature behaviour is assessed in combination with filling, packing and post-cooling deformation. Transient analysis was chosen as during the cooling stage, the cooling behaviour in the moulded part changes with time. For the present study, this is important as it gives one of the primary response variables,  $t_{cool}$ , which is influenced by the time needed for the hottest part of the component to reach the chosen ejection temperature. All of

the simulations used the same material data, process parameters and boundary conditions. This means that the part material, mould material, melt temperature, mould temperature, filling time, packing time, cooling-time input, mould opening time and coolant medium were not varied. The only design variables varied were the channel profile, coolant flow rate, and coolant inlet temperature. This configuration enables one to compare the simulation results directly throughout the entire design matrix [32].

### 2.5.1. Process Analysis Type

All simulations are run on the Transient Analysis sequence in Moldex3D, which is marked as Ct-F-P-Ct-W, which indicates cyclic cooling stages, filling stages, packing stages, transient cooling stages, and warping stages, respectively. Transient analysis mode is also chosen in place of the cycle-averaged analysis mode, which determines the temperature distribution in the mould and in the part over time during the cooling stage, instead of just determined as a single steady-state average. The extraction of the Time to Reach Ejection Temperature result, the primary thermal output measure of the study, which needs the understanding of the temperature behaviour during the entire cooling period, requires this time-resolved method.

### 2.5.2. Mesh Generation

Prior to the main simulation runs, a mesh convergence study was performed in order to determine a suitable mesh density. This study aimed to make sure that the primary thermal result was not highly sensitive to the size of the mesh and that the computation is feasible. Five different mesh levels were tested: 10 mm, 6 mm, 4.5 mm (recommended by Moldex3D), 3 mm and lastly 1.5 mm seeding. The primary convergence metric was chosen to be the time to reach the ejection temperature ( $t_{cool}$ ). Since this response is directly related to the cooling-stage performance and is also one of the main outputs used to compare the cooling-channel profiles,  $t_{cool}$  was decided to be a more practical convergence response for this study. The mesh independence study is summarised in Table 4.

**Table 4.** Mesh Convergence Study

Mesh Type	Seeding Size	Element Count (Total)	$t_{cool}$ (s)	Compute Time (min)
Coarse	10mm	71,352	236.670	10
Medium	6mm	173,953	236.610	16
Recommended	4.5mm	300,001	236.630	45
Fine	3mm	619,935	236.640	58
Extra Fine	1.5mm	2,563,220	236.630	251

As observed in Table 4 that the  $t_{cool}$  value does not vary much at various levels of mesh. The spread between the highest and lowest  $t_{cool}$  value is 0.060 s, which is less than 0.03% of the mean value. The recommended mesh with 4.5 mm seeding and 300,001 elements gives  $t_{cool}=236.630$  s. This is the same as the result of the extra-fine mesh and just 0.010 s from the result of the fine mesh. But it took 251 min per run for the extra-fine mesh while the recommended mesh required only 45 min per run. Hence, the chosen mesh for the principal simulation matrix was chosen due to its ability to give constant thermal output at significantly reduced computational cost. All 27 conformal cooling simulations and 3 baseline simulations of straight lines were then simulated using the recommended mesh. This ensured that all the simulation cases were solved with the same strategy of the mesh and that the differences in the results were not due to inconsistent mesh density.

### 2.5.3. Cooling Analysis Computation Setup

The cooling analysis was carried out by the Moldex3D Cool CFD mode by combining with 3D solid cooling channels. This mode was chosen because it can solve the behaviour of coolant flow and heat transfer in the 3-D coolant volume. This is relevant to the current study as the elliptical and teardrop profiles are not circular and hence cannot be represented by a one-dimensional equivalent channel model. A 3D cooling-channel model makes it possible to simulate the velocity field, pressure distribution and temperature behaviour in the actual cooling channel volume. The 3D Cool CFD setup also provides the output of hydraulic responses like coolant pressure drop, average Reynolds number etc. These responses can be used to thermofluidically characterise the circular, elliptical and teardrop profiles. The three profiles have similar flow area but different wetted perimeter and hydraulic diameter, and it is therefore more appropriate to consider the use of a three-dimensional coolant domain to compare profile-dependent hydraulic behaviour. The walls of the cooling channels in the simulation workflow were meshed with the surrounding mould domain in order to enable a heat exchange calculation between the mould insert and the flowing coolant. This allowed the same model to be used for the part-side thermal response and coolant-side hydraulic response evaluation in the simulation. Thermal, hydraulic, and dimensional outputs ( $T_{avg}$ ,  $T_{max}$  and  $t_{cool}$ ,  $\Delta P$ , and  $Re_{avg}$ , and  $Warp$ ) were thus included in the final dataset.

## 2.6. Output Extraction and Thermofluidic Characterisation

The necessary response variables were then obtained from the Moldex3D post-processing environment after every simulation. The outputs were chosen for representing the thermal, hydraulic and dimensional behaviour of the cooling-channel system. There were six response variables represented in the study: Average part temperature ( $T_{avg}$ ), Maximum part temperature ( $T_{max}$ ), Time to reach ejection temperature ( $t_{cool}$ ), Coolant pressure drop ( $\Delta P$ ), Average Reynolds number ( $Re_{avg}$ ), and Warpage displacement ( $Warp$ ). The three conformal cooling profiles can be compared based on the following outputs, but also based on their cooling performance, hydraulic resistance and dimensional quality [33].

### 2.6.1. Extracted Simulation Response Variables

*Average Part Temperature ( $T_{avg}$ ):* This is the average temperature of the moulded part at the end of the specified cooling stage. This response is for assessment of the overall thermal state of the part. It is an average value and is not as sensitive as the maximum temperature to isolated local hot spots. Thus,  $T_{avg}$  can be used for comparison of the overall cooling effect of the circular, elliptical and teardrop shapes.

*Maximum Part Temperature ( $T_{max}$ ):* It is the highest nodal temperature on the part at the end of the cooling stage, in degrees Celsius. It is a single value that is prone to local thermal hotspots, usually at the base of deep ribs, connection of thin-walled structures or furthest away from the cooling channels, and thus an indicator of the worst thermal scenario, rather than the overall cooling effect.  $T_{max}$  is kept as a thermal response to evaluate the possibility of part overheating and its influence on ejection integrity and post-ejection deformation.

*Time to Reach Ejection Temperature ( $t_{cool}$ ):* It is the time (in seconds) taken for the very last node in the part to cool to the material ejection temperature of 102.93°C, as defined in the Moldex3D material data set for PP\_POLYFORTFPP20T. This is the minimum duration of cooling phase required for

safe part ejection without deformation damage, and hence is the primary factor affecting the minimum cycle time for a given profile and process condition. This is different from the cooling time input of 30 s, which governs the duration of the cooling phase where the coolant is flowing;  $t_{cool}$  is a separate output that measures the amount of time required for the part to thermally equilibrate below the specified ejection temperature [15].

*Coolant Pressure Drop ( $\Delta P$ ):* A hydraulic penalty is calculated for each cooling-channel profile and operating condition, using a pressure-drop calculation for the coolant. Parameters influencing the pressure drop in a given coolant medium are flow rate, length of channels, hydraulic diameter, bends, shape of profile and local wall-flow behaviour. The conformal route is the same for the three conformal profiles used in this study, and so the differences in pressure drop between the circular, elliptical and teardrop are primarily due to the cross-section geometry and the operating conditions. The pressure-drop response is significant since greater cooling performance may be needed to accommodate higher coolant flow, and a greater flow may mean greater pumping needs. Hence,  $\Delta P$  is considered one of the minimised responses for the multi-response optimisation. This will avoid the optimisation choosing a condition which will provide a good thermal performance but will cause an unnecessarily high hydraulic penalty. [7, 18].

*Coolant Reynolds Number ( $Re_{avg}$ ):* The average Reynolds number ( $Re_{avg}$ ) is the mean of the coolant Reynolds number in the cooling channel. It is used to indicate the flow regimes to determine whether the flow of the coolant is predominantly transitional or turbulent.  $Re_{avg}$  is not considered to be a direct performance objective during the optimisation stage. It is, however, utilised to describe the condition of coolant flow and to assist a pressure-drop and thermal-response discussion. While Reynolds number is relevant to cooling performance, there is a possibility of having too high a Reynolds number with no proportional cooling increase, but rather a pressure drop increase [23].

*Part Warp (Warp):* This is the maximum sum of nodal displacement from the nominal CAD geometry after the mould has opened and cooled, in millimetres. Warp is caused by uneven thermal shrinkage: areas that remain warmer longer will have higher residual thermal stresses, which relax as the part is ejected, distorting the part. Given the impact of cross-section profile on temperature uniformity, warp is also used as a response variable to reflect the dimensional quality of the part as a result of different profiles' thermal performance.

### 2.6.2. Hydraulic Diameter ( $Dh$ )

Hydraulic diameter is used to compare the circular, elliptical and teardrop profiles from a hydraulic viewpoint. The hydraulic diameter is the diameter of the channel for a circular channel. The hydraulic diameter of a non-circular channel is based on the internal area of a channel and the wetted perimeter. This will enable the comparison of the elliptical and teardrop profile by a like hydraulic unit of measure. In profiled conformal cooling channels, the use of geometric and hydraulic indicators is particularly significant since the cross-section may not be circular and thus change the behaviour of the flow and the cooling performance of the channel [31]. For the elliptical and teardrop cross-sections, the hydraulic diameter is equivalent to the internal flow diameter, which is defined as:

$$Dh = \frac{4A}{P} \quad (1)$$

Where  $Dh$  is the hydraulic diameter,  $A$  the internal cross-sectional flow area and  $P$  the wetted perimeter. Values for area and perimeter were taken from the SolidWorks cross-section measurements. Table 5 presents the hydraulic diameters calculated.

**Table 5.** Calculated Hydraulic Diameter

Profile	Area, $A$ (mm <sup>2</sup> )	Wetted Perimeter, $P$ (mm)	Hydraulic Diameter, $Dh$ (mm)
Circular	78.54	31.42	10.00
Elliptical	78.55	32.38	9.70
Teardrop	78.52	32.50	9.66

From Table 5, it can be seen that the hydraulic diameter of circular profile is highest, followed by elliptical and teardrop profiles. The difference in the cross-sectional areas is not large, so the difference in the hydraulic diameters is primarily due to difference in the wetted perimeter. The teardrop profile has the largest wetted perimeter, and smallest hydraulic diameter. The latter are then used for interpretation of the Reynolds-number response.

### 2.6.3. Flow Velocity ( $V$ )

The mean cross-sectional flow velocity ( $V$ ) indicates the speed at which the coolant travels through the cooling channels at a specific flow rate. This value is an important component for calculating the Reynolds number and determines the kinetic energy required for effective convective heat transfer. Since Moldex3D defines flow conditions using the volumetric flow rate ( $Q$ ), rather than direct velocity. According to the principle of continuity, the mean flow velocity is given by:

$$V = \frac{Q}{A} \quad (2)$$

Where  $V$  is the mean velocity of the coolant,  $Q$  is the flow rate through the channel and  $A$  is the cross section of the flow area in the channel. This relationship is only considered as one of the interpretations of the nominal flow condition, as the detailed coolant-flow solution is directly obtained from Moldex3D.

Because the cross-sectional area of the circular, elliptical and teardrop profiles is similar, the mean velocity of the coolant for each profile at a given flow rate will be very similar. Hence, the comparison of the profiles is not due to a big difference between the nominal flow velocity. The difference in main velocity is between the flow-rate levels selected. The velocity difference between a given profile, however, at a fixed flow rate is small due to the similar cross section of all the profiles at a given flow rate; the mean velocity is around 0.42 m/s for 2 L/min, 1.05 m/s for 5 L/min and 2.10 m/s for 10 L/min. This helps to uphold the equal area design principle applied in the study. The profiles are compared under similar nominal coolant-throughput conditions and differences in hydraulic and thermal behaviour are primarily related to wetted perimeter, hydraulic diameter, profile orientation and the local flow distribution.

### 2.6.4. Reynolds Number ( $Re$ )

The Reynolds number is used for the interpretation of the flow regime of the coolant inside the cooling channel. In this study,  $Re_{avg}$  is directly taken from the volume-averaged value of each simulation run that is calculated in the Moldex3D CFD cooling module. It is not directly used as an optimisation

goal but as a flow-regime indicator for diagnostic use. It's important to note that Reynolds number is not inherently “good” or “bad” as a higher Reynolds number could reflect better coolant mixing, but could also correspond to a higher pressure drop. Thus, the condition of coolant flow is described by  $Re_{avg}$  and  $\Delta P$  is used as the hydraulic penalty in the optimisation [23]. The governing equation for  $Re$  in the duct is:

$$Re = \frac{\rho V D_h}{\mu} \quad (3)$$

where  $\rho$  is the density of the coolant,  $V$  is the mean velocity of the coolant,  $D_h$  is the hydraulic diameter, and  $\mu$  is dynamic viscosity. For this study, this relationship indicates that the Reynolds numbers can be varied in three different ways. In the first place, the greater the flow rate of the coolant, the greater the mean velocity  $V$ , which will have a significant effect on making  $Re$  greater. Secondly, a higher coolant inlet temperature will reduce the dynamic viscosity of water, thus leading to a higher  $Re$  at the same nominal flow rate. Third, even with the flow rate and the cross-sectional area kept almost the same, small changes are found due to the differences in hydraulic diameter.

Thus, most significant changes in  $Re_{avg}$  are likely to be due to coolant flow rate and coolant temperature. The 2L/min case is considered the low-flow regime, with the majority of the final simulation results lying in the transitional regime. The 5 L/min condition transitions the coolant flow into the turbulent region for all of the coolant flow profiles, and the 10 L/min condition is a high turbulent flow case. This flow-regime change is significant because it provides an insight into why the cooling performance initially improves with increasing flow rate but becomes lower with a greater pressure-drop penalty with further increases in flow rate.

Although profile geometry has an effect on  $Re_{avg}$  it is not as large as changing the flow rate. The mean velocity of the three profiles (circular, elliptical and teardrop) at the same volumetric flow rate are nearly the same because the cross-section areas of the three profiles are approximately equal. Hence, the differences of  $Re_{avg}$  with profiles are primarily associated with the local flow behaviour and hydraulic diameter. From the values of the hydraulic diameter in Table 5, it is believed that the circular profile will have the highest  $Re_{avg}$  value, and the next highest is the elliptical followed by the teardrop profile. This anticipated trend is later compared to the results of the Moldex3D Reynolds-number extraction in Chapter 3.

## 2.7. Response Surface Methodology

More than one process variable affects the thermal, hydraulic and dimensional performance of the conformal cooling channels. In this study, coolant inlet temperature and coolant volumetric flow rate affect average part temperature, maximum part temperature, cooling time, pressure drop, Reynolds number and warpage displacement. These relationships are not necessarily linear, as more coolant flow may improve heat removal at lower flow rates, but offer less improvement at higher flow rates. Meanwhile, the pressure drop may be a nonlinear function of flow rate. Hence, Response Surface Methodology was employed to model the input factors and simulation output responses. To evaluate linear, quadratic and interaction effects within one modelling framework, response surface methodology was chosen. However, unlike other simulation approaches, RSM models a continuous response surface for the range of operating conditions tested. This enables the visualisation of response behaviour, the estimation of values at intermediate operating conditions and optimisation.

Similar RSM-based methods have been utilised in research on warpage modelling and optimisation of straight drilled and conformal cooling channels for injection moulding applications [34].

### 2.7.1. RSM Input Factors and Response Variables

The RSM analysis was carried out using two continuous input factors, namely coolant inlet temperature ( $T_c$ ) and coolant flow rate ( $Q$ ). One combined model did not explicitly include the cross-sectional profile as a categorical factor. Rather, individual RSM models were created for the circular, elliptical and teardrop conformal cooling profiles. The advantage of this approach was that it allowed the effect of  $T_c$  and  $Q$  to be evaluated within each of the profiles, as well as the difference in the response behaviour between the three profile geometries. The physical factor levels for the Moldex3D simulation matrix were coolant inlet temperature of 15°C, 25°C, and 35°C, as well as coolant flow rate of 2 L/min, 5 L/min, and 10 L/min. These physical units are used when reporting the simulation conditions and the JASP Response Optimiser Solution. But, regression coefficient tables and polynomial equations will be exported in coded-coefficient form. Thus, A and B in the fitted RSM equations represent coded values of coolant inlet temperature and coolant flow rate, respectively, and not the actual values of  $T_c$  and  $Q$ . The symbols in the regression equations and the physical RSM input factors are shown in the following Table 6.

**Table 6.** RSM input factors, and physical levels, and coded equation symbols

Factor	Symbol	Level 1	Level 2	Level 3
Coolant inlet temp	A	15°C	25°C	35°C
Flow Rate	B	2 L/min	5 L/min	10 L/min

The levels in Table 6 refer to the physical values that are used for the Moldex3D simulations. The JASP Response Optimiser Solution will also give the optimum settings in physical units, °C and L/min. However, the regression equations that JASP exports are in coded units, meaning A and B in the equations are coded versions of  $T_c$  and  $Q$ , respectively, not the actual physical values. The following six response variables were modelled:  $T_{avg}$ ,  $T_{max}$ ,  $t_{cool}$ ,  $\Delta P$ ,  $Re_{avg}$ , and  $Warp$ . There were three conformal profiles and six response variables analysed for each conformal profile, resulting in a total of 18 response surface models to be fitted. The three straight-line baseline simulations were not considered for RSM-fitting because they are not a conformal cross-section profile variant, and they are a different route for the cooling channel.

### 2.7.2. Second-Order Polynomial Model

Since the behaviour of the response may involve curvature and interaction effects, a second-order polynomial model was chosen. For instance, the effect of the coolant flow rate on cooling time could be more pronounced at low flow rates and less pronounced at high flow rates, whereas the effect of the flow rate on pressure drop could be more pronounced at high flow rates. Such non-linear behaviour would not be described by a first-order model, which only models a flat response plane. Similarly, recent conformal-cooling optimisation research has employed a simulation-based approach to assess the impact of the cooling-channel design variables and the cooling-rate improvement [28, 34, 35]. The Second-order polynomial is generalised by:

$$\hat{y} = \beta_0 + \beta_1 A + \beta_2 B + \beta_{11} A^2 + \beta_{22} B^2 + \beta_{12} AB \quad (4)$$

where,  $\hat{y}$  is the predicted response;  $A$  is the coded variable corresponding to coolant inlet temperature ( $T_c$ , °C);  $B$  is the coded variable corresponding to the coolant flow rate ( $Q$ , L/min);  $\beta_0$ , intercept of the coded response-surface model;  $\beta_1$  and  $\beta_2$ , linear coefficients; and  $\beta_{11}$ ,  $\beta_{22}$ , and  $\beta_{12}$ , quadratic and interaction coefficients, respectively. JASP displays the equations that have been fitted, but the levels of the factors and the output from the optimiser are in terms of the physical units of °C and L/min. For each response variable and each conformal profile, the model was fitted separately. The obtained equations were then used to produce the response surface plots and to determine the significance of the factors as well as to predict the response at any point within the range of the experimental conditions. Table 7 shows specific physical interpretation of each term in the context of this study.

**Table 7.** Physical interpretation of the second-order polynomial terms for this study

Term	Coefficient	Meaning
$A$	Coded Variable	Coded variable corresponding to coolant inlet temperature, $T_c$
$B$	Coded Variable	Coded variable corresponding to coolant flow rate, $Q$
$\beta_0$	Intercept	Predicted response at the centre-point conditions
$\beta_1 A$	Linear – Coolant Temp	Main effect of Coolant inlet temperature
$\beta_2 B$	Linear – Flow Rate	Main effect of Coolant flow rate
$\beta_{11} A^2$	Quadratic – Coolant Temp	Curvature in the Coolant temperature direction
$\beta_{22} B^2$	Quadratic – Flow Rate	Curvature in the Flow rate direction
$\beta_{12} AB$	Interaction	Combined effect of coolant inlet temp and flow rate

### 2.7.3. RSM Design Structure and Model Adequacy

Each conformal cooling profile has nine RSM simulation runs for three levels of coolant inlet temperature and three levels of coolant flow rate. The same nine combinations of  $T_c$  and  $Q$  were used for the circular, elliptical and teardrop profiles. This results in equivalent response-surface datasets for each profile and facilitates comparing the profile-specific models under the same operating conditions. There are 6 terms in each second-order model, the intercept, 2 linear terms, 2 quadratic terms and one interaction term. Each response model has nine points of the simulation, so there are three degrees of freedom left after model fitting. The resulting degrees of freedom structure is shown in Table 8 below.

**Table 8.** Degrees of freedom for each profile-response RSM model

Source	Degrees of Freedom
Linear Terms	2
Quadratic Terms	2
Interaction Term	1
Error	3
Total	8

It should be noted that the error left, at the end of the above Table 8, is residual error. The residual error is not a measure of pure experimental error because the design points in the simulation matrix are not replicated. It, rather, stands for the approximation error that occurs between the polynomial approximation and the deterministic output of the Moldex3D simulation. Thus, the model adequacy

assessment is to check the capability of the chosen second-order polynomial model to describe the simulation data in the design space tested. A model adequacy matrix was used for the evaluation of the fitted RSM models. This matrix represents the statistical measure that is applied to determine the appropriateness of the response surface models for response interpretation, interpolation and optimisation. Table 9 below shows the evaluation indicators.

**Table 9.** Model evaluation metrics for fitted RSM models

Metric	Definition	Purpose
$R^2$	Proportion of total variation in the response explained by the model	Overall goodness of fit
Adjusted $R^2$ (Adj $R^2$ )	$R^2$ corrected for number of model terms relative to observations	Used to check the model fit reliability after accounting for linear, quadratic and interaction terms
Predicted $R^2$ (Pred $R^2$ )	Estimates the predictive ability of the fitted model within the tested design space	Used to assess the response surface suitability for interpolation and optimisation
Standard error of regression (S)	Shows typical model error in response units	A smaller value relative to response range indicates better practical model accuracy
ANOVA model of significance	Evaluates the fitted model to explain a statistically meaningful portion of response variation	Used as a supporting indicator of model adequacy, not as proof of physical validation
Residual plots	Show if the model errors have systematic patterns	Randomly distributed residuals support the use of fitted model for interpretation

The indicators in Table 9 are used to evaluate the mathematical adequacy of the fitted response surfaces. A good model should have a high  $R^2$ , adjusted  $R^2$  and predictive  $R^2$  and a low standard error of regression, S, compared to the range of the response. Residual plots are also examined to make sure that there are no systematic trends in the fitting errors. The distribution of the residuals can be random and the statistics of the model fit can be good, so that the fitted response surface can be used within the range of the factors tested for interpolation and optimisation. The amount of these indicators of adequacy is not experimental validation of the physical moulding process. For the purpose of this study, they only confirm the appropriateness of the polynomial models to represent the Moldex3D simulation responses with reasonable accuracy. The true model-fit values are presented in Chapter 3 when the quality of the eighteen response surface models that were fitted are examined prior to interpreting the response surfaces and optimisation results.

#### 2.7.4. RSM Implementation in JASP

Response surface analysis was performed in JASP, the statistical environment used to fit the RSM models and output the model results. JASP was chosen because it offers the necessary output for regression, ANOVA, residuals, model-fit and response-surface in a uniform statistical workflow [36]. The software has been described in literature as a graphical statistical platform for common statistical analyses, where the analysis procedures are carried out by the existing statistical packages. The simulation results of Moldex3D were created into three distinct data sets: circular conformal cooling channel, elliptical conformal cooling channel and teardrop conformal cooling channel. Each set of data had nine simulation runs, which included the three coolant inlet-temperature levels and three coolant flow-rate levels. The following six response variables ( $T_{avg}$ ,  $T_{max}$ ,  $t_{cool}$ ,  $\Delta P$ ,  $Re_{avg}$ ,  $Warp$ ) were imported along with the two input factors (Tc, Q) for each profile.

Coolant inlet temperature and coolant flow rate were considered as continuous scale variables and used their physical values in the RSM setup. The fitted separate second-order response surface model for each response and each conformal profile led to six fitted response surface models for each conformal profile and eighteen fitted RSM models in total. The results chapter's regression equations, coefficient tables, ANOVA results, model-fit statistics, and residual plots and response surface plots were all captured from the JASP outputs. The regression equations are presented in internally coded units; input factors and the interpretation of the responses are related to the physical parameters of coolant inlet temperature and coolant flow rate. Thus, the values of the coefficients are used to interpret the direction of the factors, the curvature and the interaction behaviour and the operating conditions are still expressed in °C and L/min.

## 2.8. Methodological Scope, Assumptions and Limitations

This study presents a methodology that is based on a controlled comparison of three cross-section profiles of conformal cooling channels using simulation. Analyses are presented for the circular, elliptical and teardrop profiles for the same part geometry, polymer and mould material, conformal channel route and fixed process settings. Thus, the results presented here are valid in the simulation domain chosen and should only be compared as relative results for the defined battery-casing case. The study does not aim to develop a general rule for the cooling channel design for all injection moulding tools, part geometries and polymers. The entire workflow was carried out using three primary software. The geometry of the part, the mould and cooling channels were generated by SolidWorks. The injection moulding, cooling and warpage simulation was done using Moldex3D and the thermal, hydraulic and dimensional response variables were extracted. All response surface models were fitted using JASP, and model adequacy and statistical outputs for the responses were obtained and used for their interpretation. The functions of the different software are summarised in Table 10.

**Table 10.** Software tools used in the methodological workflow

Software	Role in Methodology	Main Outputs used in the Study
SolidWorks	CAD modelling of part and Cooling - channel profiles	Part geometry, circular, elliptical, teardrop channel geometry
Moldex3D	Injection Moulding, Cooling and Warpage Simulation	$T_{avg}$ , $T_{max}$ , $t_{cool}$ , $Re_{avg}$ , $\Delta P$ , $Warp$
JASP	Response surface modelling and statistical evaluation	RSM equations, coefficient tables, ANOVA, residual plots, model-fit statistics and response surface plots

It is made sure that the Moldex3D material data, process settings and cooling channel boundary conditions are consistent to compare the three profiles. The same simulation setup is used for all the cases in this study, so the relative differences between the profiles are of primary interest. The results are thus interpreted as comparative predictions and not experimentally measured production values, but based on the simulations. Physical moulding trials can add to the variation resulting from machine behaviour, sensor accuracy, coolant supply stability, actual variation of material batches, condition of the tool surface and manufacturing tolerances. The RSM models are also limited by the selected design space. The models were only fitted for coolant inlet temperatures of 15°C, 25°C and 35°C, and coolant flow rates of 2, 5 and 10 L/min, and the response surfaces are used for interpretation within these ranges. The optimiser values are operating conditions predicted by the RSM and are not extra Moldex3D runs.

The manufacturability of the non-circular internal channels is outside the main scope of this methodology. While the simulation is created using the internal channel geometry designed, actual manufactured inserts could be constrained by the limitations of additive-manufacturing, internal surface roughness, powder removal, minimum channel feature size, overhangs and post-processing access. This is significant as recent research has demonstrated that the surface roughness of conformal cooling channels can affect the channel's coolant pressure, Reynolds number and flow velocity; and research on self-supporting conformal channels has indicated that manufacturability may affect the choice of channel shape for injection moulding toolings that are non-circular. The straight-line cooling channel is given just as a reference baseline. It serves to put the overall thermal impact of conformal routing at equal coolant conditions into perspective. The circular, elliptical and teardrop conformal profiles are the main ones that are compared in terms of methodology. In general, the methodology offers a structured and repeatable approach to reveal profile-level trends, trade-offs and RSM predicted operating regions. Additional tasks involve confirmation simulations at the predicted optimum points, experimental measurement of the coolant pressure and physical validation of the parts quality [37].

## **2.9. Chapter Summary**

This chapter presented the methodology used to compare circular, elliptical and teardrop conformal cooling channel profiles. The study was conducted as a controlled simulation-based comparison with the same part geometry, mould material, polymer material, conformal channel route and the same injection moulding process parameters. The variables of the main interest were the profile of the cooling channel, the flow rate of the coolant and the inlet coolant temperature. The conformal cooling simulation matrix comprised of 27 runs with three different channel profiles, three different flow rates (2, 5 and 10 L/min), and three different coolant inlet temperatures (15, 25 and 35 °C), while three straight-line cooling simulations were performed at 5 L/min, at 15 °C, 25 °C and 35 °C as a reference. The geometry of the moulded part was a simplified geometry based on a battery casing, the virtual mould was designed as a P20 steel insert. The circular, elliptical and teardrop cooling channels were modelled in SolidWorks with approximately equal cross-sectional areas to ensure comparable nominal coolant flow capacity. The profiles chosen were the circular as the reference and the elliptical as well as the teardrop as modified non-circular profiles. All conformal channels were located on the same route with a constant standoff of 15 mm, so that the focus of the comparison was on the cross-sectional geometry of the channel. Injection moulding, cooling and warpage simulation was done using Moldex3D. A mesh convergence study was carried out, and a seeding size of 4.5 mm with 300,001 elements was chosen as it yielded stable cooling-time results at a lower computational cost. The main responses evaluated were average part temperature, maximum part temperature, time to reach ejection temperature, coolant pressure drop, average Reynolds number and warpage displacement. The hydraulic diameter, mean coolant velocity and Reynolds number were used for thermofluid characterisation. Differences in hydraulic behaviour were primarily related to wetted perimeter, hydraulic diameter and local flow effects, since the channel areas were similar. Finally, response surface methodology analysis was performed using JASP to obtain 18 second-order RSM models for each of the three profiles, in order to compare the thermal, hydraulic and dimensional performance of the three profiles.

### 3. Results and Discussion

This chapter discusses the results and discussion of the Moldex3D simulation matrix created in Chapter 2 to be used for the comparative evaluation of the cross-section profiles of conformal cooling channels. In this simulation matrix, there are 27 conformal cooling channel runs, and 3 straight-line baseline runs as described in the simulation framework. There are three cross-section profiles (circular, elliptical and teardrop profiles), and three coolant flow rates (2, 5 and 10 L/min) and three coolant inlet temperatures (15, 25 and 35°C) considered in the conformal cooling simulations. The straight-line baseline simulations are used to assess the thermal benefit of conformal cooling. Six response variables are obtained within each simulation: average part temperature ( $T_{avg}$ ), maximum part temperature ( $T_{max}$ ), time to reach ejection temperature ( $t_{cool}$ ), coolant pressure drop ( $\Delta P$ ), volume-averaged Reynolds number ( $Re_{avg}$ ) and total warpage displacement ( $Warp$ ). Then, each conformal profile and each response is analysed using response surface methodology RSM, resulting in 18 second-order models fitted to each response. Coolant flow rate ( $Q$ ) and coolant inlet temperature ( $T_c$ ) are continuous scale factors in the final RSM analysis, and the response surfaces are presented in terms of engineering units for the tested operating space. Firstly, the raw simulation response data is presented, followed by a discussion on model adequacy, thermal behaviour, hydraulic behaviour, factor effects, multi-response optimisation, cross-profile comparison and comparison with the straight-line baseline [27]. All the RSM JASP results, as per profiles, are added in Appendix 5, 6 and 7, for circular, elliptical and teardrop profiles respectively.

#### 3.1. Simulation Response Data

The entire set of simulation response data for the twenty-seven runs of the conformal cooling channel is presented in the following Table 11. A channel profile abbreviation, the coolant flow rate and the coolant inlet temperature are used to identify each run. In the case of CL-5-25, CL indicates the circular conformal cooling channel, 5 is the flow rate of the coolant in L/min, and 25 is the inlet temperature of the coolant in °C. The run-identification structure enables comparison of the influence of profile geometry, coolant flow rate and coolant temperature consistently throughout the complete simulation matrix. Comparative simulation studies are typical when performing conformal cooling research to assess cooling performance, cycle-time behaviour and thermal performance prior to physical mould manufacturing, particularly in the case of additively manufactured cooling channels.

Six response variables ( $T_{avg}$ ,  $T_{max}$ ,  $t_{cool}$ ,  $\Delta P$ ,  $Re_{avg}$  and  $Warp$ ) are obtained from Moldex3D.  $T_{avg}$  is the average part temperature at the end of the defined cooling stage and  $T_{max}$  is the maximum part temperature at the same cooling stage. Both of these thermal responses are used in conjunction with each other as  $T_{avg}$  gives the general thermal response of the part while  $T_{max}$  represents the localised hot-spot behaviour. The response  $t_{cool}$  is the time it takes to cool the hottest area of the part to the chosen ejection temperature and is therefore directly related to the cooling stage time and the potential for cycle time. The pressure drop of the coolant  $\Delta P$  is a measure of the hydraulic resistance of the cooling circuit, and  $Re_{avg}$  is a flow-regime indicator. Finally,  $Warp$  is the total warpage displacement after cooling and ejection and is used as the dimensional-quality response. These variables give a thermal, hydraulic and dimensional overall assessment of the three conformal cooling channel profiles. Full raw simulation response tables, as per profile, along with input process parameters are given in Appendix 4.

**Table 11.** Full Simulation Run Data from Moldex3D and additional 3 Straight cooling channel baseline runs

Run ID	Q (L/min)	Tc (°C)	$T_{avg}$ (°C)	$T_{max}$ (°C)	$t_{cool}$ (s)	$\Delta P$ (kPa)	$Re_{avg}$	Warp (mm)
CL-2-15	2	15	48.881	128.701	95.199	4	2955.952	0.743
CL-2-25	2	25	55.724	132.233	98.544	4	3508.093	0.76
CL-2-35	2	35	61.412	135.448	102.51	3	4075.821	0.773
CL-5-15	5	15	36.299	123.457	89.586	19	6377.085	0.716
CL-5-25	5	25	44.076	127.405	93.978	18	8015.47	0.735
CL-5-35	5	35	52.051	131.531	98.525	17	9808.318	0.754
CL-10-15	10	15	31.119	121.552	86.922	64	12490	0.71
CL-10-25	10	25	39.754	125.856	92.104	62	15930	0.73
CL-10-35	10	35	48.526	130.268	97.227	61	19550	0.749
EL-2-15	2	15	47.894	128.008	95.773	4	2748.41	0.741
EL-2-25	2	25	54.28	131.376	99.149	4	3257.195	0.756
EL-2-35	2	35	60.726	134.765	103.18	3	3799.826	0.772
EL-5-15	5	15	36.016	123.263	89.663	18	6005.583	0.717
EL-5-25	5	25	43.934	127.336	95.62	17	7523.249	0.736
EL-5-35	5	35	51.795	131.334	99.784	16	9165.332	0.754
EL-10-15	10	15	31.026	121.405	87.506	61	11740	0.709
EL-10-25	10	25	39.81	125.745	93.914	59	14920	0.728
EL-10-35	10	35	48.326	130.013	98.931	58	18240	0.748
TD-2-15	2	15	48.494	120.788	91.325	4	2645.312	0.75
TD-2-25	2	25	54.791	124.416	94.902	4	3135.234	0.765
TD-2-35	2	35	61.237	128.201	100.35	3	3656.934	0.781
TD-5-15	5	15	36.061	115.626	86.358	19	5915.928	0.725
TD-5-25	5	25	43.934	120.224	91.23	18	7179.421	0.744
TD-5-35	5	35	51.903	124.793	95.639	17	8790.302	0.762
TD-10-15	10	15	31.004	113.717	84.349	66	11260	0.715
TD-10-25	10	25	39.7	118.605	89.707	64	14330	0.735
TD-10-35	10	35	48.434	123.514	94.51	63	17540	0.755
SL-5-15	5	15	82.434	144.250	167.06	0.873	5456.52	0.764
SL-5-25	5	25	87.475	146.951	180.73	0.775	6787.79	0.780
SL-5-35	5	35	92.623	149.786	203.43	0.693	8287.00	0.801

A number of general trends can be observed in the raw data before incorporation of any parameter model. In all three conformal profiles,  $T_{avg}$ ,  $T_{max}$ , and  $t_{cool}$  decreases steadily with increasing flow rate, and  $\Delta P$  and  $Re_{avg}$  increase with flow rate. This shows a thermal-hydraulic tradeoff. A rise in the temperature of coolant increases  $T_{avg}$ ,  $T_{max}$  and  $t_{cool}$  in all profiles and at all flow rates, which is consistent with the decrease in thermal driving force between the coolant and mould wall. The teardrop application of the profile results in significantly lower values of  $T_{max}$  than the circular and elliptical at all equivalent operating conditions, which is a pattern also quantified in the cross-profile comparison.

### 3.2. RSM Model Adequacy and Validation

The simulation response data from Table 11 was analysed by the response surface methodology (RSM) introduced in Chapter 2. Each conformal cooling channel profile was associated with a different second-order response surface model. A total of eighteen RSM models were obtained as three conformal profiles, and six response variables were analysed. Coolant flow rate ( $Q$ ) and coolant inlet temperature ( $T_c$ ) were both continuous scale factors and were used as such in the final analysis. Thus, flow-rate levels were set to 2, 5 and 10 L/min, and the coolant inlet temperature levels were set to 15, 25 and 35°C, respectively. This enabled the fitted response surfaces to be representative of the actual physical spacing of the process variables tested, particularly the coolant flow rate, which did not have a uniform interval between the tested response levels. Prior to the analysis of the factor effects, response surfaces and optimisation results, it is important to check if the fitted models are able to capture the Moldex3D simulation results. The coefficient of determination ( $R^2$ ), adjusted coefficient of determination (adj  $R^2$ ), predictive coefficient of determination (pred  $R^2$ ) and standard error of the regression ( $S$ ) were used to assess model adequacy. These indicators provide information on the reliability of the fitted response surface for interpolation and optimisation in the tested design space.

#### 3.2.1. Coefficient of Determination and Predictive Fit

The model-fit statistics of the eighteen final RSM models based on the scales are given in the following Table 12. The coefficient of determination ( $R^2$ ) is the value proportional of the response variation accounted for by the fitted model. The adjusted coefficient of determination (adj  $R^2$ ) is a measure that takes into account the number of terms that are being fit in the model, and checks if the fitted model remains strong after including linear, quadratic and interaction terms. The expected predictive ability of the model in the tested factor range is evaluated using the predictive coefficient of determination (pred  $R^2$ ). The standard error of regression ( $S$ ) is the typical error of prediction in the original response unit, e.g. °C, seconds, kPa or millimetres.

**Table 12.** RSM Model Fit Statistics

Profile	Response	$R^2$	Adj $R^2$	Pred $R^2$	$S$
Circular	$T_{avg}$	0.999	0.997	0.988	0.525 °C
Circular	$T_{max}$	0.999	0.998	0.99	0.214 °C
Circular	$t_{cool}$	0.999	0.998	0.992	0.203 s
Circular	$\Delta P$	1	1	0.999	0.343 kPa
Circular	$Re_{avg}$	1	1	1	40.43
Circular	$Warp$	0.997	0.993	0.972	0.002 mm
Elliptical	$T_{avg}$	0.999	0.998	0.991	0.423 °C
Elliptical	$T_{max}$	0.999	0.998	0.99	0.205 °C
Elliptical	$t_{cool}$	0.995	0.986	0.947	0.592 s
Elliptical	$\Delta P$	1	1	0.999	0.343 kPa
Elliptical	$Re_{avg}$	1	1	1	28.75
Elliptical	$Warp$	0.999	0.997	0.988	0.001 mm
Teardrop	$T_{avg}$	0.999	0.998	0.991	0.443 °C

Profile	Response	R <sup>2</sup>	Adj R <sup>2</sup>	Pred R <sup>2</sup>	S
Teardrop	$T_{max}$	0.999	0.996	0.984	0.286 °C
Teardrop	$t_{cool}$	0.997	0.991	0.967	0.462 s
Teardrop	$\Delta P$	1	1	0.999	0.343 kPa
Teardrop	$Re_{avg}$	1	1	1	65.15
Teardrop	$Warp$	0.999	0.998	0.992	0.000928 mm

Table 12 indicates that all eighteen fitted models of response surface have good adequacy within the investigated simulation domain. The R<sup>2</sup> values are between 0.995 and 1.000, which means the second-order models account for nearly all the variation in the response in the Moldex3D data. The goodness of fit of the adjusted R<sup>2</sup> values is close to the goodness of fit of the R<sup>2</sup> values, which indicates that the terms used in the model have not been used to inflate their fit. The range of the predictive R<sup>2</sup> values is 0.947 to 1.000, which reflects acceptable predictive capability of the models for interpolation in the range selected. The least successful predictive model is the elliptical  $t_{cool}$  response, which has pred R<sup>2</sup>=0.947. This however is still well above the commonly accepted minimum value for predictive adequacy of 0.80. The pressure-drop and Reynolds-number models are found to be in nearly perfect agreement since these responses are largely dominated by systematic hydraulic relationships with coolant flow rate and coolant temperature. The thermal-response models also exhibit high fit quality with a prediction error of less than 0.6 s for  $t_{cool}$  and less than 0.6°C for the temperature responses. Thus, the developed RSM models are deemed to be adequate for interpretation of the responses, surface plotting and multi-response optimisation. The results of these model adequacy checks are considered to be a validation of the fitted response surfaces with the deterministic simulation data, rather than an experimental validation of the physical moulding process. The study is not accompanied by physical moulding trials or confirmation simulations at the points predicted by the optimiser, so the models of the RSM are used as an interpolation and optimisation tool within the tested simulation space. Hence, the latter optimum values are shown as the RSM-predicted operating conditions.

### 3.2.2. Residual Diagnostics

The ANOVA results also confirm the models of the fitted response surfaces are adequate. The overall second-order models are statistically significant for all 3 conformal cooling profiles and all 6 responses within the deterministic simulation data set. This validates that the model structure chosen can capture the main tendency of the responses as the coolant flow rate and coolant inlet temperature change. For the hydraulic responses, the most evident and systematic effects are found for the coolant flow rate with respect to the hydraulic responses. This is to be expected since the higher the flow rate, the more velocity the coolant will have, leading to a higher Reynolds number and higher hydraulic resistance of the cooling circuit. Both coolant inlet temperature and coolant flow rate affect the fitted response surfaces for the thermal responses, but in different ways. The thermal driving force between the heated polymer/mould region and the coolant is mainly controlled by the coolant inlet temperature and the convective removal capacity of the cooling channel is controlled by the coolant flow rate. The quadratic flow-rate terms in the thermal and hydraulic models are significant and indicate a non-linear relationship between flow rate and its effect. Specifically, the thermal gain due to the increased flow rate diminishes with an increase in flow rate, and the pressure-drop penalty escalates rapidly.

This favours the later optimisation result as the preferred operating region is not the highest tested flow rate, but one with a moderate flow rate.

The residual plots also were checked to determine if the fitted models exhibit systematic error patterns. For all the response models, the range of the residuals is small relative to the total range of the response, and there are no large unexplained deviations. The pressure-drop and Reynolds-number models, in particular, exhibit very regular behaviour, as these responses are primarily determined by the predictable hydraulic relationships. The thermal-response models exhibit somewhat greater residuals, particularly for cooling time, although the magnitude of the residuals is considered acceptable for the purposes of interpolation within the factor space tested. So, the RSM models fitted are deemed to be appropriate for the interpretation of the responses and for multi-response optimisation. The results of adequacy however, should be viewed in the context of the study. The ANOVA and residual statistics are used to check the validity of the fitted response surfaces with the Moldex3D simulation data, but not with the experimental data from the moulding process. No experimental moulding trials were conducted at the optimiser-predicted points within the tested simulation domain, so the RSM optimums presented later in this chapter are considered as predicted operating conditions within the tested simulation domain.

### **3.3. Effect of Process Parameters on Thermal Responses**

The thermal response analysis is done to assess the effect of coolant flow rate, coolant inlet temperature and cross-section profile of the channel on the temperature state and cooling-time behaviour of the moulded part. Three different thermal responses are considered: average part temperature ( $T_{avg}$ ), maximum part temperature ( $T_{max}$ ) and time to reach ejection temperature ( $t_{cool}$ ). These responses are various measures of cooling performance. The average part temperature is an indication of the overall thermal level of the moulded part at the end of the defined cooling stage, and the maximum part temperature is indicative of localised hot-spot behaviour. Cooling time response is a measure of the time the hottest area takes to reach the desired ejection temperature and thus is directly related to potential cycle time savings. The cycle time, warpage and thermal response are also examined as they are all directly related to the productivity and quality of the injection-moulding process and are evaluated in similar conformal-cooling studies [27, 35]. For the present simulation results, profile geometry is not a significant factor for the thermal responses as compared to coolant inlet temperature and coolant flow rate for average part temperature. But if localised thermal behaviour is taken into account, then profile geometry becomes more significant. This difference is significant because  $T_{avg}$  is an indicator of the overall cooling status of the part, while  $T_{max}$  and  $t_{cool}$  are more indicative of the local hot spots and heat removal effectiveness near the critical areas. Hence, the three thermal responses are discussed separately in the following subsections.

#### **3.3.1. Average part Temperature ( $T_{avg}$ )**

$T_{avg}$  represents the average temperature of the moulded part at the end of the specified cooling phase. It is used as a general indicator of the overall thermal state of the part, after the same cooling time has been applied for all the simulation cases. The smaller the  $T_{avg}$ , the more heat that has been extracted from the polymer during the known cooling window. Hence, this response would be beneficial to compare the bulk cooling performance of the circular, elliptical and teardrop conformal cooling channel profiles for a range of coolant inlet temperatures and flow rates.  $T_{avg}$  should however, be considered as a response of the overall thermal response as it is not a good indicator of the presence

of localised high-temperature areas, which are better represented by  $T_{max}$  and  $t_{cool}$ . The response surface plots of  $T_{avg}$  are presented in Fig. 9.

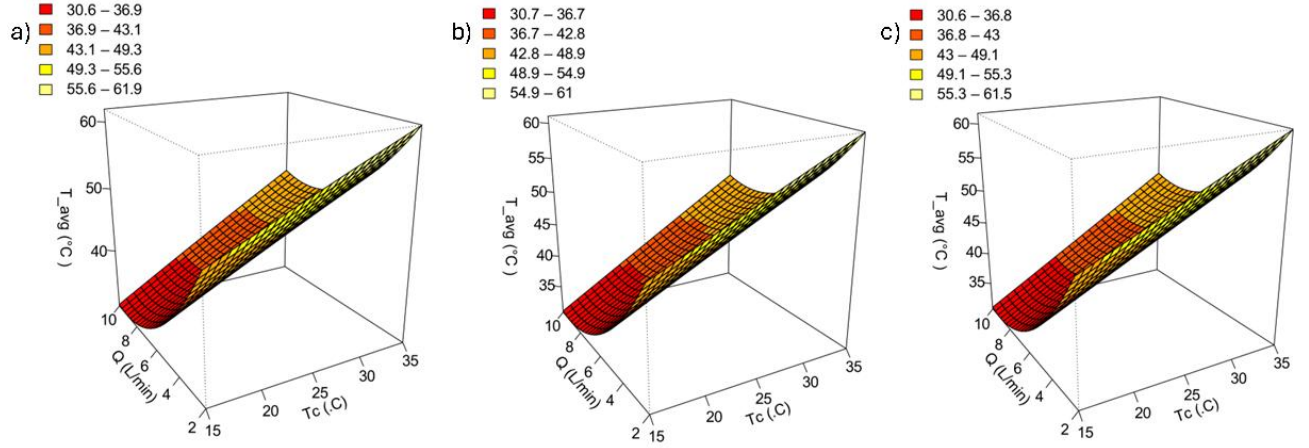


**Fig. 9.** RSM response surface plots for Average part temperature ( $T_{avg}$ ) as a function of flow rate and coolant temperature: a) circular profile, b) elliptical profile, c) teardrop profile

The response surfaces in Fig. 9 are mathematically represented by the fitted RSM equations. They are used to determine the contribution of each input factor to the average part temperature prediction, and to aid in the subsequent profile comparison. The linear terms reflect the primary direction of the change, and the quadratic and interaction terms reveal if the response changes nonlinearly over the operating conditions examined. So, the equations are useful in converting the surface plots to provide a more meaningful numerical interpretation of the  $T_{avg}$  response. The fitted RSM equations for  $T_{avg}$  in coded units are:

For Circular Profile:

$$T_{avgCL} = 41.933 + 7.712A - 7.770B - 0.137A^2 + 5.728B^2 + 1.162AB \quad (5)$$

For Elliptical Profile:

$$T_{avgEL} = 41.794 + 7.741A - 7.290B - 0.044A^2 + 5.246B^2 + 1.065AB \quad (6)$$

For Teardrop Profile:

$$T_{avgTD} = 41.697 + 7.762A - 7.564B + 0.047A^2 + 5.548B^2 + 1.117AB \quad (7)$$

Where  $A$  represents the coded variable corresponding to coolant inlet temperature ( $T_c$ ), and  $B$  represents the coded variable corresponding to coolant flow rate ( $Q$ ) in the internally coded RSM model. Therefore,  $A$  and  $B$  should not be substituted using the direct physical values of  $T_c$  and  $Q$ .

The three equations exhibit the same general response behaviour. In all profiles, the coefficient of the coolant inlet temperature is positive, that is, the higher the  $T_c$ , the higher the  $T_{avg}$ . For all profiles, the flow rate of the coolant has a negative coefficient, which means that an increase in  $Q$  decreases  $T_{avg}$ . Both variables have linear coefficients of similar magnitude, suggesting that the average part temperature is dependent upon both the coolant temperature and flow rate. The positive  $B^2$  coefficients indicate that the effect of flow rate on  $T_{avg}$  is diminishing returns: the higher the flow rate,

the less improvement in  $T_{avg}$ . This also applies to the raw Moldex3D data. For the circular profile at  $T_c=25^\circ\text{C}$ ,  $T_{avg}$  decreases from  $55.724^\circ\text{C}$  at 2 L/min to  $44.076^\circ\text{C}$  at 5 L/min, and then to  $39.754^\circ\text{C}$  at 10 L/min. The maximum cooling improvement ( $11.648^\circ\text{C}$ ) is obtained when the flow is increased from low to medium, and the smallest cooling improvement ( $4.322^\circ\text{C}$ ) is obtained when the flow is increased from medium to high. The same response pattern is observed in the elliptical and teardrop profiles (Table 12). The effect of the coolant inlet temperature is more straightforward. In the three profiles,  $T_{avg}$  always increases as  $T_c$  increases at a given flow rate. For example, in the circular profile at 5 L/min,  $T_{avg}$  increases from  $36.299^\circ\text{C}$ , at  $T_c=15^\circ\text{C}$ , to  $44.076^\circ\text{C}$ , at  $T_c=25^\circ\text{C}$ , and to  $52.051^\circ\text{C}$ , at  $T_c=35^\circ\text{C}$ . This is to ensure that the thermal driving force for heat removal is greater for a lower coolant inlet temperature and thus results in a lower average part temperature. The basic observation, that the three channel profiles generate the same mean part temperature at all conditions in the experimental domain, can be verified by a direct comparison of  $T_{avg}$  across all three profiles at the same conditions, as presented in the following Table 13.

**Table 13.**  $T_{avg}$  comparison across all three profiles at all operating conditions

Q (L/min)	$T_c$ ( $^\circ\text{C}$ )	CL $T_{avg}$ ( $^\circ\text{C}$ )	EL $T_{avg}$ ( $^\circ\text{C}$ )	TD $T_{avg}$ ( $^\circ\text{C}$ )	Max difference ( $^\circ\text{C}$ )
2	15	48.881	47.894	48.494	0.987
2	25	55.724	54.28	54.791	1.444
2	35	61.412	60.726	61.237	0.686
5	15	36.299	36.016	36.061	0.283
5	25	44.076	43.934	43.934	0.142
5	35	52.051	51.795	51.903	0.256
10	15	31.119	31.026	31.004	0.115
10	25	39.754	39.81	39.7	0.110
10	35	48.526	48.326	48.434	0.200

The above table indicates that the part temperature average is only slightly influenced by the cross-section profile. The maximum difference between profiles is  $1.444^\circ\text{C}$  at 2 L/min, and  $T_c=25^\circ\text{C}$ , and  $0.283^\circ\text{C}$  or less at 5 and 10 L/min. Thus, the main control of  $T_{avg}$  is the coolant flow rate and coolant inlet temperature, with the cross-section profile having a secondary effect on the average thermal response. This indicates that the geometry of a profile is not the primary distinguishing feature for the bulk part temperature; it has a more significant effect later in the local maximum temperature and cooling-time responses.

### 3.3.2. Maximum Part temperature ( $T_{max}$ )

Maximum part temperature ( $T_{max}$ ) is the temperature, at a point within the part, which is highest at the end of the specified cooling period.  $T_{max}$  is more sensitive to the behaviour of local hot-spots and thus would better indicate the effectiveness of cooling in the most critical part region, although  $T_{avg}$  could be used to describe the overall thermal condition of the part. This response is significant as locally elevated temperatures may cause a delay in solidification, extend the cooling time, and contribute to non-uniform shrinkage after ejection.  $T_{max}$ , therefore, provides very valuable information in determining if a cooling-channel profile can adequately cool the slowest-cooled area of a part. It is one of the most critical indicators of thermal conditions in this study, as the prime advantage of profile modification is anticipated to be presented in the local heat removal instead of

merely the average part temperature. Response surface plots for  $T_{max}$  are shown in the following Fig. 10.

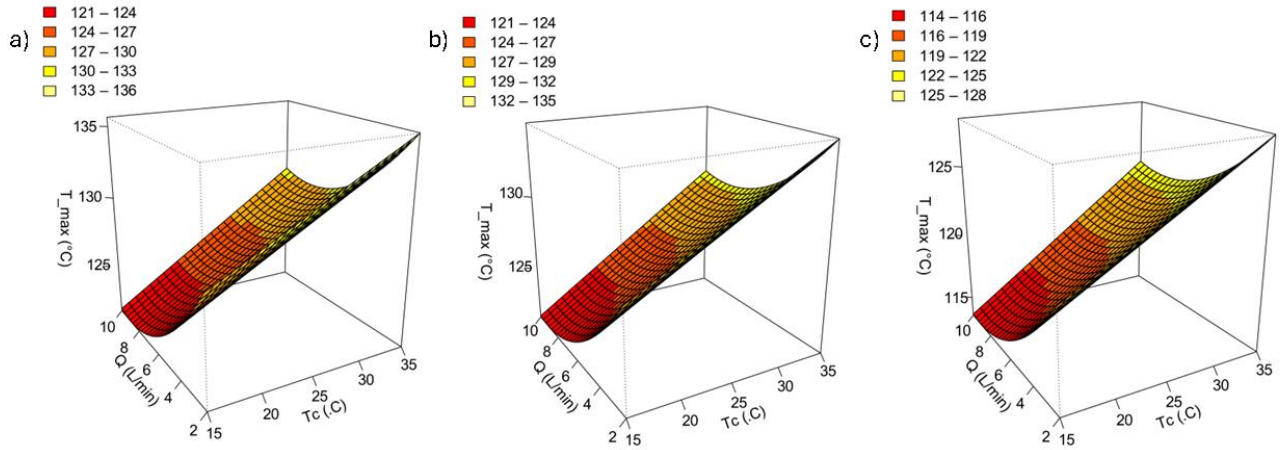


**Fig. 10.** RSM response surface plots for Maximum part temperature ( $T_{max}$ ) as a function of flow rate and coolant temperature: a) Circular Profile, b) Elliptical Profile, c) Teardrop Profile

As seen in the surface plot in Fig. 10, decreasing the coolant inlet temperature and increasing the flow rate of coolant decreases the  $T_{max}$ . But the most pronounced difference is not just the trend with the process conditions, but also the relative placement of the response surfaces. The teardrop profile is still significantly lower than the circular and elliptical profiles in the operating space tested, suggesting a definite improvement in local hot-spot cooling. The circular and elliptical profiles have very similar response surfaces and are very close throughout the range tested. The equations that were fitted give the mathematical form of the  $T_{max}$  response surfaces in Fig. 10. The use of these is to quantify the effect on the predicted maximum part temperature of the coolant inlet temperature, coolant flow rate, and shape of the profile. The fitted RSM equations for  $T_{max}$  per profile are:

For Circular Profile:

$$T_{maxCL} = 126.533 + 3.962A - 3.118B - 0.005A^2 + 2.480B^2 + 0.468AB \quad (8)$$

For Elliptical Profile:

$$T_{maxEL} = 126.487 + 3.942A - 2.831B - 0.021A^2 + 2.079B^2 + 0.437AB \quad (9)$$

For Teardrop Profile:

$$T_{maxTD} = 119.329 + 4.443A - 2.928B + 0.025A^2 + 2.195B^2 + 0.561AB \quad (10)$$

Where  $A$  represents the coded variable corresponding to coolant inlet temperature ( $T_c$ ), and  $B$  represents the coded variable corresponding to coolant flow rate ( $Q$ ) in the internally coded RSM model.

All three equations have a positive coefficient of  $A$ , indicating that the greater the coolant inlet temperature, the greater the  $T_{max}$ . The coefficient of  $B$  is negative, and this indicates that an increase in the flow rate of coolant results in a decrease in the value of  $T_{max}$ . The positive  $B^2$  The effects of flow rate are non-linear, meaning that the decrease in  $T_{max}$  is smaller at high flow rates. The intercept

value is the most significant difference with respect to profile. The teardrop profile has a much lower intercept than the circular and elliptical profiles, which indicates that the  $T_{max}$  response is shifted down through the entire process space. This behaviour is also confirmed by the raw Moldex3D simulation results. In the case of the circular profile, the increase of the flow rate from 2 to 10 L/min at  $T_c=15^\circ\text{C}$ , the  $T_{max}$  decreases from  $128.701^\circ\text{C}$  to  $121.552^\circ\text{C}$ . This is true of the other profiles as well, but the teardrop profile is always able to keep the maximum temperature down. At 10 L/min and  $15^\circ\text{C}$ , for instance, the teardrop profile results in  $T_{max}=113.717^\circ\text{C}$  whereas the circular profile results in  $T_{max}=121.552^\circ\text{C}$ , and the elliptical profile in  $T_{max}=121.405^\circ\text{C}$ . This validates the teardrop profile's benefit of local hot-spot cooling, and not just a slight change in the bulk part temperature. The following Table 14 compares the  $T_{max}$  across all three profiles.

**Table 14.**  $T_{max}$  comparison across conformal cooling channel profiles

Q (L/min)	Tc (°C)	CL $T_{max}$ (°C)	EL $T_{max}$ (°C)	TD $T_{max}$ (°C)	TD advantage vs CL (°C)
2	15	<b>128.701</b>	<b>128.008</b>	120.788	7.913
2	25	<b>132.233</b>	<b>131.376</b>	<b>124.416</b>	7.817
2	35	<b>135.448</b>	<b>134.765</b>	<b>128.201</b>	7.247
5	15	<b>123.457</b>	<b>123.263</b>	115.626	7.831
5	25	<b>127.405</b>	<b>127.336</b>	120.224	7.181
5	35	<b>131.531</b>	<b>131.334</b>	<b>124.793</b>	6.738
10	15	121.552	121.405	113.717	7.835
10	25	<b>125.856</b>	<b>125.745</b>	118.605	7.251
10	35	<b>130.268</b>	<b>130.013</b>	<b>123.514</b>	6.754

Note: values above the part freeze temperature of  $122.93^\circ\text{C}$  are marked in bold

As shown in Table 14, the teardrop profile is able to decrease  $T_{max}$  for all matched operating points. The advantage compared to the circular profile is between  $6.738^\circ\text{C}$  and  $7.913^\circ\text{C}$  and the elliptical profile is very close to the circular profile. This is a good indication that the influence of the profile geometry on  $T_{max}$  is far more significant than for  $T_{avg}$ . The primary thermal advantage of the teardrop profile is actually not to change the average part temperature, but to control hot spots. This difference is also evident in the freeze-temperature comparison. The 10 L/min and  $15^\circ\text{C}$  condition is the only condition which is below the PP freeze temperature for the circular and elliptical profiles. The teardrop profile, on the other hand, is under the freeze temp in five instances: TD-2-15, TD-5-15, TD-5-25, TD-10-15 and TD-10-25. That is, the teardrop profile has an acceptable local solidification behaviour in a wider range of operating conditions, such as moderate flow. The  $T_{max}$  response indicates that profile geometry definitely has an impact on the local thermal performance. The circular and elliptical profiles are found to behave in a similar way, but the teardrop profile shows a significant decrease in the maximum part temperature for the process range tested. This is significant as it demonstrates that the teardrop channel is more effective in cooling the most critical area of the part, and this is later reflected in the favourable performance of the channel in the cooling-time and optimisation analysis.

### 3.3.3. Cooling Time ( $t_{cool}$ )

Cooling time ( $t_{cool}$ ) is the time it takes for the hottest point of the moulded part to cool to the ejection temperature, which is selected to be  $102.93^\circ\text{C}$ . It is one of the most critical process responses as it is

directly linked to the cooling stage time and hence to the possible cycle time of the injection moulding process. In the conformal cooling simulations,  $t_{cool}$  ranges from 84.349 s for TD-10-15 to 103.180 s for EL-2-35. The following Fig. 11 shows the response surface plots for  $t_{cool}$ .

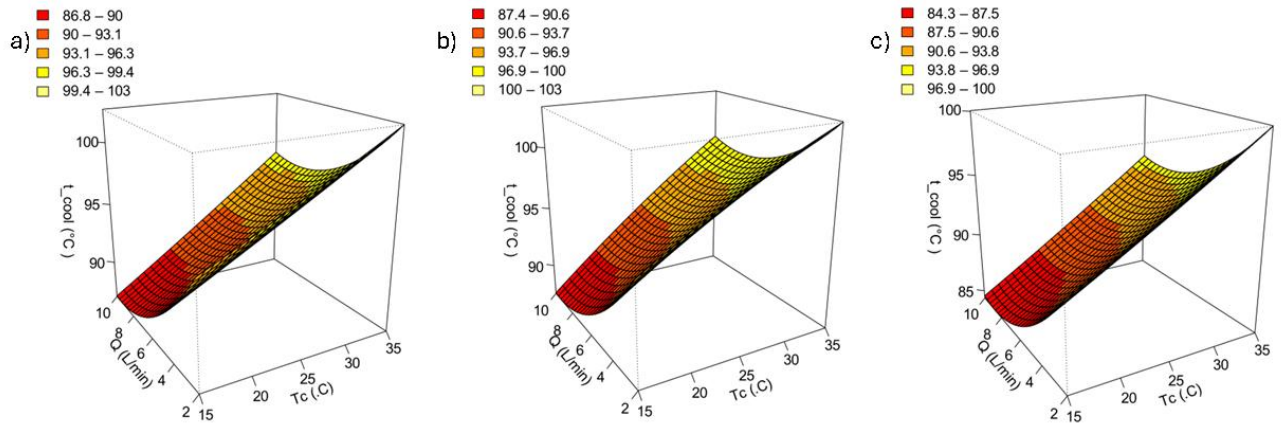


**Fig. 11.** RSM response surface plots for Cooling Time ( $t_{cool}$ ) as a function of flow rate and coolant temperature: a) Circular Profile, b) Elliptical Profile, c) Teardrop Profile

It can be seen from the surface plots in Fig. 11 that as the inlet coolant temperature is decreased and the coolant flow rate is increased, the cooling time is decreased. But the impact of these two variables is not the same. The temperature of the coolant inlet is a significant factor, as it determines the temperature driving force between the hot part region and the coolant. The flow rate also decreases  $t_{cool}$ , but the benefit diminishes at higher flow rates due to a diminishing return of the convective benefit. The mathematical form of the  $t_{cool}$  response surfaces shown in Fig. 11 is given by the fitted equations. They are used to make comparisons of the effect of the operating variables and profile geometry on the predicted cooling time. The fitted RSM equations for  $t_{cool}$  for each profile are:

For Circular Profile:

$$t_{coolCL} = 92.969 + 4.486A - 3.333B + 0.119A^2 + 2.369B^2 + 0.728AB \quad (11)$$

For Elliptical Profile:

$$t_{coolEL} = 94.422 + 4.905A - 2.958B - 0.422A^2 + 2.268B^2 + 0.955AB \quad (12)$$

For Teardrop Profile:

$$t_{coolTD} = 90.084 + 4.769A - 3.002B + 0.142A^2 + 2.345B^2 + 0.291AB \quad (13)$$

Where  $A$  represents the coded variable corresponding to coolant inlet temperature ( $T_c$ ), and  $B$  represents the coded variable corresponding to coolant flow rate ( $Q$ ).

In all three equations, the coefficient of  $A$  is positive, indicating that an increase in coolant inlet temperature will result in an increase in  $t_{cool}$ . The coefficient of  $B$  is negative, indicating that an increase in the flow rate of the coolant will lead to a decrease in  $t_{cool}$ . The  $B^2$  values are positive, indicating that the flow rate effect is nonlinear, that is, the higher the flow rate, the greater the reduction in cooling time, but the reduction is smaller as flow rate increases. The raw data indicate

that coolant inlet temperature's effect is greater than flow rate within the range tested for the circular profile. At  $Q=5$  L/min, increasing  $T_c$  from  $15^\circ\text{C}$  to  $35^\circ\text{C}$  increases  $t_{cool}$  from 89.586 s to 98.525 s, giving an increase of 8.939 s. At  $T_c=25^\circ\text{C}$ , increasing  $Q$  from 2 to 10 L/min reduces  $t_{cool}$  from 98.544 s to 92.104 s, giving a reduction of 6.440 s. This verifies that reducing coolant temperature is more effective on cooling time and increasing flow rate is an added but lesser benefit. Similarly, the diminishing return effect of flow rate is seen in the circular profile at  $T_c=25^\circ\text{C}$  as  $t_{cool}$  decreases from 98.544 s to 93.978 s for an increase in  $Q$  from 2 to 5 L/min, which is a decrease of 4.566 s. The further increase of  $Q$  from 5 to 10 L/min leads to a decrease of  $t_{cool}$  from 93.978 s to 92.104 s, which is only 1.874 s less. Thus, the greatest benefit from the cooling-time perspective is when switching from low flow to medium flow, and the greatest to highest flow offers a lesser benefit. Table 15 below gives a simple comparison of  $t_{cool}$  in all profiles and conditions.

**Table 15.**  $t_{cool}$  comparison across profiles

Q (L/min)	Tc (°C)	CL $t_{cool}$ (s)	EL $t_{cool}$ (s)	TD $t_{cool}$ (s)	TD advantage vs CL (s)
2	15	95.199	95.773	91.325	3.874
2	25	98.544	99.149	94.902	3.642
2	35	102.510	103.180	100.350	2.160
5	15	89.586	89.663	86.358	3.228
5	25	93.978	95.620	91.230	2.748
5	35	98.525	99.784	95.639	2.886
10	15	86.922	87.506	84.349	2.573
10	25	92.104	93.914	89.707	2.397
10	35	97.227	98.931	94.510	2.717

This indicates that the teardrop profile is the shortest cooling time at each matched operating condition. The teardrop advantage over the circular profile is between 2.160 s and 3.874 s. TD-10-15 achieves the shortest cooling time in the complete conformal data set,  $t_{cool}=84.349$  s. For the moderate flow rate of 5 L/min and  $15^\circ\text{C}$ , the teardrop profile results in  $t_{cool}=86.358$  s, while the circular profile results in  $t_{cool}=89.586$  s and the elliptical profile results in  $t_{cool}=89.663$  s. This validates the fact that the teardrop profile results in a uniform cooling-time reduction over the design space investigated. This decrease in cooling time is directly related to the  $T_{max}$  behaviour mentioned in Section 3.3.2. Note that the teardrop profile has a more effective reduction of the local hot-spot temperature, which means that the hottest region has a smaller thermal distance to traverse in order to attain the ejection temperature. Hence, the teardrop profile is able to reach the ejection condition earlier than the circular and elliptical profiles. This reduction in absolute time may not seem significant, but in high-volume production, this time difference can make a big difference over many moulding cycles.

The results for  $t_{cool}$  overall indicate that the teardrop profile of the cooling-channel influences not only the hot-spot regions, but also the time necessary for the part to reach the ejection condition. For the same geometry and routing arrangement, the circular and elliptical profiles do not demonstrate a significant improvement in cooling-time response when varying from circular to elliptical. However, the teardrop profile is always lower in all the matched cases, showing that its effect is not restricted to just one coolant temperature and flow rate. This behaviour is important because  $t_{cool}$  is controlled by the last region of the part to reach the ejection temperature. Thus, the answer is more dependent on what the most thermally critical area is than on the average part temperature. This is also the reason

for the teardrop profile to present a more pronounced benefit in terms of  $T_{max}$  and  $t_{cool}$ , compared to  $T_{avg}$ . That is, the main contribution of the teardrop profile is not on the bulk temperature of the entire part, but on the severity of local hot-spots, which is the most important factor to consider when determining the time that the critical region reaches the ejection condition. This is important from a process perspective because the cooling phase can't be reduced without risk of harming the part until the hottest region is cool enough. If the average part temperature is low, but there is a local hot spot that is above the ejection condition, then the part may be susceptible to distortion or dimensional instability after ejection. Thus, the results of the teardrop profile reduction of  $t_{cool}$  are more meaningful than simply an average-temperature reduction. It suggests that the teardrop geometry improves the cooling response at the controlling region of the part, which is the region that determines the minimum cooling requirement. This trend is presented graphically in Fig. 12, and it can be seen that the profile ranking in the entire conformal-cooling simulation matrix is stable; the teardrop profile has the shortest cooling time, and the circular and elliptical profiles are found to be close together. This is in agreement with the later optimisation result, which indicates that the teardrop profile has the lowest RSM-predicted cooling time of the three conformal cooling profiles.



**Fig. 12.** Comparison of cooling time ( $t_{cool}$ ) for circular, elliptical and teardrop CCC profiles under matched coolant flow rate and coolant temperature conditions

### 3.4. Effect of Process Parameters on Hydraulic and Dimensional Responses

The hydraulic response analysis is used to analyse the effects of conformal cooling channel profile on the flow behaviour and flow resistance. In this section, two responses, coolant pressure drop ( $\Delta P$ ) and average Reynolds number ( $Re_{avg}$ ), are considered. Pressure drop is an indication of the hydraulic resistance of the cooling channel and is important because higher pressure drop will require greater pumping demand from the cooling system. Reynolds number is used as an indicator of flow regime

and is used to explain the transition or turbulence of the coolant flow. These two responses need to be considered together in conformal cooling systems, since the benefit of increased flow rate can be to increase the cooling, but beyond a certain point, the benefit of increased flow rate may be negligible, while the penalty of increased pressure drop continues to increase. This is a trade-off that needs to be considered when determining a suitable range of Reynolds number values when considering conformal cooling moulds, as excessive values of the Reynolds number can lead to significant increases in pressure drop value without a corresponding increase in cooling value [23]. For the present results, the coolant flow rate is the most important parameter to control  $\Delta P$  and  $Re_{avg}$ , with the coolant inlet temperature having a secondary effect due to its influence on the coolant properties. So, the pressure drop and Reynolds number are analysed separately in the following subsections. The pressure-drop section compares the hydraulic penalty for each profile and flow-rate condition, and the Reynolds-number section describes the flow-regime behaviour.

### 3.4.1. Pressure Drop ( $\Delta P$ )

Coolant pressure drop ( $\Delta P$ ) is the hydraulic resistance of the cooling channel circuit. The lower the pressure drop, the better, as it will lessen the pumping requirements to flow the coolant through the mould. However, pressure drop should be understood in conjunction with thermal performance, as the increase in coolant flow rate can result in better heat removal and also higher hydraulic resistance. Thus, in this study,  $\Delta P$  is considered as the primary hydraulic penalty for each conformal cooling channel profile. The following Fig. 13 shows the response surface plots for coolant pressure drop  $\Delta P$ .

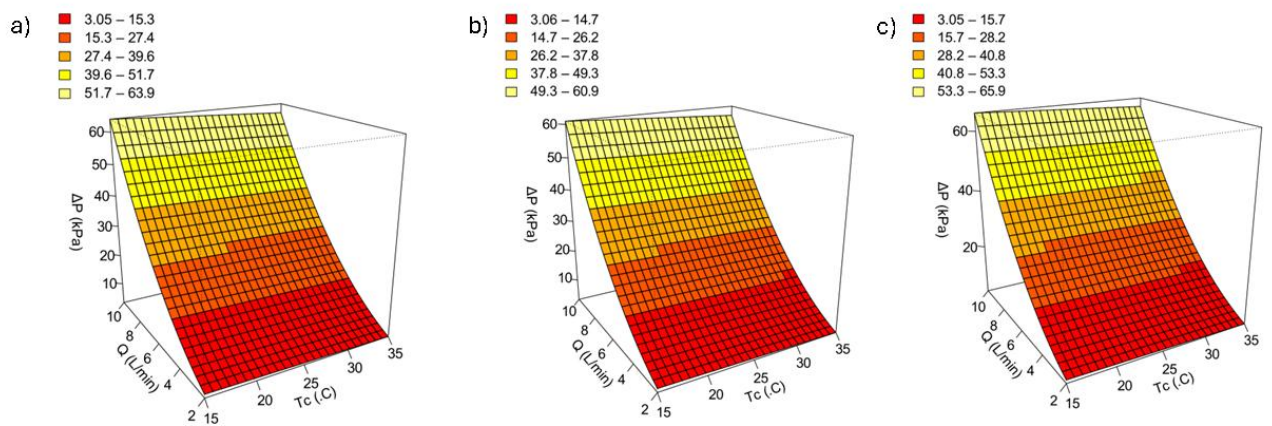


**Fig. 13.** Response surface plots of coolant pressure drop ( $\Delta P$ ) as a function of coolant inlet temperature and coolant flow rate: a) circular profile, b) elliptical profile, and c) teardrop profile

From the surface plots in Fig. 13, the pressure drop is seen to be dependent primarily on the coolant flow rate. For the low flow rate, the pressure drop values of all three profiles are very similar. The more you increase flow rate, the more the difference between the profiles, where the elliptical profile has the lowest pressure drop and the teardrop profile will have the highest pressure drop. The effect of the coolant inlet temperature is smaller than the effect of flow rate, but pressure drop decreases slightly with increasing coolant temperature. The equations for the  $\Delta P$  response surfaces presented in Fig. 13 are presented. They are used to compare the hydraulic responses of the three channel profiles, and to determine the influence of flow rate on the growth of pressure drop. The RSM model fitted equations of  $\Delta P$  for each profile are:

For Circular Profile:

$$\Delta P_{CL} = 24.822 - 1.041A + 29.333B + 8.178B^2 - 0.490AB \quad (14)$$

For Elliptical Profile:

$$\Delta P_{EL} = 23.456 - 1.041A + 27.833B + 8.044B^2 - 0.490AB \quad (15)$$

For Teardrop Profile:

$$\Delta P_{TD} = 25.022 - 1.041A + 30.333B + 8.978B^2 - 0.490AB \quad (16)$$

Where  $A$  represents the coded variable corresponding to coolant inlet temperature ( $T_c$ ), and  $B$  represents the coded variable corresponding to coolant flow rate ( $Q$ ). The  $A^2$  term is not included in the equations as it does not appear in any of the three pressure-drop models.

Pressure-drop models are fitted very well with the RSM outputs, which is characterised by  $R^2=1.000$ , adjusted  $R^2=1.000$  and predictive  $R^2=0.999$  for all three profiles. All three equations contain a strong positive coefficient for  $B$  and thus show that the pressure drop is primarily a function of the flow rate of the coolant. The  $B^2$  coefficients are also positive, indicating that this increase is not proportional. This is an indication that the pressure-drop penalty is much greater for a transition from 5 to 10 L/min than from 2 to 5 L/min. In all three profiles, the coefficient of  $A$  is negative, which means that the pressure drop is slightly decreased with an increase in coolant inlet temperature. This is due to the fact that water viscosity decreases with an increase in temperature, which makes the flow hydraulically less resistant. The comparison of the profiles shows that the elliptical profile has the lowest hydraulic resistance, and the teardrop profile has the highest. At low and medium flow rates, this difference is small, but it is more apparent at 10 L/min, for which the values of the pressure drop are 62 kPa, 59 kPa, and 64 kPa for the circular, elliptical, and teardrop profiles, respectively. So, at this operating condition, the teardrop pressure drop is 5 kPa greater than the elliptical profile and 2 kPa greater than the circular profile. Raw pressure drop values are listed in Table 16.

**Table 16.** Coolant pressure drop ( $\Delta P$ , kPa) across all three channel profiles

Q (L/min)	T <sub>c</sub> (°C)	CL $\Delta P$ (kPa)	EL $\Delta P$ (kPa)	TD $\Delta P$ (kPa)	$\Delta P$ difference (TD-EL, kPa)
2	15	4	4	4	0
2	25	4	4	4	0
2	35	3	3	3	0
5	15	19	18	19	+1
5	25	18	17	18	+1
5	35	17	16	17	+1
10	15	64	61	66	+5
10	25	62	59	64	+5
10	35	61	58	63	+5

The data from above table shows that the influence of the profile on the pressure drop is low for low flow rate and increases for high flow rate. All three profiles have a 3-4 kPa pressure drop range at 2 L/min. The teardrop and the circular profiles are just 1 kPa higher than the elliptical profile, at 5 L/min. The teardrop profile shows a difference of 5 kPa, however, at 10 L/min. This means that the

teardrop profile is hydraulically more disadvantageous and is only apparent during high flow conditions. The pressure-drop results, overall, indicate that the coolant flow rate is the most significant hydraulic variable, with profile geometry being a secondary, but significant, variable. The elliptical profile is the most hydraulically favourable, while at high flows, the teardrop profile causes the greatest pressure drop. But this loss of pressure needs to be balanced by the thermal benefits of the teardrop profile, particularly the reduction in  $T_{max}$  and  $t_{cool}$ . This is discussed later in the multi-response optimisation section.

### 3.4.2. Average Reynolds Number ( $Re_{avg}$ )

The main flow-regime indicator used for the coolant in the conformal cooling channels is the average Reynolds number ( $Re_{avg}$ ). It can be used to show if the flow of the coolant is predominantly laminar, transitional or turbulent in the cooling-channel volume. For this study, the traditional flow-regime classification is used: laminar flow is considered to be for  $Re < \sim 2300$ , transition for  $\sim 2300 < Re < \sim 4000$ , and turbulent for  $Re > \sim 4000$ . The level of coolant mixing and the ability of the coolant to remove heat from the mould wall is dependent on the flow regime, and this interpretation is important. In this current comparison,  $Re_{avg}$  is not considered as an optimisation variable. Instead, it is utilised as a diagnostic hydraulic response whose purpose is to aid understanding of the coolant-flow condition created by each profile and operating point. This is important as a higher Reynolds number does not necessarily indicate better performance overall. Increased  $Re_{avg}$  may signify greater coolant movement and greater turbulence as well as greater pressure-drop penalty. Hence  $Re_{avg}$  is used in conjunction with pressure drops and thermal responses and not on its own. The response surface plots for  $Re_{avg}$  are shown in Fig. 14.

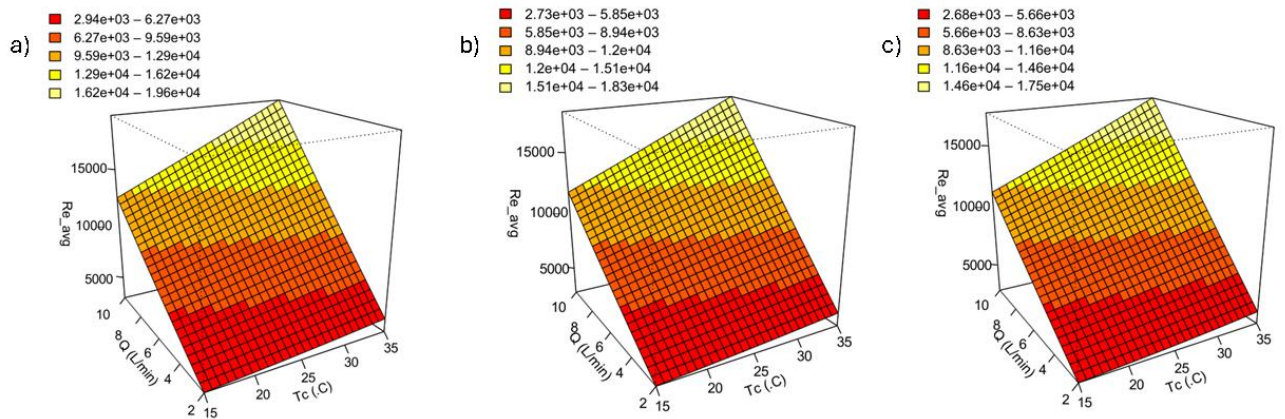


**Fig. 14.** Response surface plots for average Reynolds number ( $Re_{avg}$ ) as a function of coolant inlet temperature and coolant flow rate: a) circular profile, b) elliptical profile, and c) teardrop profile

As seen in the surface plots of Fig. 14,  $Re_{avg}$  is seen to increase significantly with the coolant flow rate and also with the coolant inlet temperature. The effect of flow rate is predominant since the increase in  $Q$  directly increases the coolant velocity in the channel. The influence of coolant temperature is also seen as the higher coolant temperature results in a lower water viscosity and hence a higher Reynolds number at the same nominal flow rate. Thus, the maximum  $Re_{avg}$  values are found at the maximum flow rate and maximum coolant inlet temperature. The plotted form of the  $Re_{avg}$  response surfaces presented in Fig. 14 are obtained from the fitted equations. These are applied to compare behaviour of the three channel profiles under the flow regime and to determine the hydraulic

behaviour as a function of coolant flow rate and coolant temperature. The RSM model fitted equations of  $Re_{avg}$  for each profile are:

For Circular Profile:

$$Re_{avgCL} = 9579.312 + 2058.651A + 6238.356B + 58.342A^2 + 133.438B^2 + 1481.612AB \quad (17)$$

For Elliptical Profile:

$$Re_{avgEL} = 8987.816 + 1898.485A + 5849.095B + 49.710A^2 + 96.615B^2 + 1359.488AB \quad (18)$$

For Teardrop Profile:

$$Re_{avgTD} = 8637.242 + 1804.457A + 5615.420B + 86.528A^2 + 66.320B^2 + 1321.702AB \quad (19)$$

Where  $A$  represents the coded variable corresponding to coolant inlet temperature ( $T_c$ ), and  $B$  represents the coded variable corresponding to coolant flow rate ( $Q$ ).

The coefficient of  $B$  is much bigger than the coefficient of  $A$  in all three equations, which means that the flow rate is the most important parameter that affects  $Re_{avg}$ . The positive  $A$  coefficient indicates that increasing the coolant inlet temperature also increases  $Re_{avg}$ , but by a lesser effect than due to increase in flow rate. The positive sign of the interaction term  $AB$  indicates that flow rate's effect increases with increasing coolant temperature, since as the temperature of the coolant increases, the viscosity of the coolant decreases. This explains why the highest Reynolds numbers are obtained at  $Q=10$  L/min and  $T_c=35^\circ\text{C}$ . The profile ranking is the same in all operating conditions. The circular profile has the highest  $Re_{avg}$ , the elliptical profile has the next highest  $Re_{avg}$  and the teardrop profile has the lowest  $Re_{avg}$ . This ranking is based on the hydraulic diameter rank of the three profiles. The cross-sectional area of the profiles is almost the same, and the difference of the Reynolds number is primarily associated with the hydraulic diameter and the flow behaviour at the considered point. Thus, the circular profile will have the highest Reynolds number as it has the largest hydraulic diameter, and the teardrop profile will have the lowest Reynolds number as it has the smallest hydraulic diameter. The following Table 17 shows the  $Re_{avg}$  for all three profiles.

**Table 17.**  $Re_{avg}$  for all three profiles

Q (L/min)	Tc (°C)	CL $Re_{avg}$	EL $Re_{avg}$	TD $Re_{avg}$	Flow regime
2	15	2955.952	2748.41	2645.312	Transitional
2	25	3508.093	3257.195	3135.234	Transitional
2	35	4075.821	3799.826	3656.934	Transitional / borderline turbulent for CL
5	15	6377.085	6005.583	5915.928	Turbulent
5	25	8015.47	7523.249	7179.421	Turbulent
5	35	9808.318	9165.332	8790.302	Turbulent
10	15	12490	11740	11260	Turbulent
10	25	15930	14920	14330	Turbulent
10	35	19550	18240	17540	Turbulent

As tabulated in the above table, the 2 L/min cases are primarily in the transition region. The only exception is the circular profile at  $Q=2$  L/min and  $T_c=35^\circ\text{C}$  with  $Re_{avg}=4075.821$ , which is just above the traditional turbulent threshold. All three profiles are in the turbulent regime at 5 L/min and 10 L/min. This confirms that the main flow-regime transition is between 2 L/min and 5 L/min flow. Higher flow rates (e.g., 10 L/min) create greater turbulence intensity at the expense of the pressure drop penalty mentioned in Section 3.4.1. The overall results of the  $Re_{avg}$  indicate that flow rate is the most influential parameter to control the coolant flow regime, and coolant temperature is the secondary parameter with a consistent trend. The teardrop profile has the lowest Reynolds number, and the circular profile has the highest Reynolds number. However, the lower  $Re_{avg}$  of the teardrop profile does not lower the thermal advantage. From that, it is seen that the teardrop profile still yields the lowest  $T_{max}$  and the shortest  $t_{cool}$  as shown in Sections 3.3.2 and 3.3.3, respectively. This implies that the thermal advantage of the teardrop profile is primarily due to its profile geometry and the local behaviour of heat removal, but not necessarily to the highest Reynolds number.

### 3.4.3. Warpage Displacement (*Warp*)

The deviation of the moulded part from the nominal CAD shape after cooling down and ejection is called Warpage displacement (*Warp*). In this study, it serves as the main dimensional-quality response since it is an indicator of how far the final part is from the desired part shape. A warpage value indicates the dimensional stability, assembly accuracy and the risk of problems with fits in the final component. Warpage is primarily due to differential cooling or differential shrinkage of the part inside the mould. Regions that are hotter than others for longer shrink last after other regions have solidified. This difference in shrinkage puts internal stresses into the material and can relax after ejection, causing the part to bend, twist or deform. Thus, in addition to the behaviour of the coolant flow, the local temperatures, the position of the cooling channels, the geometry of the profile and the behaviour of its material shrinkage can all affect the warpage. For this reason, the warpage is also provided with the thermal and hydraulic responses. Although the use of a "cooling-channel" profile may decrease the maximum temperature and the cooling time, it should not produce too much dimensional deformation. In the present comparison, the warpage response is used to help quantify whether or not the circular, elliptical, and teardrop profiles have similar dimensional behaviour for the same coolant flow rate and coolant inlet temperature. Fig 15 shows the response surface plots for *Warp*.

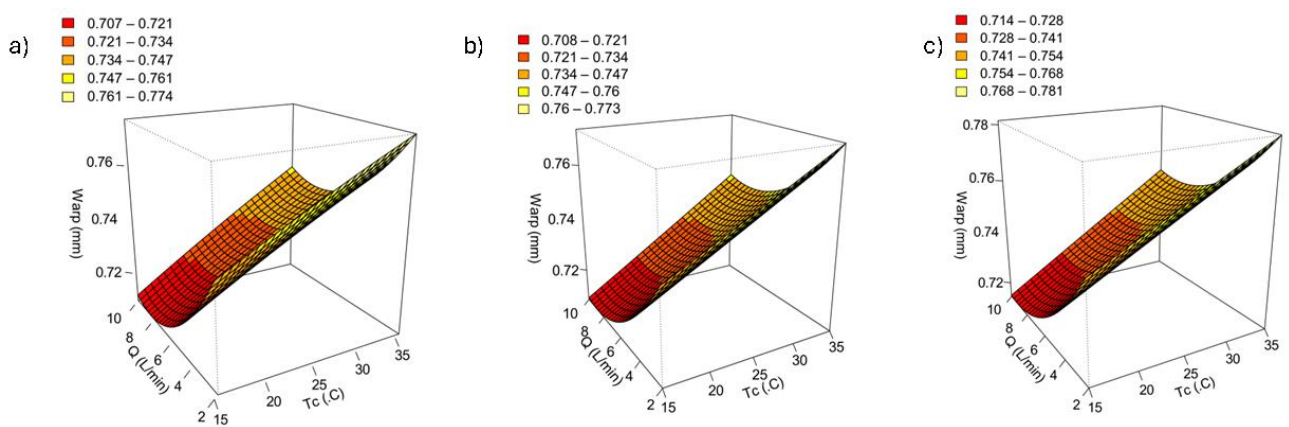


**Fig. 15.** Response surface plots of warpage displacement (*Warp*) as a function of coolant inlet temperature and coolant flow rate: a) circular profile, b) elliptical profile, and c) teardrop profile

As can be seen from the surface plots in Fig. 15, the higher the coolant inlet temperature, the higher is the warpage and the lower the coolant flow rate, the higher is the warpage. But the total fluctuation is not large compared to the one mentioned above for thermal and hydraulic response. From the three profiles it is seen that the surface shapes are very similar, which means that the effect of cross-section profile on the final warpage displacement is limited. The only difference is under the same operating conditions, the teardrop profile produces slightly higher values of warpage than the circular and elliptical profiles, although these differences are quite small. The equations fitted for the *Warp* response surfaces in Fig. 15 give the mathematical form of the surfaces. They are employed to determine the relative importance of inlet coolant temperature, coolant flow rate, and the profile geometry on the dimensional response predicted. The RSM model fitted equations of *Warp* displacement for each profile are:

For Circular Profile:

$$Warp_{CL} = 0.731 + 0.018A - 0.014B - 0.001A^2 + 0.014B^2 + 0.002AB \quad (20)$$

For Elliptical Profile:

$$Warp_{EL} = 0.731 + 0.018A - 0.014B + 0.000A^2 + 0.011B^2 + 0.002AB \quad (21)$$

For Teardrop Profile:

$$Warp_{TD} = 0.739 + 0.018A - 0.015B + 0.000A^2 + 0.011B^2 + 0.002AB \quad (22)$$

Where  $A$  represents the coded variable corresponding to coolant inlet temperature ( $T_c$ ), and  $B$  represents the coded variable corresponding to coolant flow rate ( $Q$ ).

The coefficient of  $A$  is positive in all three equations, indicating that warpage is increased with an increase in the inlet coolant temperature. The coefficient of  $B$  is negative, which shows that increasing the coolant flow rate reduces warpage. This behaviour is similar to the thermal-response results, as a decrease in the coolant temperature and an increase in the coolant flow rate result in a decrease in the thermal non-uniformity that leads to the shrinkage-related deformation. The magnitude of the higher-order coefficients is small, indicating that the response in warpage is near linear over the range of operating conditions tested. This is also reflected in the raw Moldex3D data. The influence of coolant inlet temperature and flow rate on warpage of the circular profile is in the expected direction; that is, as coolant inlet temperature increases, warpage also increases, while it decreases only by a small margin when flow rate increases; however, the magnitude of the changes is small. Table 18 shows the raw warpage values.

**Table 18.** Warpage Displacement (mm) across all three profiles

Q (L/min)	Tc (°C)	CL <i>Warp</i> (mm)	EL <i>Warp</i> (mm)	TD <i>Warp</i> (mm)	Max Difference (mm)
2	15	0.743	0.741	0.750	0.009
2	25	0.760	0.756	0.765	0.009
2	35	0.773	0.772	0.781	0.009
5	15	0.716	0.717	0.725	0.009
5	25	0.735	0.736	0.744	0.009
5	35	0.754	0.754	0.762	0.008

Q (L/min)	Tc (°C)	CL Warp (mm)	EL Warp (mm)	TD Warp (mm)	Max Difference (mm)
10	15	0.710	0.709	0.715	0.006
10	25	0.730	0.728	0.735	0.007
10	35	0.749	0.748	0.755	0.007

This table reveals that of all the responses in the study, warpage is the least profile sensitive. The total warpage lies within 0.709 to 0.781 mm for all conformal cooling runs with a total spread of 0.072 mm; the largest difference between any two of the profiles is 0.009 mm at matched operating conditions. This validates the results, which show that the warpage is much less sensitive to the cross-section profile than to  $T_{max}$  and  $t_{cool}$ . The results of warpage are that the dimensional response is dominated by the coolant inlet temperature and the coolant flow rate, and the effect due to profile geometry is very small. Compared with the circular and elliptical profiles, the teardrop profile causes slightly more warpage, but less than 0.010 mm at all matched operating conditions. Hence, no appreciable dimensional-quality loss is incurred within the chosen simulation domain associated with the thermal benefit of the teardrop profile. This is significant as the teardrop profile offers lower  $T_{max}$  and shorter  $t_{cool}$  with similar warpage level to the other two conformal cooling profiles.

### 3.5. Factor Significance Analysis

The thermal, hydraulic and dimensional responses were each analysed in the previous sections. This section provides an overview of the general effect of the coolant inlet temperature and coolant flow rate on the overall results of all responses using the fitted RSM model coefficients. The idea is not so much to repeat the discussion on each response, but to note which factor controls each response and how that will impact the later optimisation. The regression equations reported by JASP will be in the internal coded units and can be compared within the tested design space in terms of the direction and relative strength of the factor effects. A in this section is coolant inlet temperature (Tc) and B is coolant flow rate (Q).

#### 3.5.1. Linear Effects of Coolant Temperature and Flow Rate

The linear coefficients indicate the predominant direction of change due to coolant inlet temperature and flow rate. Table 19 shows linear coefficients for each of the six response variables and all three conformal cooling channel profiles. These coefficients are used for the RSM models for the circular, elliptical and teardrop profiles.

**Table 19.** Linear regression coefficients for coolant temperature (A) and flow rate (B) in the fitted RSM models

Response	Profile	A (Tc Coefficient)	B (Q Coefficient)	Dominant factor
$T_{avg}$ (°C)	Circular	+7.712	-7.77	$Q \approx Tc$
	Elliptical	+7.741	-7.29	Tc
	Teardrop	+7.762	-7.564	Tc
$T_{max}$ (°C)	Circular	+3.962	-3.118	Tc
	Elliptical	+3.942	-2.831	Tc
	Teardrop	+4.443	-2.928	Tc

Response	Profile	A (Tc Coefficient)	B (Q Coefficient)	Dominant factor
$t_{cool}$ (s)	Circular	+4.486	-3.333	Tc
	Elliptical	+4.905	-2.958	Tc
	Teardrop	+4.769	-3.002	Tc
$\Delta P$ (kPa)	Circular	-1.041	+29.333	Q
	Elliptical	-1.041	+27.833	Q
	Teardrop	-1.041	+30.333	Q
$Re_{avg}$	Circular	+2058.651	+6238.356	Q
	Elliptical	+1898.485	+5849.095	Q
	Teardrop	+1804.475	+5615.42	Q
Warp (mm)	Circular	+0.018	-0.014	Tc
	Elliptical	+0.018	-0.014	Tc
	Teardrop	+0.018	-0.015	Tc

The coefficient pattern is consistent for the thermal responses. The thermal response of  $T_{avg}$ ,  $T_{max}$  and  $t_{cool}$  increases with the increase of coolant inlet temperature in all profiles because the coefficient for coolant temperature is positive. Physically, this is due to the fact that thermal driving force for heat removal is less with warmer coolant. The flow-rate coefficient is negative for each of the thermal models, indicating that as the flow rate of the coolant is raised, the part is cooled more rapidly and the part temperature decreases. The magnitude of the temperature coefficient is generally larger than that of the flow-rate coefficient, in this case, for  $T_{max}$  and  $t_{cool}$ , which shows that for the behaviour of the local hot-spot temperature and cooling-time, coolant inlet temperature is more important than flow-rate as a linear factor. The impacts of coolant flow rate and coolant temperature are more balanced for  $T_{avg}$ . The circular model has nearly equal coefficient values: +7.712 (Tc) and -7.770 (Q). This proves that both factors have a strong influence on the average part temperature. In the elliptical and teardrop models, the effect of coolant temperature is slightly more influential, while the effect of flow rate is nearly as influential. This also strengthens the previous interpretation that process conditions exert a major influence on the control of  $T_{avg}$  as opposed to profile geometry.

The factor pattern of the hydraulic responses is different. The coefficient of flow rate for pressure drop is highly positive in all three profiles (circular = +29.333, elliptical = +27.833 and teardrop = +30.333). These values are much larger than the coolant-temperature coefficient of -1.041. Hence, the flow rate of the coolant is the main factor on which pressure drop depends. The negative temperature coefficient is indicative that with an increase in coolant temperature, the pressure drop decreases a little, which is in line with the decrease in water viscosity as the temperature increases. Coolant flow rate is also the primary parameter in determining the Reynolds-number response. The circular, elliptical and teardrop flow-rate coefficients are +6238.356, +5849.095 and +5615.420, respectively. The coolant-temperature coefficients are also positive, but smaller. This verifies that  $Re_{avg}$  is also increased primarily due to increasing velocity of the coolant and the temperature of the coolant is added effect due to its viscosity reduction. Coefficient pattern for warpage is consistent with thermal responses: warpage increases with coolant temperature and warpage decreases (not significantly) with flow rate. The absolute values of the coefficients are, however small, which verifies that the sensitivity of warpage is much smaller than the thermal and hydraulic sensitivities.

The linear coefficient analysis, overall, also demonstrates separation between the thermal and hydraulic control mechanisms. The inlet temperature of the coolant is the most important parameter for the  $T_{max}$ ,  $t_{cool}$  and  $Warp$ , while the flow rate of the coolant is the most important parameter for the  $\Delta P$  and  $Re_{avg}$ . Both factors have a significant influence on the average part temperature. This means that in order to improve the cooling system, one has to make a compromise: decrease the coolant temperature to improve thermal performance, but increase the flow rate to improve the heat removal, which strongly increases the hydraulic resistance. The quadratic, interaction and multi-response optimisation analyses are used to further assess this trade-off.

### 3.5.2. Quadratic and Interaction Effects

The quadratic and interaction coefficients indicate the presence of linear or nonlinear behaviour between the responses within the range studied. The  $A^2$ ,  $B^2$  and AB coefficients for the fitted RSM models are summarised in the following Table 20.

**Table 20.** Quadratic ( $A^2$ ,  $B^2$ ) and interaction (AB) coefficients in the fitted RSM model

Response	Profile	$A^2$ Coefficient	$B^2$ Coefficient	AB Coefficient
$T_{avg}$ (°C)	Circular	-0.137	+5.728	+1.162
	Elliptical	-0.044	+5.246	+1.065
	Teardrop	0.047	+5.548	+1.117
$T_{max}$ (°C)	Circular	-0.005	+2.48	+0.468
	Elliptical	-0.021	+2.079	+0.437
	Teardrop	+0.025	+2.195	+0.561
$t_{cool}$ (s)	Circular	+0.119	+2.369	+0.728
	Elliptical	-0.422	+2.268	+0.955
	Teardrop	+0.142	+2.345	+0.291
$\Delta P$ (kPa)	Circular	+0.000	+8.178	-0.49
	Elliptical	+0.000	+8.044	-0.49
	Teardrop	+0.000	+8.978	-0.49
$Re_{avg}$	Circular	+58.342	+133.438	+1481.612
	Elliptical	+49.71	+96.615	+1359.488
	Teardrop	+86.528	+66.32	+1321.702
$Warp$ (mm)	Circular	-0.000833	+0.014	+0.002
	Elliptical	+0.000167	+0.011	+0.002
	Teardrop	+0.000	+0.011	+0.002

Maximum nonlinearity is related to the coolant flow rate. The positive  $B^2$  coefficients for the thermal responses show that as the flow rate increases, the thermal returns decrease. This is consistent with the previous findings that showed a greater improvement in going from low to medium flow than medium to high flow. The same  $B^2$  effect is even greater in pressure drop, the  $B^2$  coefficients are +8.178 for circular, +8.044 for elliptical and +8.978 for teardrop. This validates that a drop in pressure rises non-linearly in relation to the flow rate. The  $A^2$  coefficients are all small, indicating that the coolant inlet temperature is essentially linear in the range of the experiments. The largest interaction effects are for  $Re_{avg}$ , with the AB coefficients being considerably larger than for the other responses.

This is a result of the effect of flow rate and coolant temperature on coolant velocity and viscosity. In the thermal responses, the interaction terms are there but of lesser magnitude, so that  $Q$  and  $T_c$  interact, but the main response behaviour is still dominated by their linear and flow-rate curvature effects.

### 3.5.3. Overall Factor Ranking and Interpretation

The coefficient analysis verifies that the conformal cooling problem is not a single-factor improvement problem but rather is a multi-response trade-off. The thermal responses are improved from the lower coolant inlet temperature due to the higher thermal driving force for heat removal. The higher the flow rate to the coolant, the better it cools, but the positive  $B^2$  terms indicate that the improvement is diminished as the flow rate is increased. Meanwhile, the pressure drop rises sharply, in a nonlinear fashion, with flow rate. Hence, the maximum flow-rate condition is not necessarily the most advantageous operating situation. The results of the coefficient analysis are summarised in Table 21.

**Table 21.** Overall factor influence based on fitted RSM coefficient behaviour

Response	Primary Factor	Secondary Factor	Main Higher-Order Behaviour
$T_{avg}$	$Q \approx T_c$ (near equal)	Profile geometry (minor)	Strong ( $Q^2$ ) curvature
$T_{max}$	$T_c$	$Q$ , Profile Geometry	( $Q^2$ ) curvature; TD shifts response lower
$t_{cool}$	$T_c$	$Q$ , Profile Geometry	( $Q^2$ ) curvature; TD gives shorter cooling time
$\Delta P$	$Q$	$T_c$ (negligible)	Strong ( $Q^2$ ) pressure-drop growth
$Re_{avg}$	$Q$	$T_c$	Strong ( $Q \times T_c$ ) interaction
$Warp$	$T_c$	$Q$	Small ( $Q^2$ ) and ( $Q \times T_c$ ) effects

Thermal performance is basically enhanced by reducing coolant temperature and increasing adequate coolant flow; hydraulic performance is primarily constrained by the pressure drop penalty at high flow. Profile geometry is only slightly affecting  $T_{avg}$  and  $Warp$  but is clearly affecting  $T_{max}$  and  $t_{cool}$ . The teardrop profile optimises the local hot-spot control and cooling time, and the elliptical profile has a good hydraulic characteristic because of its low-pressure drop behaviour. In general, it is concluded that the optimum operating condition should be chosen by multi-response optimisation using the factor-effect analysis to understand the reasons. Any solution needs to lower thermal responses while minimising any additional hydraulic drag. This forms the foundation for the desirability-based optimisation in the following section.

### 3.6. Multi-Response Optimisation Results

In factor-effect analysis conducted in Section 3.5, it was concluded that the performance of a cooling channel cannot be judged by a single response. A reduced coolant inlet temperature and increased coolant flow rate yield better thermal response, and higher coolant flow rates result in a higher coolant pressure drop. Hence, thermal performance and hydraulic resistance can be coupled with the dimensional quality, and optimisation problem should consider all of them. Therefore, multi-response optimisation was carried out with the fitted RSM models. Five responses were optimised, namely the average part temperature ( $T_{avg}$ ), maximum part temperature ( $T_{max}$ ), cooling time ( $t_{cool}$ ), coolant pressure drop ( $\Delta P$ ) and warpage displacement ( $Warp$ ). An indicator of the flow regime ( $Re_{avg}$ ) was

not considered as an optimisation objective, as it is not a direct response of the flow to the minimisation/maximisation of the objective function. In this case,  $Re_{avg}$  was only used to interpret the coolant-flow condition. The selected responses were consolidated with the composite desirability approach in this study. In this method, each response is transformed into an individual desirability in a range of 0 to 1, and then these individual desirabilities are aggregated into a single optimisation index [34]. The composite desirability is calculated by:

$$D = (d_1 \times d_2 \times \dots \times d_k)^{\frac{1}{k}} \quad (23)$$

where  $D$  is the composite desirability value, and  $k$  is the number of responses that are in the optimisation.

In all the selected five responses, they were minimised and were given the same importance, the optimisation is a balance between the cooling performance, pressure drop and warpage. The optimisation was carried out individually for the three different profiles of conformal cooling channels, namely circular, elliptical and teardrop. This was to determine the optimum operating condition for each of the profiles and compare the effect of the combined optimum of the profiles. The optimum values reported in the following section are not additional runs directly simulated using Moldex3D, but rather the operating conditions within the tested design space that are optimum as predicted by the fitted RSM models.

### 3.6.1. Optimisation Results by Cooling Channel Profile

The results of optimisation for each profile are shown in Table 22 below. This table provides a summary of the predicted optimum coolant flow rate, coolant inlet temperature, composite desirability and corresponding response values for each conformal cooling channel profile. This comparison is intended to find which of the three profiles, circular, elliptical or teardrop, will offer the best overall thermal response, pressure drop and warpage.

**Table 22.** RSM-predicted optimum conditions as response values for each CCC profile

Response/Parameter	Circular Profile	Elliptical Profile	Teardrop Profile
Composite Desirability (D)	0.989	0.989	0.993
Q (L/min)	4.73	5.273	4.713
T <sub>c</sub> (°C)	15.611	15.701	16.023
T <sub>avg</sub> (°C)	30.646	27.557	30.618
T <sub>max</sub> (°C)	120.89	120.029	113.717
t <sub>cool</sub> (s)	86.922	87.506	83.736
ΔP (kPa)	6.24	6.071	5.083
Warp (mm)	0.704	0.699	0.715

The optimum coolant inlet temperature predicted for all profiles is still near the low end of the range tested, with a temperature of 15.611°C to 16.023°C. The optimum flow rate is predicted to be moderate (4.713 to 5.273 L/min) and not the highest flow rate tested (10 L/min). This validates the fact that the most favourable multi-response region is not achieved by increasing the coolant flow to its maximum. Instead, the optimiser chooses a flow-rate range which has a lower pressure drop and better thermal performance.

The desirability of the circular profile is  $D=0.989$ . At this optimum point, the predicted pressure drop is 6.240 kPa, the predicted cooling time is 86.922 s, and the predicted maximum part temperature is 120.890°C. The results show that the circular shape can provide a high ratio of cooling capacity to pressure loss at a moderate flow. The elliptical profile also provides a composite desirability of  $D=0.989$ . It is predicted to have optimum values at  $Q=5.273$  L/min,  $T_c=15.701$ °C. The lowest predicted warpage value is 0.699 mm for the elliptical profile and a low predicted pressure drop of 6.071 kPa. This corresponds to the previous hydraulic-response interpretation that the elliptical profile is desirable when pressure drop and dimensional stability are paramount. The teardrop profile has the highest composite desirability of  $D=0.993$ . Its predicted optimum occurs at  $Q=4.713$  L/min and  $T_c=16.023$ °C. At this point, the predicted  $T_{max}$  is 113.717°C and the predicted  $t_{cool}$  is 83.736 s, which are the lowest values among the three profile optimums. As such, the teardrop profile continues to be the preferred profile when the primary objective is to achieve reduction of the local hot-spot and cooling-time improvement. The overall results of the optimisation show that the trade-off highlighted in the factor-effect analysis is true. Low coolant temperature is found to increase cooling performance, with a weaker effect on pressure drop than high flow rate, which is found to increase thermal response but with a stronger effect on the pressure drop. The optimum solutions are in a low temperature and moderate flow region accordingly. After optimisation, all three profiles give good performance, but the teardrop profile has the highest desirability, and the lowest predicted maximum part temperature and predicted cooling time.

### 3.6.2. Interpretation of the Optimised Operating Region

The results from optimisation indicate the optimal operating region is mainly located at the lower limit for the coolant temperature and around the middle of the coolant flow range. The predicted optimum inlet temperature of the coolant for all three profiles is between 15.611°C and 16.023°C, and the predicted optimum flow rate of the coolant is between 4.713 L/min and 5.273 L/min. This confirms that the best region is not at the maximum flow rate tested (10 L/min), but rather at a moderate flow rate region where the thermal responses are better without the high pressure drop that is present at the highest flow rate tested. The pressure drop predicted at the optimal points are low for all three profiles, ranging from 5.083 kPa for teardrop profile to 6.240 kPa for circular profile. This is significant, since the results of the pressure-drop analyses in Section 3.4.1 indicated that the pressure drop rises significantly at high flow rates. Optimisation is not just for the best cooling condition, but an optimisation for a balance of cooling performance, hydraulic resistance and warpage.

The circular and elliptical shapes have similar values of the composite desirability ( $D=0.989$ ), but their thermal performance is less than that of the teardrop shape at the optimum predicted value. The circular profile yields  $T_{max}=120.890$ °C and  $t_{cool}=86.922$  s, whereas the elliptical profile yields  $T_{max}=120.029$ °C and  $t_{cool}=87.506$  s. The teardrop profile results in  $T_{max}=113.717$ °C and  $t_{cool}=83.736$  s, compared to. Thus, the teardrop profile offers the maximum reduction in the hot-spot area, and the fastest predicted cooling time of the three optimum solutions. These desirability differences have been found to be small,  $D=0.989$ , for the circular and elliptical profiles and  $D=0.993$ , for the teardrop profile. Thus, it is not necessarily better to consider the teardrop profile as being superior only because of the desirability score. The choice is primarily supported by the values of the responses that correspond to the desirability value of the desirability result, namely the lower value of  $T_{max}$  and the shorter value of  $t_{cool}$ . The elliptical profile is still appealing in terms of hydraulics and dimension, with

the lowest predicted warpage of 0.699 mm, and low predicted pressure drop of 6.071 kPa. With hydraulic resistance as well as thermal performance being taken into consideration, however, the teardrop profile makes the best overall compromise. In general, the optimisation results suggest that the best operating condition for the conformal cooling system studied is a low inlet coolant temperature and moderate coolant flow. This operating region will not sustain the hydraulic penalty of the highest flow-rate operating condition but will ensure that good thermal performance is maintained. Which one of the three profiles is selected as the preferred profile is the teardrop channel, which provides the composite desirability of high and the best hot-spot and cooling-time response among the three profiles in the test simulation domain. The ideal values are not confirmation runs from Moldex3D, but rather are the RSM prediction values.

### 3.7. Cross-Profile Performance Comparison

The responses to thermal, hydraulic, dimensional and optimisation were analysed separately in the previous sections. This section will compare the three conformal cooling channel profiles side-by-side to determine the overall cooling channel performance. The comparison is done with the raw Moldex3D response data, the fitted RSM models and the result of multi-response optimisation. This is to find out if the circular, elliptical or teardrop cross-section offers the best combination of cooling ability, hydraulic resistance and dimensional stability. The profile comparison demonstrates that there is no one 'best' profile in each response. The teardrop profile functions best on the primary thermal responses mostly, the maximum part temperature  $T_{max}$  and cooling time  $t_{cool}$ . The elliptical profile is most effective in hydraulic resistance, having the least pressure drop at the same conditions of operation. Many responses are close to the elliptical profile, but not as good at reducing the hot spot as the teardrop profile. The overall comparison is summarised in Table 23.

**Table 23.** Overall performance comparison of conformal cooling channels profiles

Response	Best Profile	Intermediate Profile	Weakest Profile	Main Observation
$T_{avg}$	All nearly equivalent	—	—	Max profile difference = 1.444°C; at (Q = 5) L/min, max difference ≤ 0.283°C
$T_{max}$	Teardrop	Elliptical	Circular	Teardrop reduces $T_{max}$ by 6.738–7.913°C compared with circular
$t_{cool}$	Teardrop	Circular / Elliptical	Elliptical / Circular	Teardrop reduces $t_{cool}$ by 2.160–3.874 s compared with circular
$\Delta P$	Elliptical	Circular	Teardrop	Elliptical gives the lowest pressure drop; TD–EL difference reaches 5 kPa at 10 L/min
$Re_{avg}$	Circular	Elliptical	Teardrop	Ranking follows hydraulic diameter: CL > EL > TD
Warp	All nearly equivalent	—	—	Max profile difference at matched conditions = 0.009 mm
Desirability D	Teardrop	Circular / Elliptical	—	TD = 0.993; CL = 0.989; EL = 0.989

As seen in the above table, the greatest profile-dependent improvement is for  $T_{max}$  and  $t_{cool}$ . The teardrop profile will reduce maximum part temperature under all matched operating conditions and

will also provide the shortest cooling time. It is good to see that this is not average part temperature reduction but local hot-spot control that is the key benefit of the teardrop profile. The  $T_{avg}$  response is a function of the cross-section profile for low flow rates, but it is nearly profile independent at medium and high flow rates, meaning that bulk part temperature is controlled primarily by the coolant flow rate and coolant inlet temperature and not by cross-section profile.

The hydraulic ranking is different. The elliptical profile results in the lowest pressure drop at matched conditions, particularly at higher flow rates, with the teardrop profile resulting in the highest pressure drop at matched conditions. The thermal advantage of the teardrop profile should, however, be considered in conjunction with the pressure drop. The teardrop profile is still found to be the most desirable one in the results of the optimisation due to its hydraulic disadvantage being offset by its improved  $T_{max}$  and  $t_{cool}$  under the chosen response weighting. The Reynolds-number comparison reveals that the circular profile results in the maximum  $Re_{avg}$ , with the elliptical shape and teardrop shape being next, as shown. The maximum Reynolds number, however, does not necessarily represent the maximum thermal performance. The teardrop profile has the lowest  $Re_{avg}$  even though it has the lowest  $T_{max}$  and shortest  $t_{cool}$ . Thus, the thermal benefit of the teardrop profile is not only due to greater flow intensities. It has primarily to do with the cross-section geometry and how it affects the local heat-removal behaviour. The cross-profile comparison of the profiles indicates that the teardrop profile is the best profile to consider when thermal performance is a primary concern, since it offers the highest hot-spot reduction and the fastest cooling time. The elliptical profile is the best one to use when hydraulic resistance is the primary factor, and the circular profile is a good reference case with even, but less distinctive, performance. When all the responses are considered together, the teardrop profile is the best overall compromise for the selected battery-casing geometry and simulation conditions. It has the greatest advantage in the local thermal behaviour, with a practically equal warpage response for circular and elliptical profiles.

### 3.8. Conformal Cooling Channel and Baseline Straight Cooling Channel Comparison

The three profiles of conformal cooling channels were compared to the straight-line cooling channel baseline to assess the improvement in cooling performance due to the conformality of the channels. The performance of the straight-line baseline was simulated at  $Q=5$  L/min for 15°C, 25°C and 35°C at the inlet of the coolant. These conditions are similar to the centre flow rate condition in the conformal cooling design matrix, making it possible to compare the straight-line baseline with the three conformal profiles using the same flow rate of the coolant and the same temperature of coolant. The conformal cooling channels are normally regarded as having more uniform and efficient cooling than straight channels, due to their ability to closely conform to the mould cavity surface and minimise the distance between the cooling path and thermally critical areas [38]. The results of the thermal comparison for straight-line baseline and conformal cooling profiles are shown in Table 24 below.

**Table 24.** Thermal response comparison (conformal cooling channels vs straight line cooling channels baseline)

Response	Tc (°C)	SL	CL	EL	TD	CCC Improvements vs SL
$T_{avg}$ (°C)	15	82.434	36.299	36.016	36.061	56.0–56.3%
	25	87.475	44.076	43.934	43.934	49.8–49.8%
	35	92.623	52.051	51.795	51.903	43.8–44.1%

Response	Tc (°C)	SL	CL	EL	TD	CCC Improvements vs SL
$T_{max}$ (°C)	15	144.25	123.457	123.263	115.626	14.4–19.8%
	25	146.951	127.405	127.336	120.224	13.3–18.2%
	35	149.786	131.531	131.334	124.793	12.2–16.7%
$t_{cool}$ (s)	15	167.06	89.586	89.663	86.358	46.4–48.3%
	25	180.73	93.978	95.62	91.23	47.1–49.5%
	35	203.43	98.525	99.784	95.639	51.0–53.0%

The comparison is based on the average part temperature ( $T_{avg}$ ), maximum part temperature ( $T_{max}$ ) and cooling time ( $t_{cool}$ ) as these responses are directly linked to the cooling advantage of the conformal channel geometry. All three of the conformal cooling channel profiles present a significant improvement in the thermal responses as compared to the straight-line baseline in the table. The average part temp is lowered by about 43.8-56.3%, depending on the coolant inlet temp and profile. The reduction in the cooling time is also significant (46.3% to 53.0%). These reductions verify that the conformal channel path offers better thermal performance by virtue of having the route of the coolant closer to the part geometry than the straight-line channel route having an ineffective heat conduction distance.

From a process quality perspective, the decrease of  $T_{max}$  is smaller than both  $T_{avg}$  and  $t_{cool}$ , but still significant. For the straight-line baseline, the  $T_{max}$  is found to be 146.951°C, at Tc=25°C; and for the teardrop conformal profile, the  $T_{max}$  is found to be 120.224°C, at Tc=25°C. This equates to a drop in temperature of 26.727°C. The  $T_{max}$  is also reduced significantly by the circular and elliptical profiles; the teardrop profile offers the greatest reduction in  $T_{max}$  for each matched baseline condition, of the conformal profiles. The main benefit of conformal cooling is not just the profile shape, but channel route, which is confirmed by the baseline comparison. Even the most basic conformal cross-section (circular), decreases the cooling time from 180.730 s to 93.978 s when Q=5 L/min and Tc=25°C. This indicates that the primary advantage compared to straight line cooling is the conformality, and the profile geometry further influences the local response of the thermal field in the conformal channel group.

An increase in the pressure drop of the coolant is achieved with the thermal improvement. The matched flow rate straight-line baseline pressure drop in the system at 15°C, 25°C and 35°C are 0.873kPa, 0.775kPa and 0.693kPa, respectively. At the same baseline conditions (15, 25, 35 °C), the pressure drops of the conformal cooling channels are 18–19 kPa, 17–18 kPa, and 16–17 kPa, respectively, which amounts to an increase of pressure drops of 20.6–24.5 times over the straight-line baseline. This is a confirmation of hydraulic penalty of conformal channel routing, but the absolute values of the pressure drop are moderate within the tested flow range. The overall results of the straight-line baseline comparison support the thermal advantage of the conformal cooling for this geometry of the battery casing. The major advantage is the conformal routing of the channel, which significantly lowers the average temperature of the parts and cooling times, in comparison to the straight-line channel. The teardrop profile gives the best local reduction of hot-spots, and the elliptical profile is still hydraulically favourable among the conformal profiles. Thus, the basic comparison is in favour of conformal cooling as the main step towards the optimisation of the straight-line cooling, and the profile geometry as a secondary step in conformal geometry optimisation.

### 3.9. Results Interpretation and Limitations

The results indicate that the selection of conformal cooling channel profile should depend on the priority of the desired performance and not be based on one of the response variables. Average part temp and warpage curves are similar for both the circular and the elliptical and teardrop profiles, but are more distinct for maximum part temp, cooling time and pressure drop. When considering the profile comparison, therefore, it is most meaningful to consider it in the context of local hot spot control, cooling time reduction and hydraulic resistance. In a thermal sense, the teardrop profile is the best profile as it provides the lowest maximum part temperature and the fastest cooling time. This means that there is better cooling of the critical hot-spot region locally. The hydraulic consideration is more favourable for elliptical profile as it offers minimum pressure drop at similar operating conditions. The circular shape serves as a good reference with balanced behaviour but is not dominant in the thermal and hydraulic responses. This is corroborated by the optimisation results. The optimum operating range does not necessarily coincide with the maximum measured flow rate and includes a region of low hydraulic head loss and low flow rate; this is the thermal improvement area. This indicates that the cooling channel design is a compromise between cooling and the pressure penalty. In this trade-off, the teardrop shape offers the best compromise for the chosen optimisation objective due primarily to the lower maximum part temperature and the shorter cooling time. The results obtained should be analysed in the context of the simulation scope. The study is conducted on one geometry of the moulded part, one polymer material, one conformal channel route and three cross-section profiles with close to the same cross-sectional area. However, the results and findings of the selected simulation case should not be applied directly to all injection moulding applications as they are conclusions. The study also concentrates on the responses of thermal, hydraulic and warpage from Moldex3D simulation, but without physical moulding experiments, measured part temperatures, or experimental cooling time validations. Furthermore, the manufacturability of the non-circular channels, such as the limits of metal additive manufacturing, the internal surfaces operation, removal of powder residues, and accessibility of post-processing, is also not comprehensively assessed. The optimiser values are also RSM-predicted values and not further confirmation runs in Moldex3D. However, further confirmation would need to be achieved by further simulations at the optimum points predicted, by sensitivity analysis for varying channel layouts and part geometries and/or by experimental testing with manufactured mould inserts. The scope should be taken into account when evaluating the profile ranking and its practical applicability of the proposed teardrop cooling-channel profile.

### 3.10. Chapter Summary

This chapter presented the Moldex3D simulation results, RSM analysis, multi-response optimisation and engineering interpretation for the circular, elliptical and teardrop conformal cooling channel profiles. Coolant inlet temperature and flow rate were found to be important factors on the thermal, hydraulic and dimensional responses, whereas profile geometry dominated on the local thermal behaviour. The differences in profile for average part temperature ( $T_{avg}$ ) were small at 1.444 °C on average, and only 0.283 °C between flow rates of 5 and 10 L/min. The profile effect was more pronounced for maximum part temperature ( $T_{max}$ ) with the teardrop profile being 6.738–7.913 °C cooler than the circular profile and 2.160–3.874 s faster for cooling time ( $t_{cool}$ ). From the hydraulic results it was found that the coolant flow rate primarily controls the pressure drop and Reynolds number. Pressure drop rose non-linearly with flow rate, indicating that very high flows are not

efficient. The lowest pressure drop was found to be for the elliptical profile, and the highest for the teardrop profile, with a maximum difference of 5 kPa at 10 L/min. The circular profile achieved the highest mean Reynolds number, but did not lead to the best thermal response. The least profile sensitive response was warpage with a difference of a maximum of 0.009 mm. The models were fitted and the  $R^2$  values ranged between 0.995 and 1.000, while the predicted  $R^2$  values ranged between 0.947 and 1.000. The optimum ranges of coolant flow-rate and coolant inlet temperature were found to be 4.713-5.273 L/min and 15.611-16.023 °C, respectively, by multi-response optimisation. The teardrop profile had the greatest desirability ( $D=0.993$ ) compared to the circular ( $D=0.989$ ) and elliptical ( $D=0.989$ ) profiles, primarily because of the lower predicted  $T_{max}$  and  $t_{cool}$ . The conformal cooling resulted in a reduction of up to 43.8–56.3% for  $T_{avg}$  and up to 46.3–53.0% for  $t_{cool}$  compared to the straight-line baseline at 5 L/min. The teardrop profile exhibited the best overall thermal performance and tolerable pressure-drop behaviour.

## 4. Economic and Environmental Impact Analysis

Based on the results presented in Chapter 3, it was shown that the cross-section profile of conformal cooling channels has an effect on the thermal and hydraulic performance of the injection moulding cooling system. The profile shape (circular profile) was taken as the reference conformal profile shape, and the elliptical and teardrop profiles were considered as modified profile shapes. The teardrop profile exhibited the best thermal characteristics, primarily because of reduced maximum part temperature and reduced time to ejection temperature. The elliptical profile had the least tendency to pressure drop and is applicable in situations where a pressure drop is the limiting criterion. The straight-line cooling channel is only added to this chapter as a secondary baseline, to give an industrial perspective to the general impact of conformal routing. It is important to interpret these simulation findings from an economic and environmental point of view. Cooling time is a significant component of the injection moulding cycle, and even a slight reduction in the time to ejection temperature may be significant in high-volume production. But the variation in conformal profile shapes is expected to be less than that between straight-line and conformal cooling. Thus, the profile level results are considered as optimisation effects and not as complete process level changes. This has been verified by earlier studies that demonstrate that conformal cooling can contribute to a more uniform cooling, reduce cycle time, and enhance part quality, and that the final energy and cost benefits are dependent on machine, mould, material and production conditions [12, 39].

The analysis in this chapter is developed as a scenario-based impact assessment. The model is mainly based on the simulation results from Chapter 3, such as time to ejection temperature, maximum part temperature, and pressure drop and is integrated with specified production assumptions. No physical moulding test or measured data in the factories were available, so the results should be considered as a potential impact for industry in the simulated range, but not as actual production savings.

### 4.1. Basis and Assumptions of the Profile-Based Impact Model

The economic and environmental assessment has been created as a scenario-based profile comparison model. This was done because the present work is simulation-based and does not use industrial production data. The model doesn't aim to predict the cost or energy consumption of any particular factory. Rather, it illustrates how the observed differences between circular, elliptical and teardrop conformal profiles might impact indicators related to production, given a transparent set of assumptions.

The primary comparison is done at the same operating condition (5L/min coolant flow rate and 25°C coolant inlet temperature). This condition was chosen because it was in the middle of the simulation matrix, and to be able to compare all three conformal profiles under the same coolant operating condition. The circular conformal profile is the reference profile, as circular channels are the traditional and most frequently adopted channel cross-section in the design of cooling channels. The elliptical profile is considered as the hydraulic-efficiency alternative, and the teardrop profile is considered as the thermal-performance alternative. The straight-line cooling case (5L/min, 25°C) is only added as a second baseline to illustrate the general difference between straight-line routing and conformal routing.

For the matched condition chosen, the circular profile had  $t_{cool}=93.978$  s, the elliptical profile had  $t_{cool}=95.620$  s, and the teardrop profile had  $t_{cool}=91.230$  s. Thus, the teardrop profile resulted in a 2.748

s decrease in time to reach ejection temperature as compared to the circular conformal reference, which is about a 2.92% reduction in cooling time as seen in the profile level. This improvement is minor, but is similar to the thermal improvement noticed in Chapter 3 with the teardrop, where the maximum part temperature was reduced from 127.405°C to 120.224°C at the same operating condition. This means that the teardrop profile not only offers shorter cooling time, but also greater hot-spot reduction. At this condition, however, the elliptical profile did not decrease the cooling time when compared to the circular profile; it decreased the pressure drop from 18 kPa to 17 kPa, however, which is more desirable if the main design parameter is the hydraulic resistance. The fixed non-cooling portion of the injection moulding cycle was calculated using the fixed parameters of filling, packing and mould-opening times used in the simulation setup:

$$t_{non-cooling} = t_{fill} + t_{pack} + t_{open} \quad (24)$$

Where  $t_{non-cooling}$  is the non-cooling cycle time (s),  $t_{fill}$  is the fixed filling cycle time (s),  $t_{pack}$  is the fixed packing cycle time (s) and  $t_{open}$  is the fixed mould opening time (s). Substituting the fixed parameter values of each stage gives a total non-cooling time ( $t_{non-cooling}$ ) of 17.31 s. The estimated total cycle time for each cooling profile is then calculated as:

$$t_{cycle} = t_{non-cooling} + t_{cool} \quad (25)$$

where  $t_{cycle}$  is the estimated injection moulding total cycle time, and  $t_{cool}$  is the simulated time to reach the ejection temperature, as per the profile.

All profiles use the same non-cooling time to give the productivity comparison as a function of the simulated cooling-time difference. This method is suitable for relative comparison, but not as if the calculated cycle time is the actual industrial cycle time. In practice, the actual cycle time would also be influenced by machine movement, mould opening/closing characteristics, ejection parameters, safety margin of the process, strategy of production control, and part-quality requirements. The scenarios model assumptions are summarised in Table 25. Values derived from the simulation are differentiated from assumed production and cost values in the table. This distinction is necessary as Moldex3D simulation gives technical output results like  $t_{cool}$ ,  $T_{max}$  and  $\Delta P$ , but cannot give factory-specific results like annual production volume, electricity price, machine hourly cost, emission factor, or additional tooling cost.

**Table 25.** Assumption basis for profile-based economic and environmental model

Parameter	Symbol	Value used in model	Assumption basis
Reference conformal profile	-	Circular, 5 L/min, 25°C	Standard conformal cross-section used as the profile reference
Hydraulic-efficiency profile	-	Elliptical, 5 L/min, 25°C	Selected because it showed the lowest pressure-drop tendency among conformal profiles
Thermal-performance profile	-	Teardrop, 5 L/min, 25°C	Selected because it gave the lowest $T_{max}$ and shortest $t_{cool}$ at the matched condition
Secondary conventional baseline	-	Straight-line, 5 L/min, 25°C	Included only for contextual comparison with conventional cooling
Fixed non-cooling time	$t_{non-cooling}$	17.31 s	Calculated from fixed simulation inputs

Parameter	Symbol	Value used in model	Assumption basis
Time to reach ejection temperature	$t_{cool}$	From Chapter 3	Direct Moldex3D simulation output
Maximum part temperature	$T_{max}$	From Chapter 3	Direct Moldex3D simulation output used for hot-spot interpretation
Coolant pressure drop	$\Delta P$	From Chapter 3	Direct Moldex3D simulation output used for hydraulic-power estimation
Annual production volume	$V_a$	500,000 parts/year	Medium-volume production scenario; replace with factory production data for industrial use
Average machine power	$P_m$	15 kW	Scenario value; actual value depends on machine size, drive type and operating state
Electricity price	$C_e$	0.20 €/kWh	Scenario value; replace with local industrial electricity tariff
Machine hourly rate	$C_h$	40 €/h	Scenario value representing machine-time cost; replace with company costing data
Grid emission factor	$EF_{grid}$	0.25 kg CO <sub>2</sub> /kWh	Scenario value; replace with national or factory-specific electricity emission factor
Pump efficiency	$\eta_p$	0.6	Scenario value used to convert ideal hydraulic power into approximate pump demand
Additional profile-specific tooling cost	$C_t$	8,000 €	Scenario value representing additional manufacturing cost of non-circular conformal insert; replace with supplier quotation

The technical differences between the profiles are obtained from the results of the simulation, and the economic and environmental inputs are considered as scenario parameters. This makes sure that the effect of the profile isn't exaggerated. For instance, the teardrop profile offers just a small percentage of reduction in  $t_{cool}$  over the circular profile, however this may be economically significant if used in high production volumes. Likewise, the elliptical profile is not the profile which provides the shortest cooling time, but may be desirable from a hydraulic efficiency perspective or due to pump-capacity restrictions. Table 25 gives assumed values, which should be substituted for measured values or values supplied by the manufacturer in the industrial application. The annual production volume is best derived from the production plan, the electricity price from the electricity contract of the factory or also from a database for official industrial electricity prices and the cost of the profile-specific tooling from the mould insert manufacturer. This is in line with the energy evaluation studies that have been carried out with injection-moulding machines, where accurate energy and environmental evaluation is only possible with the use of machine-specific and process-specific data, and not with generic data [39, 40, 41].

#### 4.2. Productivity Impact of Cooling Channel Profile Selection

The first production level impact of cooling channel profile selection is related to cycle time. In injection moulding, the number of parts produced per hour is directly connected to the total cycle time. Since the same part geometry, mould material, polymer material, coolant flow rate and coolant inlet temperature are used for the profile comparison, the productivity effect is evaluated from the difference in the simulated time to reach ejection temperature. The number of possible cycles per hour is calculated as:

$$N = \frac{3600}{t_{cycle}} \quad (26)$$

Where  $N$  is the number of cycles per hour and  $t_{cycle}$  is the estimated cycle time (s), as per the profile. The profile level productivity difference can then be calculated by comparing each profile with the circular conformal profile as reference:

$$I_N = \frac{N_{profile} - N_{circular}}{N_{circular}} \times 100 \quad (27)$$

Where  $I_N$  is the productivity change compared with the circular conformal profile in %,  $N_{profile}$  is the number of cycles per hour for the selected elliptical or teardrop profile, and  $N_{circular}$  is the number of cycles per hour for the circular conformal profile, here used as reference. The circular profile is taken as the reference as this is the standard conformal cooling profile. Next, the elliptical and teardrop profiles are compared with it, and the effect that the change in the channel cross-section has on production is assessed. The matched condition of 5 L/min and 25°C is chosen because it is the mid-range operating point for the simulation matrix. The calculated productivity comparison is shown in Table 26 below.

**Table 26.** Estimated productivity impact of conformal cooling channel profile selection at 5L/min and 25 °C range

Profile	$t_{cool}$ (s)	Estimated $t_{cycle}$ (s)	Cycles/h, N	Productivity change compared with circular profile (%)	Annual machine hours per 500,000 parts
Circular	93.978	111.288	32.35	Reference	15,456.67 h
Elliptical	95.62	112.93	31.88	-1.45%	15,684.72 h
Teardrop	91.23	108.54	33.17	2.53%	15,075.00 h

Results in Table 26 indicate that the profile level productivity impact is less than the straight-line versus conformal cooling difference, but still significant for repeat production. The teardrop conformal profile saves an estimated 2.748 s of cycle time when compared to the circular conformal profile. This results in the productivity gain of approximately 2.53% at the matched condition. This results in an estimated machine-time saving of ~381.67 h/year over the assumed annual part production volume of 500,000 parts and the circular conformal profile. Thus the teardrop profile is not a large process-level change on its own, but does offer a small and useful cycle time benefit when the mould is being used on high volume production. The opposite trend is observed with the elliptical profile. It provides slightly more time to reach ejection temperature than the circular profile at the desired condition. Hence, it is less productive than the circular and teardrop profiles. However, this does not mean that the elliptical profile is not useful. The primary benefit of it is not to reduce cooling time but to reduce the tendency to create a high pressure drop, since it is the lowest pressure drop tendency among conformal profiles. This implies that cycle time alone can't be used to make the profile decision. If maximum thermal performance and shorter cycle time is the production goals, the teardrop profile is more favourable. The elliptical profile is still relevant if the limiting factor is hydraulic resistance or capacity of the coolant loop. The difference in straight-line and conformal cooling is far greater than the difference in conformal profile shapes. For this reason, the industrial significance of the profile comparison is not to be understood as an alternative to the general conformal cooling benefit, but as an optimisation benefit once the conformal cooling has been

determined. In this study, the teardrop profile is the most favourable producing effect in the conformal cooling group, and the straight-line comparison only validates the general conformal routing benefit.

### 4.3. Energy Usage and Hydraulic Operating Trade-Off

The second impact of profile selection is related to energy use and hydraulic operating requirements. Though the time to reach the ejection temperature is influenced by the profile of the cooling channel, so is the coolant pressure drop. The two effects should be taken together as the best thermal profile is not always the best hydraulic profile. Based on previous energy studies for injection moulding, it is found that the energy consumption depends on the injection moulding machine, mould, and material and process parameters and thus the energy results should be considered as process-specific rather than universal values [39, 40]. The machine energy per part is estimated in the simplified scenario model based on the average machine power and estimated cycle time:

$$E_{machine,part} = P_m \times \frac{t_{cycle}}{3600} \quad (28)$$

Where  $E_{machine,part}$  is the machine energy per part in kWh/part,  $P_m$  is the assumed average machine power in kW, and  $t_{cycle}$  is the calculated cycle time in seconds. The annual machine energy is then calculated as:

$$E_{machine,annual} = E_{machine,part} \times V_a \quad (29)$$

Where  $V_a$  is the annual production volume. Finally, the approximate hydraulic power required to overcome the coolant pressure drop is calculated as:

$$P_{hyd} = \frac{Q \cdot \Delta P}{\eta_p} \quad (30)$$

Where  $P_{hyd}$  is the hydraulic power in W,  $Q$  is the coolant volumetric flow rate in  $m^3/s$  (equivalent to  $8.33 \times 10^{-5} m^3/s$ , for the case of 5 L/min),  $\Delta P$  is the coolant pressure drop in Pa, and  $\eta_p$  is the assumed pump efficiency of 0.60 as a real pump is not always 100% efficient. The calculated energy and hydraulic comparison is shown in Table 27 below.

**Table 27.** Estimated machine-energy and hydraulic-power comparison of the CCC profiles at 5L/min and 25°C

Profile	$\Delta P$ (kPa)	Estimated machine energy per part (kWh/part)	Annual machine energy for 500,000 parts (kWh/year)	Approx. pump power at ( $\eta_p = 0.60$ ) (W)
Circular	18	0.4637	2,31,850	2.500
Elliptical	17	0.4705	2,35,270.83	2.361
Teardrop	18	0.4523	2,26,125	2.500

From the results in Table 27, it is seen that the teardrop profile has the lowest estimated machine energy per part as it has the shortest estimated cycle time. Under the assumed production volume and machine-power scenario, the teardrop conformal profile is capable of reducing the annual energy demanded by the machine by about 5,725 kWh/year when compared to the circular conformal profile. This saving is not due to a reduction in pressure drop but rather by the reduction in cycle time. Thus,

the advantage of the teardrop profile is primarily on the thermal aspect. The estimated machine energy is slightly higher at the selected matched condition for the elliptical profile than the circular profile due to a longer simulated time to reach ejection temperature. But, it provides the smallest pressure drop of all conformal profiles. Hence, this has led to a slightly reduced calculated ideal hydraulic power and estimated pump power for the elliptical profile. This is because the absolute pressure-drop values are still low with regard to pump power in this case, where the difference is small (5 L/min). In this case, the potential hydraulic saving of the elliptical profile is not significant, but it might be more significant in a mould with longer cooling circuits, a higher flow rate, more parallel/serial channels or limited coolant-pump capacity.

The comparison illustrates the principal benefit of the profile selection. When looking to minimise hot spots, cooling time and time-dependent machine energy, the teardrop profile is more favourable. The elliptical shape is more desirable where low hydraulic resistance is desired. For the practical conformal reference, the circular profile still gets the most balanced behaviour, and it is easier to read the geometry with it. Thus, the selection of the profile should be based on the priority of production. For the present simulation domain, the teardrop profile is the best thermal and time-based energy option, while the elliptical profile is the best hydraulic option. Also, it should be noted that the calculated pump power is very small as compared to the assumed machine power. For instance, the pump power of the circular and teardrop profiles is approximately 2.5 W, and the machine power assumed is 15 kW. It is not to say that pressure drop is not a critical factor. It simply indicates that for the particular short circuit simulation condition, the effect on the energy under cycle time reduction is sufficiently high compared to the pumping-energy difference. In an actual production system, additional hose and fitting losses, manifold losses, cooling losses, losses due to surface roughness and flow-control equipment would have to be added prior to making a final coolant-system decision.

#### 4.4. Environmental and Economic Impact of Profile Selection

The influence of the environmental effect of the profile selection is predominantly associated with the difference in the estimated machine operating time [42]. The teardrop profile would also provide the lowest time-dependent machine energy consumption in the scenario model since it results in the lowest estimated cycle time at the selected matched condition. Compared with the circular profile the elliptical profile has the lowest pressure-drop tendency, however, a longer cooling time compared to the circular profile at this condition, which leads to longer estimated machine operating time. This demonstrates that the environmental implications of the choice of profile vary depending on the desired outcome, either thermal productivity or hydraulic efficiency. The annual machine-hour saving compared with circular conformal profile is calculated as:

$$H_{saved} = \frac{V_a(t_{cycle,circular} - t_{cycle,profile})}{3600} \quad (31)$$

Where  $H_{saved}$  is the annual machine time saved in h/year,  $V_a$  is the annual production volume in parts/year,  $t_{cycle,circular}$  is the estimated cycle time of the circular conformal profile in seconds,  $t_{cycle,profile}$  is the estimated cycle time of the selected profile in seconds. The annual machine-energy saving is therefore calculated as:

$$E_{saved} = H_{saved} \times P_m \quad (32)$$

Where  $E_{saved}$  is the annual energy saving in kWh/year,  $H_{saved}$  is the annual machine time saved in h/year, and  $P_m$  is the assumed average machine power in kW. Thus, the corresponding CO<sub>2</sub> reduction can be estimated as:

$$CO2_{saved} = E_{saved} \times EF_{grid} \quad (33)$$

Where  $CO2_{saved}$  is the estimated carbon dioxide reduction in kg CO<sub>2</sub>/year,  $E_{saved}$  is the annual energy saving in kWh/year, and  $EF_{grid}$  is the assumed electricity grid emission factor in kg CO<sub>2</sub>/kWh. Scaling this into annual cost savings estimated from machine-time saving and electricity saving:

$$C_{annual} = (H_{saved} \times C_h) + (E_{saved} \times C_e) \quad (34)$$

Where  $C_{annual}$  is the estimated annual saving in €/year,  $C_h$  is the assumed machine hourly rate in €/h, and  $C_e$  is the assumed electricity price in €/kWh. Finally, a simple payback period for AM additional tooling cost can be calculated as:

$$PB = \frac{C_t}{C_{annual}} \quad (35)$$

Where  $PB$  is the payback period in years,  $C_t$  is the assumed AM tooling cost for the injection mould insert in €, and  $C_{annual}$  is the estimated annual savings in €/year. The following Table 28 shows the calculated environmental and economic impact values calculated using the above equations. The circular profile is used as a conformal reference case.

**Table 28.** Calculated impact of elliptical and teardrop profiles on energy savings and CO<sub>2</sub> reduction at matched process conditions selected

Profile	Machine hours saved compared with circular (h/year)	Energy saving compared with circular (kWh/year)	CO <sub>2</sub> reduction compared with circular (kg CO <sub>2</sub> /year)	Estimated annual saving (€/year)	Simple payback period
Circular	0	0	0	0	Reference
Elliptical	-228.05	-3,420.83	-855.21	-9,806.39	Not applicable
Teardrop	381.67	5,725.00	1,431.25	16,411.67	0.49 years

The results indicate that in selected scenario, the teardrop profile provides the best economic and environmental benefit as it has a lower estimated cycle time than the circular profile. The estimated savings are 381.67 hours of machine time per year and 5,725 kWh per year with an assumed production rate of 500,000 parts per year. This equals to an estimated reduction of 1,431.25 kg CO<sub>2</sub>/year and annual savings of some 16,411.67 €/year. Assuming that there is an extra tooling cost of 8,000 €, which is specific to the tool, the simple payback period is about 0.49 years. In this scenario, the saving for elliptical profile is not provided since the simulated cooling time for it is higher than that of the circular profile at 5 L/min and 25°C. This result should not be taken as a statement of overall suitability of the profile, however. It's value is related to reduced hydraulic resistance, which may be more significant for longer cooling circuits, increased flow rates, and/or pump-capacity restrictions. Hence, the teardrop profile is more useful for energy and production cost reduction, which are time-dependent, and elliptical profile remains useful from a hydraulic-design point of view. The values in Table 28 are an estimated potential impact only. The electricity price, machine hourly rate, grid emission factor and extra tooling cost are assumed in the case. In industrial applications,

these values need to be substituted with data obtained on site in the factory, like measured electricity consumption, real production volume, quotation for mould inserts, coolant-system performance, etc.

#### 4.5. Practical Implementation and Conformal Profile Selection

The final decision on which cooling channel profile to use for the cooling should not be made on the thermal result of the simulation alone. For the present study, the teardrop profile results in the best thermal performance, however, other factors must be taken into consideration for industrial applications such as manufacturability, surface quality, powder removal, inspection, pressure drop and tooling cost. The shape, size, location, mechanical strength and coolant pressure drop are all factors that should be accounted for in making the design of conformal cooling channels, which are typically made possible through additive manufacturing or hybrid additive-subtractive manufacturing [38]. This is particularly relevant for non-circular conformal cooling channels and the manufacturability. While circular channels are well known, some additive or hybrid manufacturing processes can have challenges in manufacturing internal channels, as overhangs may be an issue [43]. Another important factor is the quality of the internal surface. The geometry of the channels used in the simulations for this study are idealised and the surfaces of real additively manufactured channels may be rougher. This can affect the flow, pressure drop and the transfer of the heat of the coolant. Thus, the pressure drop results may be regarded as the best simulation results until the profile is made and tested. The roughness of the surface has also been observed to influence the flow behaviour and efficiency of cooling channel in additively manufactured conformal cooling channels [37]. The following Table 29. Summarises the practical interpretation and implementation concerns as per each profile.

**Table 29.** Per-profile strength, implementation concern and practical interpretation

Profile	Main strength in this study	Main implementation concern	Practical interpretation
Circular	Standard conformal reference with balanced behaviour	Does not give the strongest hot-spot reduction	Suitable when a conventional and lower-risk conformal profile is preferred
Elliptical	Lowest pressure-drop tendency among conformal profiles	Weaker cooling-time result at the selected condition	Suitable when hydraulic resistance or pump limitation is important
Teardrop	Lowest $T_{max}$ and shortest $t_{cool}$	Requires manufacturability, surface quality and cleaning verification	Suitable when hot-spot control and cycle-time reduction are the main priorities

Hence, the selection of the profile should be based on production priority. If the primary objective is to minimise hot spots and minimise time to reach ejection temperature then the teardrop profile is the most desirable profile in the simulations performed. The elliptical profile is more appealing if the pressure loss of the coolant is the major concern. The circular profile is still useful as the reference conformal design as it offers well-balanced behaviour, and is easier to implement and compare. The selected profile should undergo the following before final industrial use: Manufacturability, Surface-quality assessment, Pressure testing and Physical moulding validation.

#### 4.6. Chapter Summary

This chapter interpreted the results of the cooling-channel profile from Chapter 3 from both an economic and environmental perspective. Given that the study was based on simulation, the impact

assessment was created as a scenario-based calculation model. The model involved the simulated time to reach ejection temperature, maximum part temperature, coolant pressure drop and assumed annual production volume, machine power, electricity price, machine hourly rate, grid emission factor and extra tooling cost. The difference between the circular, elliptical and teardrop conformal profiles was found to be relatively small in the productivity calculation, but may be important in the case of repeated production. At the matched condition of 5L/min and 25°C, the teardrop profile was found to have a 2.748 s lower estimated cycle time as compared to the circular conformal profile. This would translate to a potential machine-time savings of approximately 381.67 h/year for the assumed annual production volume of 500,000 parts. This means that improvement of cooling at the profile level – even if only a small one – can be useful in large volume production. This energy and hydraulic comparison revealed that there is a compromise to select the profile. The lowest machine energy consumption for the different times of operation was achieved for the teardrop profile due to the shortest cooling time. The elliptical profile was found to provide the least tendency to increase pressure drop of the conformal profiles. Thus, the teardrop profile is more advantageous if the primary goal is the reduction of hot-spots and improvement of cooling-time, and the elliptical profile is more advantageous if hydraulic resistance is the primary concern. It was found that in comparison with the circular profile, the teardrop profile resulted in an annual energy saving of 5,725 kWh/year and a carbon dioxide reduction of 1,431.25 kg CO<sub>2</sub>/year which was estimated using the environmental and economic calculation. The total assumed additional tooling cost resulted in simple payback period of 0.49 years with the estimated annual saving of 16,411.67 €/year. It is important to note that those values are indicative of potential impact as they are based on assumed production data and have not been proven with physical production. At the overall level, identification of balance between thermal performance and hydraulic behaviour of a profile was seen as practically useful. The optimum teardrop profile for the investigated range is the best thermal profile and the elliptical profile is the best hydraulic profile. For final industrial use, the cost would have to be evaluated on a factory-by-factory basis from the manufactured inserts and also validated physically in the moulding process.

## Conclusions

1. Existing studies confirm that conformal cooling channels significantly improve heat removal and reduce cooling time compared with conventional straight-line cooling channels. However, previous studies on conformal cooling have been primarily conducted with circular channel profiles. This shows that the efficiency of conformal cooling can be further improved by changing the cross-section profile of the channel. Thus, non-circular profiles (elliptical and teardrop channels) were determined to be potentially important alternatives to be explored.
2. The simulation framework was established with one geometry, one mould material, one polymer material, and one common conformal cooling route, thus the comparison can be mainly conducted on the cooling-channel profile and the operation parameters of the coolant. Three different forms of profiles for conformal cooling were chosen: circular, elliptical and teardrop. Coolant was run at three different flow rates of 2, 5 and 10 L/min and three different inlet temperatures of 15, 25 and 35°C. The performance indicators chosen were average part temperature ( $T_{avg}$ ), maximum part temperature ( $T_{max}$ ), time to reach ejection temperature ( $t_{cool}$ ), coolant pressure drop ( $\Delta P$ ), average Reynolds number and warpage displacement ( $warp$ ). These responses were used to compare the cooling systems thermally, hydraulically and dimensionally.
3. The Moldex3D simulation results demonstrated that conformal cooling channels were able to enhance the cooling effect when compared with the straight-line base case. For the conformal cooling profiles, the teardrop profile always provided the best local thermal performance, lowering the maximum part temperature and time to ejection. The elliptical profile on the other hand, exhibited better hydraulic behaviour, resulting in lower pressure drop in the cooling channel. This indicates that the optimum profile depends on the objective: either to improve the thermal properties, or to enhance the hydraulic properties.
4. The simulation and RSM comparison showed clear differences between the three conformal profiles. The teardrop profile turned out to be the best thermal profile with the lowest maximum part temperature and cooling time. Among the profiles, elliptical profile exhibited the least tendency to pressure drop and hence is favourable in situations where pressure drop is a major concern. There was little difference between warpage in profiles, the largest profile level difference being approximately 0.009 mm. The results of the RSM analysis revealed that the optimum region for the present study was at a moderate flow rate of the coolant and low coolant inlet temperature, around 4.713-5.273 L/min and 15.611-16.023°C, respectively, with teardrop profile having the highest desirability.
5. The industrial impact assessment revealed that the teardrop conformal cooling profile can be used to practically achieve cycle-time, energy and environment benefits for the selected production scenario. The representative matched operating condition teardrop profile showed the greatest improvement in cycle times over the straight-line baseline. This enhancement suggests potential opportunities for shorter machine operation times, higher production yields, lower electricity use and lower emissions associated with electricity use. The economic analysis also revealed that the extra expense incurred for conformal cooling is economical under high volume production. Hence, the teardrop conformal cooling shape is the most beneficial for the chosen geometry regarding a combination of thermal performance, cycle-time reduction and industrial applicability.

## Recommendations

1. The teardrop conformal cooling profile is recommended when the primary application is to enhance local thermal control, reduce hot spots and shorten cooling time. This profile had the best performance in the simulation results for maximum part temperature and time to reach ejection temperature. Hence, it is particularly recommended for parts with ribs, bosses, corners and other areas of localised thickness which, after the general cooling phase, are likely to retain heat. When the primary consideration for the mould design is thermal performance, the teardrop profile should be taken into consideration by the mould designer.
2. The elliptical profile is recommended if the hydraulic efficiency is more important. The teardrop profile exhibited more favourable local thermal performance while the elliptical profile exhibited more favourable pressure-drop behaviour when operating under matched conditions. This is beneficial for cooling systems where pumping power, coolant-circuit resistance or pressure are significant practical considerations. Therefore, the final decision on which profile to choose, teardrop or elliptical, should be based on the main goal of the production, either shorter cooling time or lower hydraulic resistance in an industrial application.
3. Experimental validation is recommended before industrial implementation. A mould insert with the selected conformal cooling profile should be manufactured, using metal additive manufacturing, and tested under real injection-moulding conditions. The measured cooling time, part temperature, measured pressure drop and warpage should then be used for comparison with the Moldex3D results. This is important since there are phenomena that are hard to capture in simulation, which are present in real moulds, such as surface roughness in printed channels, actual coolant flow losses, imperfect thermal contact, machine variation and material-processing variation.
4. Further research should be conducted on other non-circular channel shapes as well as other orientation of profiles and other channel's conformal routes. One representative casing-type geometry, one material system, one mould material and one conformal routing strategy was used in the present study. So these findings should be expanded to other part geometries, wall thickness distributions, polymer materials and mould materials, to make general conclusions for all injection-moulded products. Additional research would also be worth exploring to analyse hybrid cooling configurations, varying channel spacings, varying standoff distances, and varying profile shapes and channel-route optimisation.
5. In high volume injection moulding, conformal cooling should be taken into consideration for industrial applications where cooling time has a significant effect on productivity and cost. Optimised conformal cooling can help cut machine operating times, boost the production output, help achieve uniform temperatures, and minimise thermal defect waste. These enhancements can also reduce the energy usage and help make polymer production more sustainable. The increased manufacturing cost of conformal inserts must, however, be balanced against anticipated production volumes, energy savings and quality improvements. Conformal cooling is therefore best suited in situations where the volume of production is high enough to justify the extra cost of the tooling, because of the cycle-time and quality advantages.

## List of References

1. GASPAR-CUNHA, A.; MELO, João Bernardo; MARQUES, Tomás Bilau and PONTES, A. J. A review on injection molding: conformal cooling channels, modelling, surrogate models and multi-objective optimization. *Polymers*, vol. 17 (2025), no. 7, pp. 1–37. Available from: <https://doi.org/10.3390/polym17070919>
2. LIOU, Guan-Yan; SU, Wei-Jie; CHENG, Feng-Jung; CHANG, Chen-Hsiang; TSENG, Ren-Ho, et al. Optimize Injection-Molding Process Parameters and Build an Adaptive Process Control System Based on Nozzle Pressure Profile and Clamping Force. *Polymers*, vol. 15 (2023), no. 3, pp. 610. Available from: <https://doi.org/10.3390/polym15030610>
3. CHEN, Jinping; CUI, Yanmei; LIU, Yuanpeng and CUI, Jianfeng. Design and Parametric Optimization of the Injection Molding Process Using Statistical Analysis and Numerical Simulation. *Processes*, vol. 11 (2023), no. 2, pp. 414. Available from: <https://doi.org/10.3390/pr11020414>
4. FU, Junyu and MA, Yongsheng. A method to predict early-ejected plastic part air-cooling behavior towards quality mold design and less molding cycle time. *Robotics and computer-integrated manufacturing*, vol. 56 (2019), pp. 66–74. Available from: <https://dx.doi.org/10.1016/j.rcim.2018.08.004>
5. ZHAO, Nan-yang; LIAN, Jiao-yuan; WANG, Peng-fei and XU, Zhong-bin. Recent progress in minimizing the warpage and shrinkage deformations by the optimization of process parameters in plastic injection molding: a review. *International journal of advanced manufacturing technology*, vol. 120 (2022), no. 1, pp. 85–101. Available from: <https://link.springer.com/article/10.1007/s00170-022-08859-0>
6. COCA-GONZALEZ, Manuel and JIMENEZ-MARTINEZ, Moises. Warpage: Causes, manufacturing processes and future challenges: A review. *Proceedings of the Institution of Mechanical Engineers. Part L, Journal of materials, design and applications*, vol. 239 (2025), no. 6, pp. 1201–1217. Available from: <https://doi.org/10.1177/14644207241285399>
7. VENKATESH, G.; RAVI KUMAR, Y. and RAGHAVENDRA, G. Comparison of Straight Line to Conformal Cooling Channel in Injection Molding. *Materials today : proceedings*, vol. 4 (2017), no. 2, pp. 1167–1173. Available from: <https://dx.doi.org/10.1016/j.matpr.2017.01.133>
8. SHINDE, Mahesh S. and ASHTANKAR, Kishor M. Additive manufacturing–assisted conformal cooling channels in mold manufacturing processes. *Advances in Mechanical Engineering*, vol. 9 (2017), no. 5, pp. 168781401. Available from: <https://doi.org/10.1177/1687814017699764>
9. SHAYFULL, Z.; SHARIF, S.; ZAIN, Azlan Mohd; GHAZALI, M. F. and SAAD, R. Mohd. Potential of Conformal Cooling Channels in Rapid Heat Cycle Molding: A Review. *Advances in Polymer Technology*, vol. 33 (2014), no. 1, pp. 21381–n/a. Available from: <https://doi.org/10.1002/adv.21381>
10. KADIVAR, Mohammadreza; MCGRANAGHAN, Gerard; TORMEY, David; KARIMINEJAD, Mandana and MCAFEE, Marion. Comparison of Conventional and Conformal Cooling Channels in the Production of a Commercial Injection-Moulded Component. *Key engineering materials*, vol. 926 (2022), pp. 1821–1831. Available from: <https://doi.org/10.4028/p-q2k0v8>
11. MASOUDI, Soroush; DAS, Barun K.; AAMIR, Muhammad and TOLOUEI-RAD, Majid. Recent advancement in conformal cooling channels: A review on design, simulation and future trends. *Computer aided design*, vol. 186-187 (2025), pp. 103899. Available from: <https://dx.doi.org/10.1016/j.cad.2025.103899>

12. WEI, Zhihao; WU, Jiakai; SHI, Nan and LI, Lei. Review of Conformal Cooling System Design and Additive Manufacturing for Injection Molds. Springfield: AIMS Press, Jan 1, 2020. Available from: <https://www.aimspress.com/article/doi/10.3934/mbe.2020292>
13. TAN, Chaolin; WANG, Di; MA, Wenyong; CHEN, Yaorong; CHEN, Shijin, et al. Design and additive manufacturing of novel conformal cooling molds. *Materials & design*, vol. 196 (2020), pp. 109147. Available from: <https://dx.doi.org/10.1016/j.matdes.2020.109147>
14. TORRES-ALBA, Abelardo; MERCADO-COLMENERO, Jorge Manuel; DIAZ-PERETE, Daniel and MARTIN-DOÑATE, Cristina. A New Conformal Cooling Design Procedure for Injection Molding Based on Temperature Clusters and Multidimensional Discrete Models. *Polymers*, vol. 12 (2020), no. 1, pp. 154. Available from: <https://doi.org/10.3390/polym12010154>
15. KANBUR, Baris Burak; ZHOU, Yi; SHEN, Suping; WONG, Kim Hai; CHEN, Charles, et al. Metal Additive Manufacturing of Plastic Injection Molds with Conformal Cooling Channels. *Polymers*, vol. 14 (2022), no. 3, pp. 424. Available from: <https://doi.org/10.3390/polym14030424>
16. GÖKTAŞ, Mustafa and GÜLDAŞ, Abdulmecit. Production of Plastic Injection Molds with Conformal Cooling Channels by Laminated Brazing Method. *GAZI UNIVERSITY JOURNAL OF SCIENCE*, vol. 33 (2020), no. 3, pp. 780–789. Available from: <https://doi.org/10.35378/gujs.621930>
17. WAHL, Jan Philipp; NIEDERMEYER, Jens; BERNHARD, Robert; HERMSDORF, Jörg and KAIERLE, Stefan. Design of additively manufacturable injection molds with conformal cooling. *Procedia CIRP*, vol. 111 (2022), pp. 97–100. Available from: <https://dx.doi.org/10.1016/j.procir.2022.08.146>
18. SIMIYU, Laura W.; MUTUA, James M.; MUIRURI, Patrick I. and IKUA, Bernard W. Optimization of polygonal cross-sectioned conformal cooling channels in injection molding. *International journal on interactive design and manufacturing*, vol. 18 (2024), no. 3, pp. 1593–1609. Available from: <https://link.springer.com/article/10.1007/s12008-023-01226-7>
19. WANG, Yuandi and LEE, Changmyung. Design and Optimization of Conformal Cooling Channels for Increasing Cooling Efficiency in Injection Molding. *Applied sciences*, vol. 13 (2023), no. 13, pp. 7437. Available from: <https://doi.org/10.3390/app13137437>
20. NGUYEN, Van-Thuc; MINH, Pham Son; UYEN, Tran Minh The; DO, Thanh Trung; HA, Nguyen Canh, et al. Conformal Cooling Channel Design for Improving Temperature Distribution on the Cavity Surface in the Injection Molding Process. *Polymers*, vol. 15 (2023), no. 13, pp. 2793. Available from: <https://doi.org/10.3390/polym15132793>
21. VARGAS-ISAZA, Carlos; BENITEZ-LOZANO, Adrian and RODRIGUEZ, Johnatan. Evaluating the Cooling Efficiency of Polymer Injection Molds by Computer Simulation Using Conformal Channels. *Polymers*, vol. 15 (2023), no. 20, pp. 4044. Available from: <https://doi.org/10.3390/polym15204044>
22. KUO, Chil-Chyuan; XU, Jing-Yan; ZHU, Yi-Jun and LEE, Chong-Hao. Effects of Different Mold Materials and Coolant Media on the Cooling Performance of Epoxy-Based Injection Molds. *Polymers*, vol. 14 (2022), no. 2, pp. 280. Available from: <https://doi.org/10.3390/polym14020280>
23. GAO, Peng; LIU, Dun; PEI, Yutao and FENG, Shaochuan. Optimal Reynolds number of cooling water in conformal cooling molds. *Applied thermal engineering*, vol. 236 (2024), pp. 121509. Available from: <https://dx.doi.org/10.1016/j.applthermaleng.2023.121509>
24. SUN, Yupeng; DASTIDAR, Aniket Ghosh; AGAZZI, Alban; LE GOFF, Ronan and ALEXANDERSEN, Joe. Topology optimisation of conformal cooling channels in injection

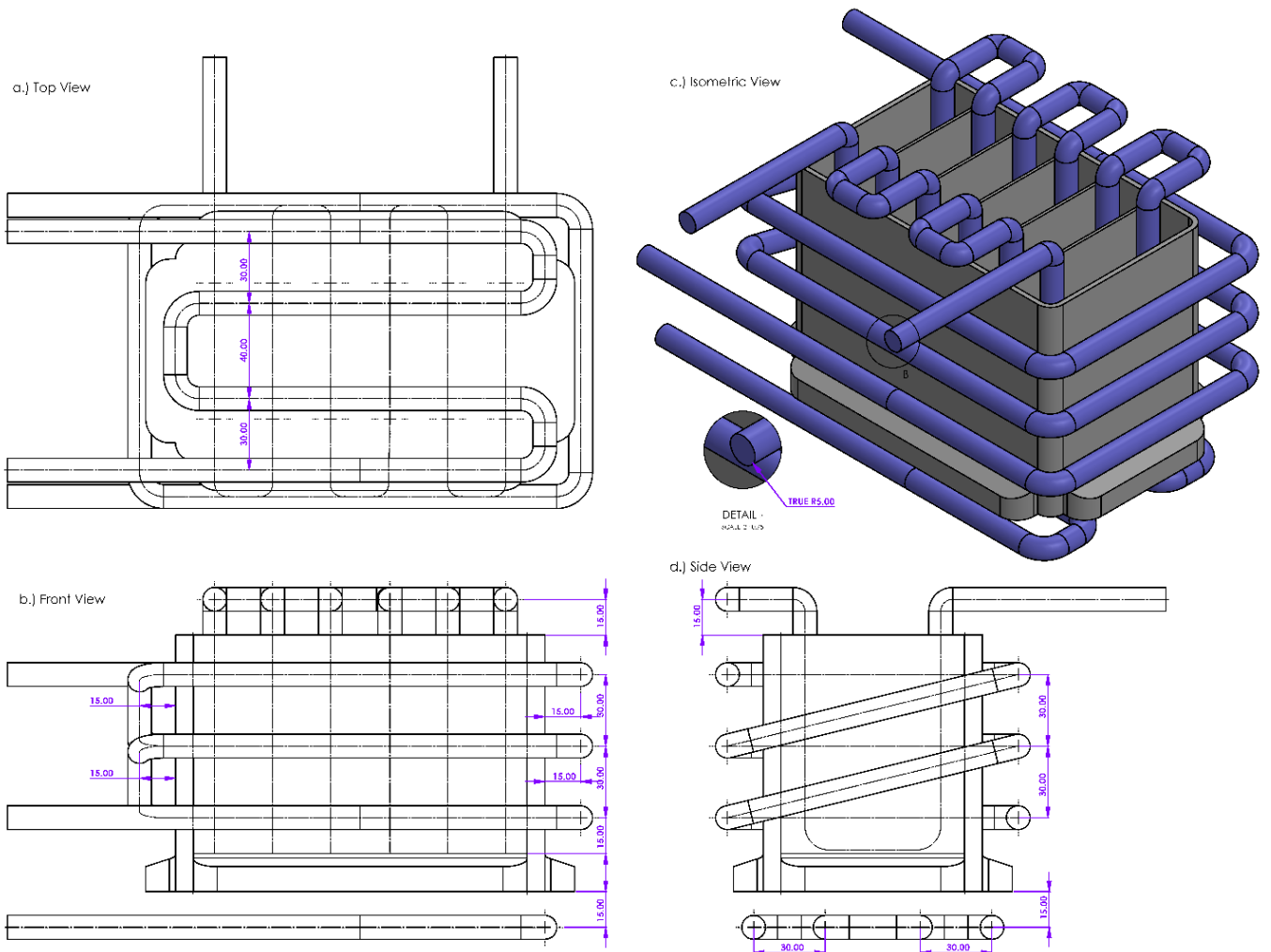
- moulding: a scaling strategy for forced convection in high Reynolds number flows. *Structural and multidisciplinary optimization*, vol. 68 (2025), no. 8. Available from: <https://link.springer.com/article/10.1007/s00158-025-04067-y>
25. MAZUR, Maciej; BRINCAT, Paul; LEARY, Martin and BRANDT, Milan. Numerical and experimental evaluation of a conformally cooled H13 steel injection mould manufactured with selective laser melting. *International journal of advanced manufacturing technology*, vol. 93 (2017), no. 1-4, pp. 881–900. Available from: <https://link.springer.com/article/10.1007/s00170-017-0426-7>
  26. WAGNER, Gabriel Mar Pinto and NÓBREGA, J. M. Conformal cooling channels in injection molding and heat transfer performance analysis through CFD - a review. *Energies (Basel)*, vol. 18 (2025), no. 8, pp. 1972. Available from: <https://doi.org/10.3390/en18081972>
  27. CLARK, Rebecca; ROCHMAN, Arif; REFALO, Paul; FARRUGIA, Philip and VELLA, Pierre. Towards sustainable injection moulding using 3D printed conformal cooling channels: a comparative simulation study. *Progress in additive manufacturing*, vol. 9 (2024), no. 5, pp. 1341–1352. Available from: <https://link.springer.com/article/10.1007/s40964-024-00609-w>
  28. LI, Jinyi; ONG, Yung Chieh and WAN MUHAMAD, Wan Mansor. Optimization Design of Injection Mold Conformal Cooling Channel for Improving Cooling Rate. *Processes*, vol. 12 (2024), no. 6, pp. 1232. Available from: <https://www.proquest.com/docview/3072665199>
  29. PURGLEITNER, Bianca; VILJOEN, David; KÜHNERT, Ines and BURGSTALLER, Christoph. Influence of injection molding parameters, melt flow rate, and reinforcing material on the weld-line characteristics of polypropylene. *Polymer Engineering and Science*, vol. 63 (2023), no. 5, pp. 1551–1566. Available from: <https://onlinelibrary.wiley.com/doi/abs/10.1002%2Fpen.26305>
  30. MYERS, Mason; MULYANA, Rachmat; CASTRO, Jose M. and HOFFMAN, Ben. Experimental Development of an Injection Molding Process Window. *Polymers*, vol. 15 (2023), no. 15, pp. 3207. Available from: <https://doi.org/10.3390/polym15153207>
  31. KUO, Chil-Chyuan and ZHU, Yi-Jun. Characterization of Epoxy-Based Rapid Mold with Profiled Conformal Cooling Channel. *Polymers*, vol. 14 (2022), no. 15, pp. 3017. Available from: <https://www.proquest.com/docview/2700757029>
  32. CHUNG, Chen-Yuan and LIU, Chuan-Jen. Metal additive manufacturing of conformal cooling channels for improving the quality of metal injection-molded products. *Advances in mechanical engineering*, vol. 16 (2024), no. 10. Available from: <https://journals.sagepub.com/doi/full/10.1177/16878132241282210>
  33. WILSON, Neil; GUPTA, Manhar; PATEL, Milan; MAZUR, Maciej; NGUYEN, Vu, et al. Generative design of conformal cooling channels for hybrid-manufactured injection moulding tools. *International journal of advanced manufacturing technology*, vol. 133 (2024), no. 1-2, pp. 861–888. Available from: <https://link.springer.com/article/10.1007/s00170-024-13754-x>
  34. MOHD HANID, Mohd Hazwan; ABD RAHIM, Shayfull Zamree; GONDRO, Joanna; SHARIF, Safian; AL BAKRI ABDULLAH, Mohd Mustafa, et al. Warpage Optimisation on the Moulded Part with Straight Drilled and Conformal Cooling Channels Using Response Surface Methodology (RSM), Glowworm Swarm Optimisation (GSO) and Genetic Algorithm (GA) Optimisation Approaches. *Materials*, vol. 14 (2021), no. 6, pp. 1326. Available from: <https://doi.org/10.3390/ma14061326>
  35. WILSON, Neil; GUPTA, Manhar; MAZUR, Maciej; PATEL, Milan J.; NGUYEN, Vu, et al. Analysis of self-supporting conformal cooling channels additively manufactured by hybrid

- directed energy deposition for IM tooling. *International journal of advanced manufacturing technology*, vol. 132 (2024), no. 1-2, pp. 421–441. Available from: <https://link.springer.com/article/10.1007/s00170-024-13291-7>
36. LOVE, Jonathon; SELKER, Ravi; MARSMAN, Maarten; JAMIL, Tahira; DROPMANN, Damian, et al. JASP: Graphical Statistical Software for Common Statistical Designs. *Journal of Statistical Software*, vol. 88 (2019), no. 2, pp. 1–17. Available from: <https://www.jstatsoft.org/index.php/jss/article/view/v088i02/v88i02.pdf>
  37. HANZLIK, Jan; VANEK, Jiri; PATA, Vladimir; SENKERIK, Vojtech; POLASKOVA, Martina, et al. The Impact of Surface Roughness on Conformal Cooling Channels for Injection Molding. *Materials*, vol. 17 (2024), no. 11, pp. 2477. Available from: <https://doi.org/10.3390/ma17112477>
  38. FENG, Shaochuan; KAMAT, Amar M. and PEI, Yutao. Design and fabrication of conformal cooling channels in molds: Review and progress updates. *International Journal of Heat and Mass Transfer*, vol. 171 (2021), pp. 121082. Available from: <https://dx.doi.org/10.1016/j.ijheatmasstransfer.2021.121082>
  39. MATARRESE, P.; FONTANA, A.; SORLINI, M.; DIVIANI, L.; SPECHT, I., et al. Estimating energy consumption of injection moulding for environmental-driven mould design. *Journal of cleaner production*, vol. 168 (2017), pp. 1505–1512. Available from: <https://dx.doi.org/10.1016/j.jclepro.2017.07.144..>
  40. ELDUQUE, Ana; ELDUQUE, Daniel; CLAVERÍA, Isabel and JAVIERRE, Carlos. Influence of material and injection molding machine’s selection on the electricity consumption and environmental impact of the injection molding process: An experimental approach. *International Journal of Precision Engineering and Manufacturing-Green Technology*, 5(1), vol. 5 (2018), no. 1, pp. 13–28. Available from: <https://link.springer.com/article/10.1007/s40684-018-0002-0..>
  41. ELDUQUE, Ana; ELDUQUE, Daniel; PINA, Carmelo; CLAVERÍA, Isabel and JAVIERRE, Carlos. Electricity Consumption Estimation of the Polymer Material Injection-Molding Manufacturing Process: Empirical Model and Application. *Materials*, vol. 11 (2018), no. 9, pp. 1740. Available from: <https://doi.org/10.3390/ma11091740>
  42. DAVIS, William; LUNETTO, Vincenzo; PRIARONE, Paolo C.; CENTEA, Dan and SETTINERI, Luca. An appraisal on the sustainability payback of additively manufactured molds with conformal cooling. *Procedia CIRP*, vol. 90 (2020), pp. 516–521. Available from: <https://dx.doi.org/10.1016/j.procir.2020.01.064>
  43. LAMARCHE-GAGNON, Marc-Étienne; MOLAVI-ZARANDI, Marjan; RAYMOND, Vincent and ILINCA, Florin. Additively manufactured conformal cooling channels through topology optimization. *Structural and multidisciplinary optimization*, vol. 67 (2024), no. 8, pp. 138. Available from: <https://doi.org/10.1007/s00158-024-03846-3>

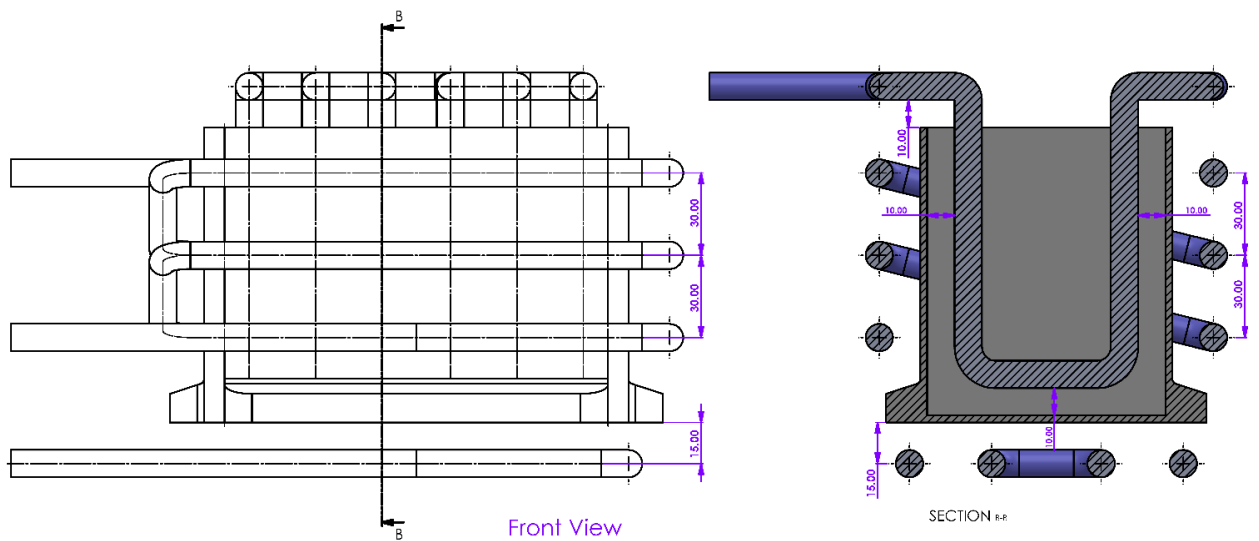
## Appendices

### Appendix 1. SolidWorks CAD of Conformal Cooling Channel Routing

#### Part Geometry with Conformal Cooling Routing (all views)

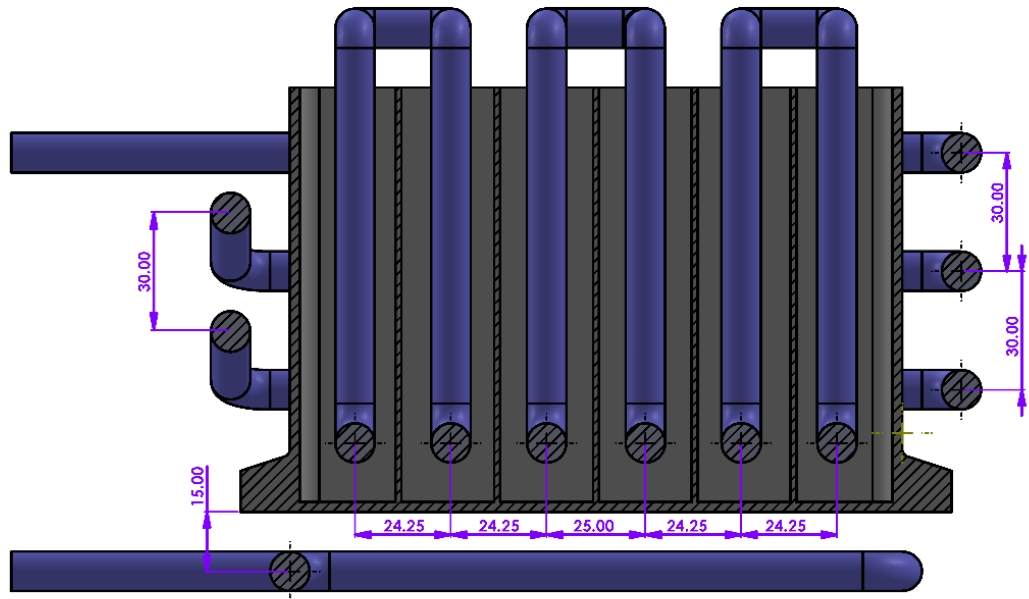


#### Part Geometry with Conformal Cooling Routing (Section View)

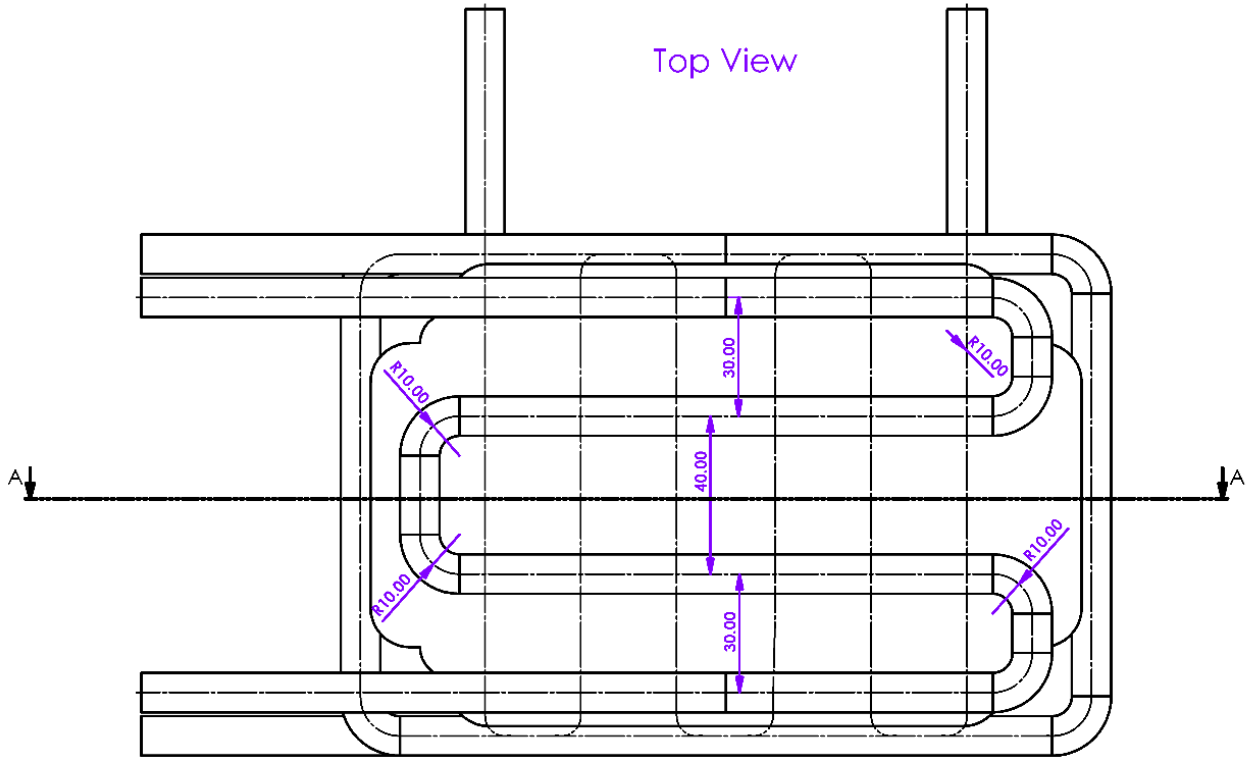


Part Geometry with Conformal Cooling Routing (Section View)

SECTION A-A



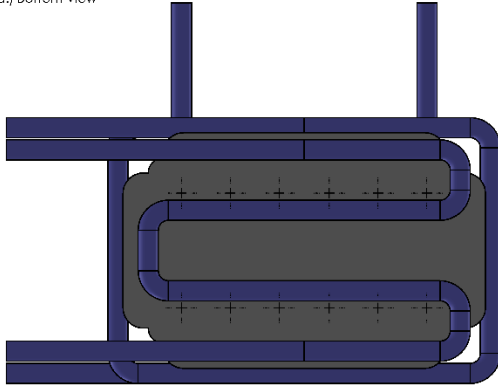
Top View



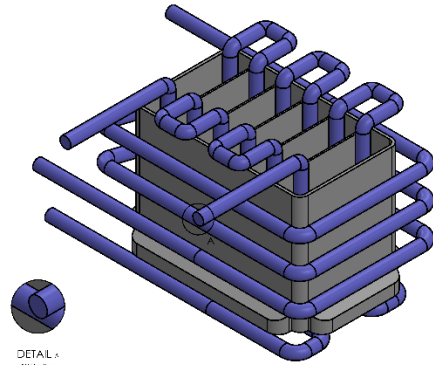
## Appendix 2. SolidWorks CAD of Part Geometry with Conformal Cooling Channels

### Part Geometry with Circular Cooling Channels (All Views)

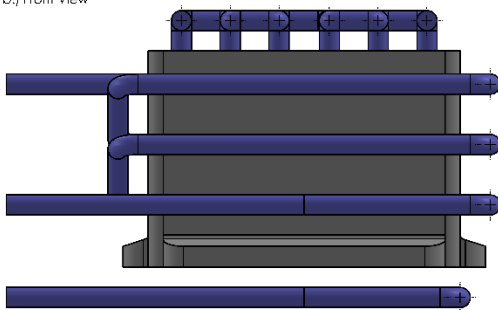
a.) Bottom View



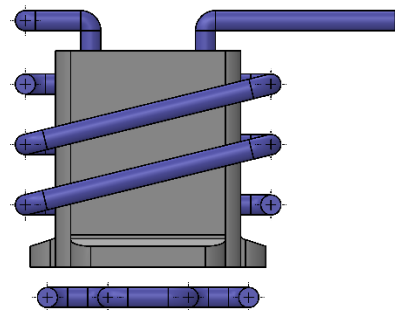
c.) Isometric View



b.) Front View

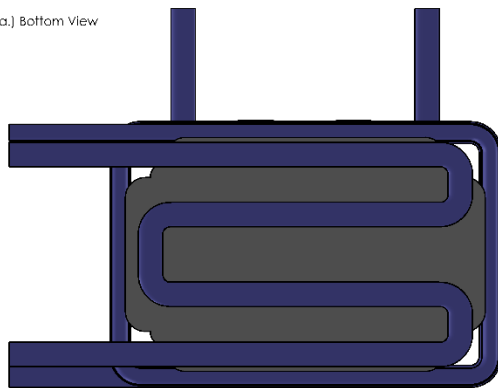


d.) Side View

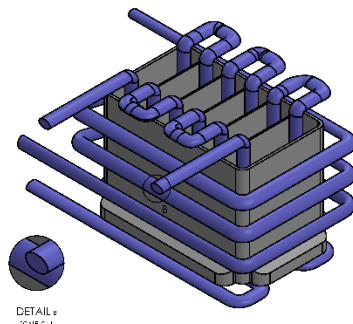


### Part Geometry with Elliptical Cooling Channels (All Views)

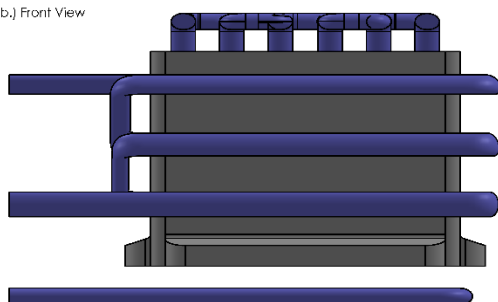
a.) Bottom View



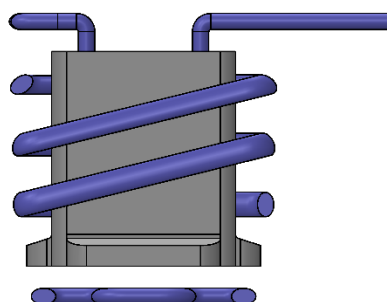
c.) Isometric View



b.) Front View

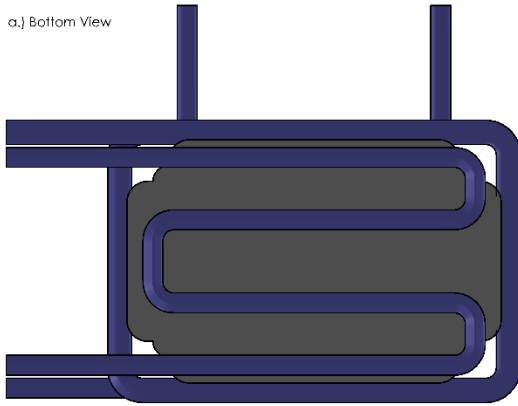


d.) Side View

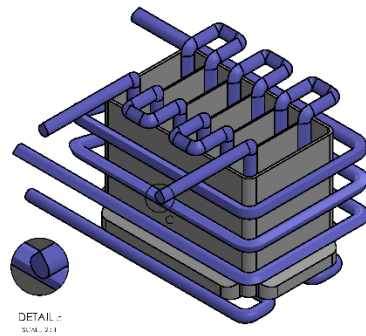


## Part Geometry with Teardrop Cooling Channels (All Views)

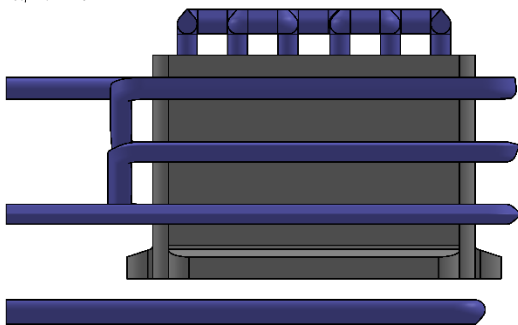
a.) Bottom View



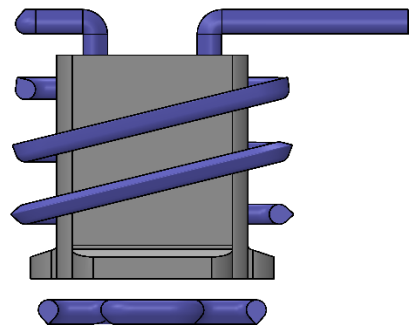
c.) Isometric View



b.) Front View



d.) Side View

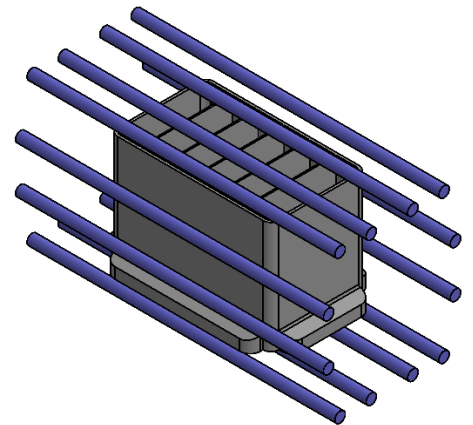


## Part Geometry with Straight-line Cooling Channels (All Views)

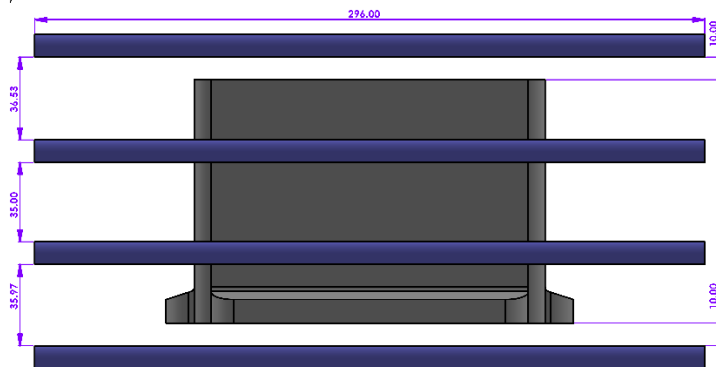
a.) Bottom View



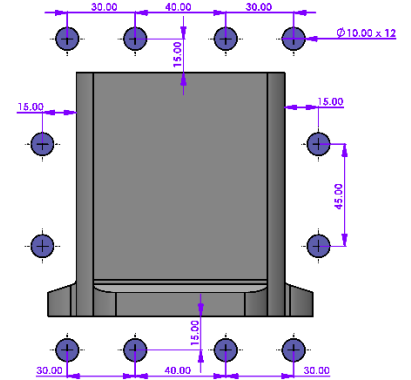
c.) Isometric View



b.) Front View

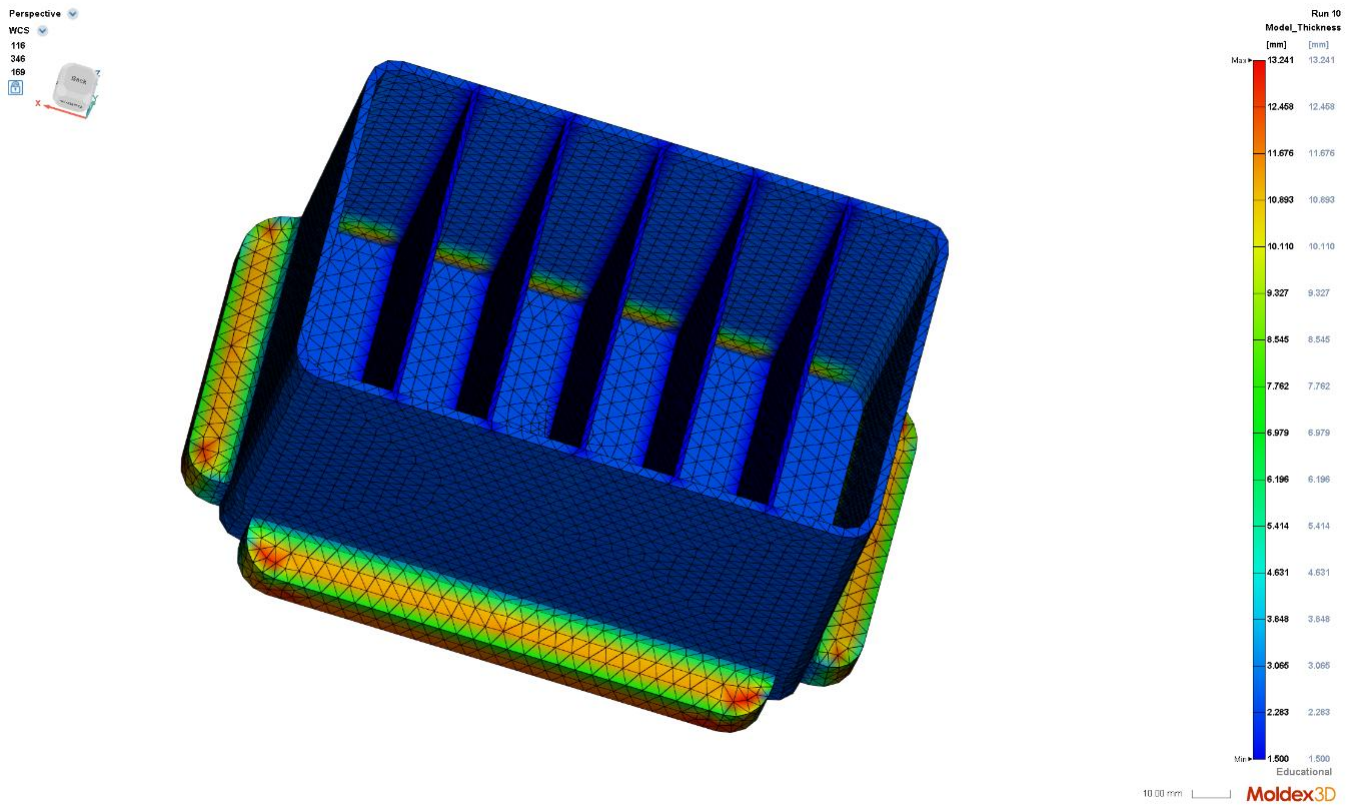


d.) Side View

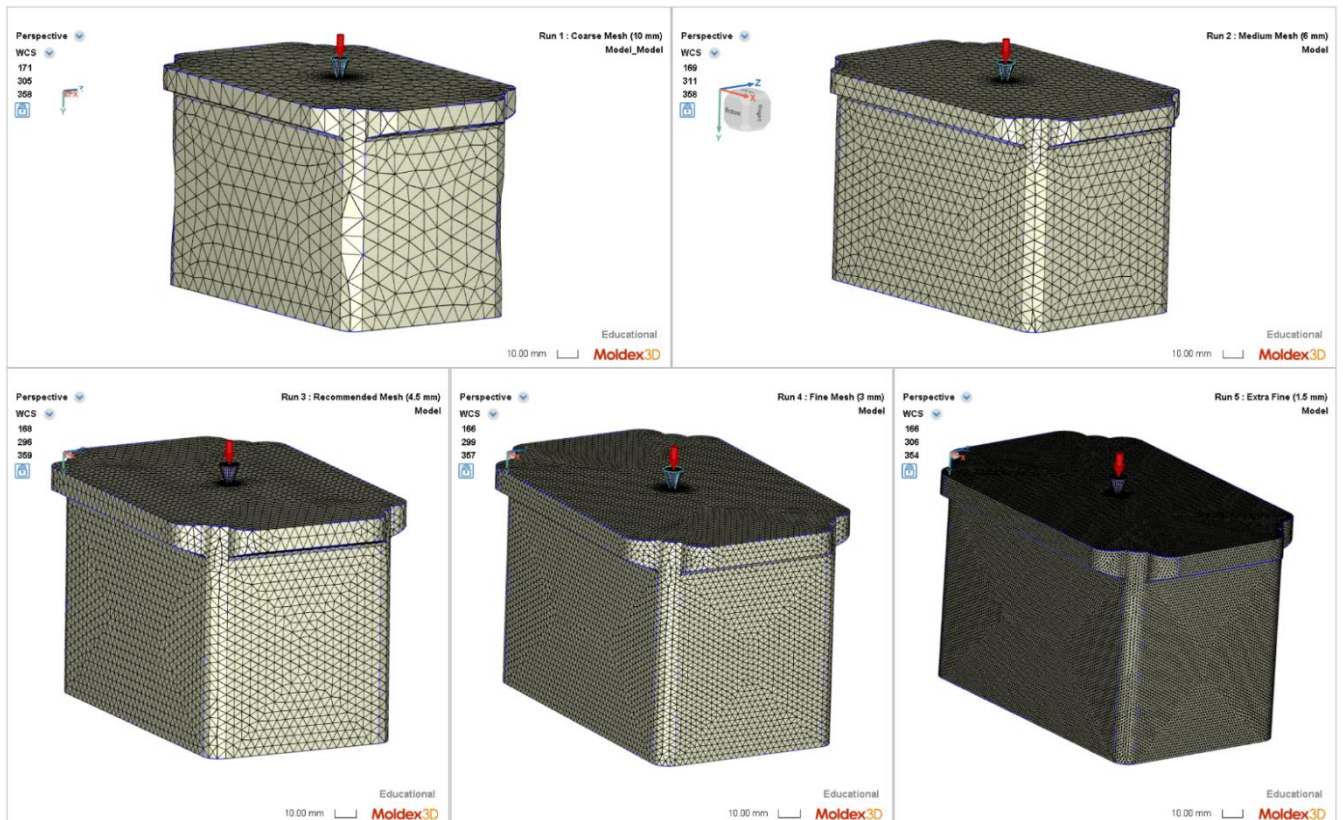


# Appendix 3. Part and Cooling Channel Models in Moldex3D Environment with Meshes

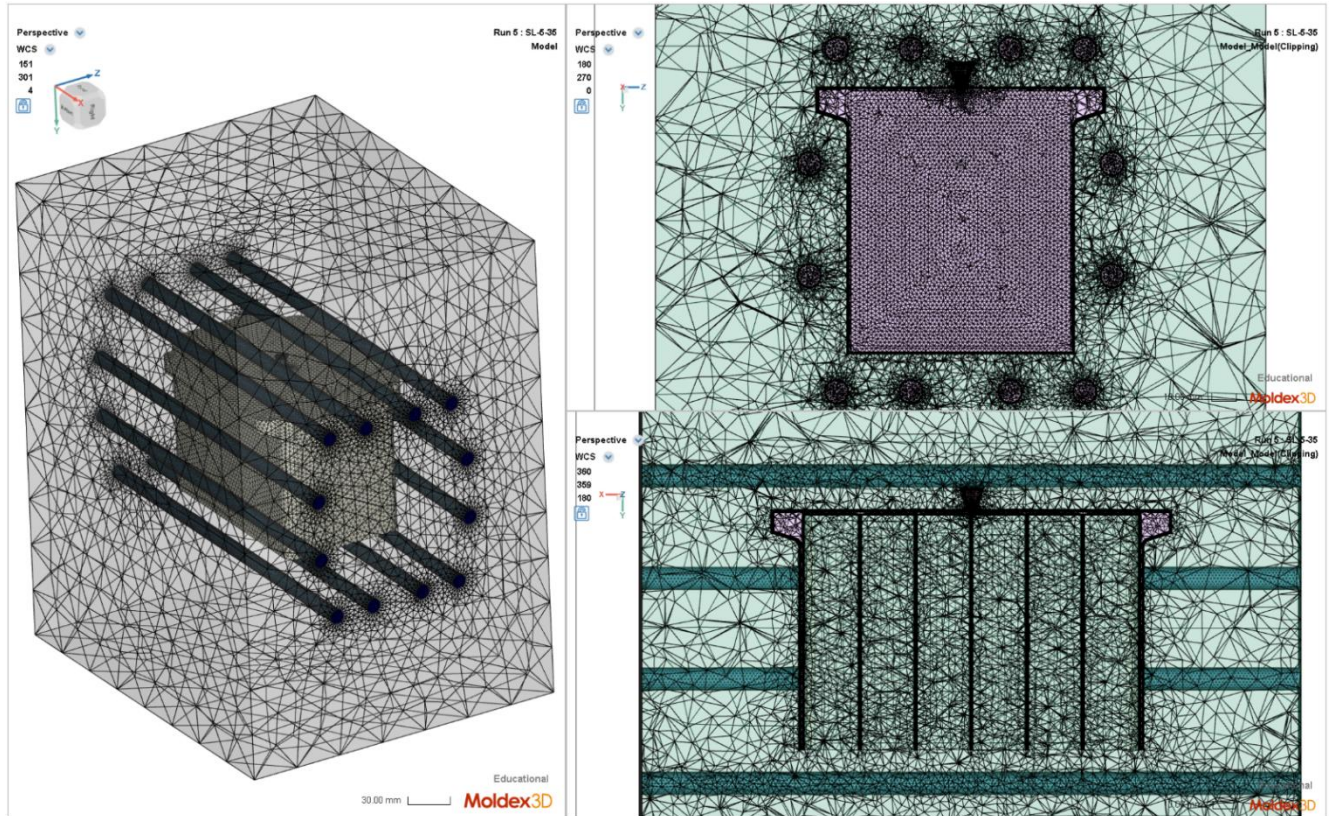
## Moldex3D: Part Thickness Estimation



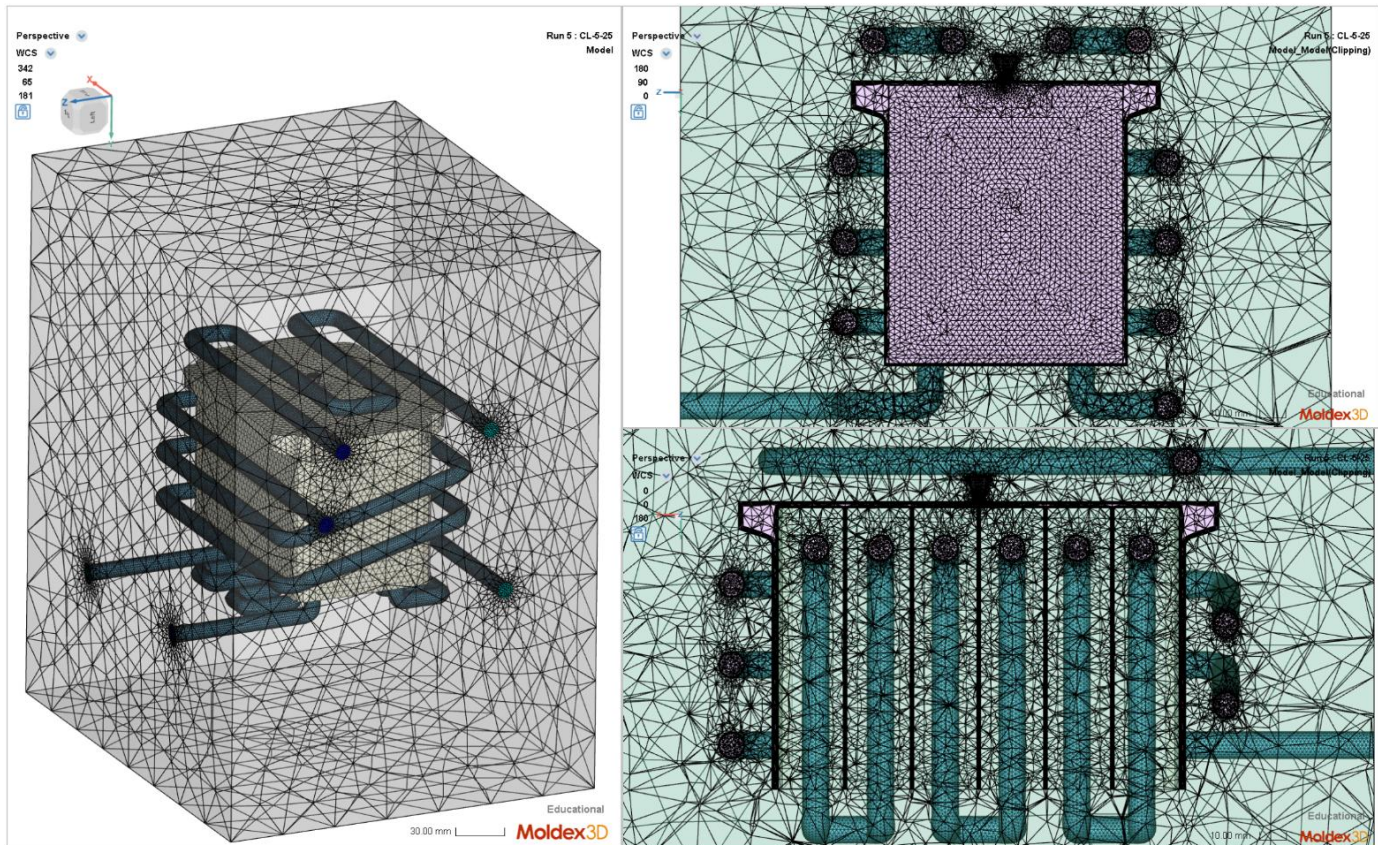
## Moldex3D: Mesh Run Comparison



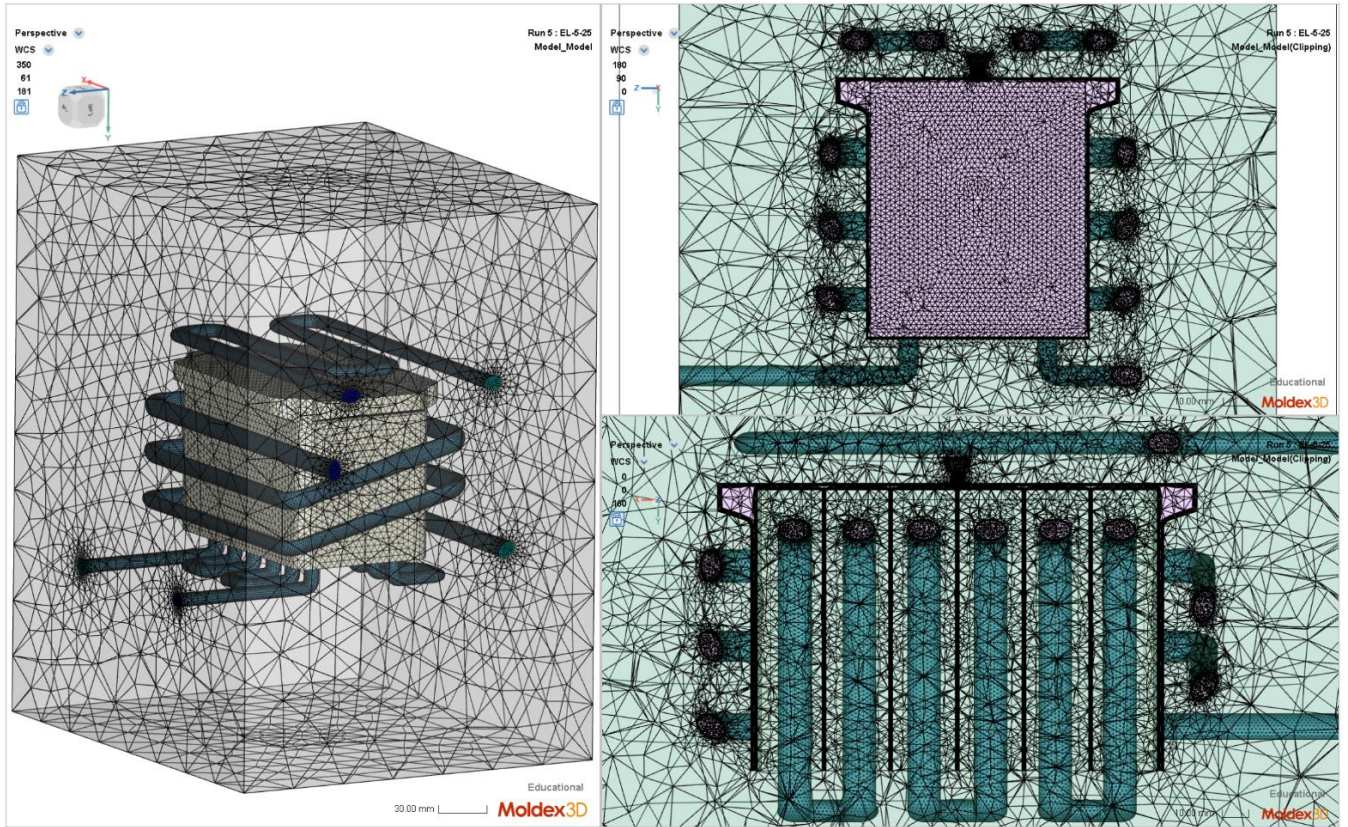
## Moldex3D: Straight-Line Cooling Channels with Mouldbase Mesh



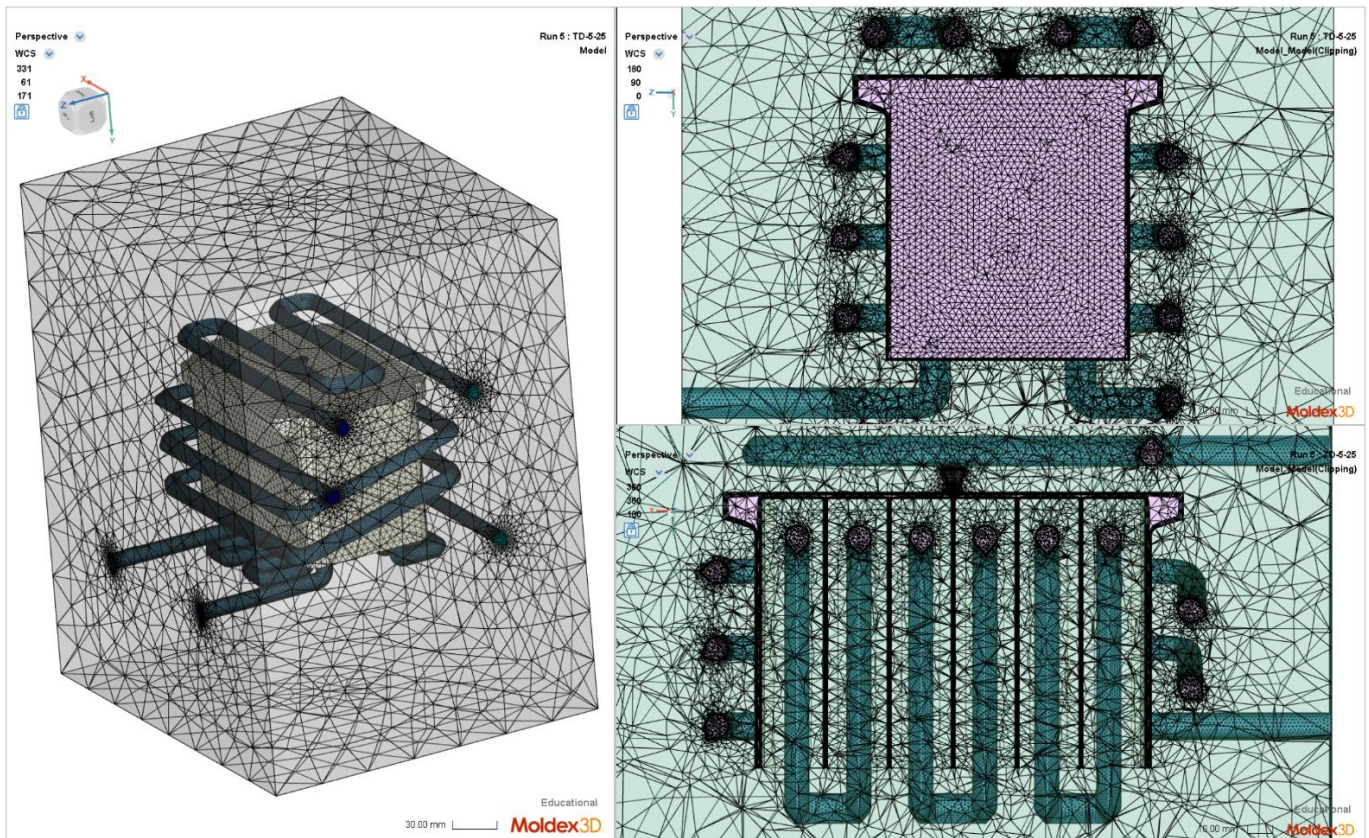
## Moldex3D: Circular Cooling Channels with Mouldbase Mesh



## Moldex3D Mesh: Elliptical Cooling Channels with Mouldbase



## Moldex3D Mesh: Teardrop Cooling Channels with Mouldbase



## Appendix 4. Moldex3D Simulation Results Data

### Simulation Results Data for Straight-Line Cooling Channels

#	1	2	3
<b>Run</b>	<b>Run 1</b>	<b>Run 2</b>	<b>Run 3</b>
<b>Run Code</b>	<b>SL-5-15</b>	<b>SL-5-25</b>	<b>SL-5-35</b>
<b>Note</b>	<b>5L/m_15°C</b>	<b>5L/m_25°C</b>	<b>5L/m_35°C</b>
<b>Material</b>			
<b>Polymer</b>	PP	PP	PP
<b>Melt Temperature Range (°C)</b>	190~250	190~250	190~250
<b>Mold Temperature (°C)</b>	40	40	40
<b>Ejection Temperature (°C)</b>	102.93	102.93	102.93
<b>Freeze Temperature (°C)</b>	122.93	122.93	122.93
<b>Process Condition</b>			
<b>Filling Time (sec)</b>	2.75	2.75	2.75
<b>Packing Time (sec)</b>	9.56	9.56	9.56
<b>Cooling Time (sec)</b>	30	30	30
<b>Cycle Time (sec)</b>	47.31	47.31	47.31
<b>Melt Temperature (°C)</b>	230	230	230
<b>Mold Temperature (°C)</b>	50	50	50
<b>Filling</b>			
<b>Melt Front Time (sec) - Max</b>	2.818	2.77	2.809
<b>Pressure (MPa) - Max</b>	17.418	17.192	16.635
<b>Packing</b>			
<b>Temperature (°C) - Max</b>	230.03	230.03	230.03
<b>Pressure (MPa) - Max</b>	8.925	8.81	8.518
<b>Cooling</b>			
<b>Average Temperature (°C) - Max</b>	144.25	146.951	149.786
<b>Average Temperature (°C) - Avg</b>	82.434	87.475	92.623
<b>Time to Reach Ejection Temperature (sec) - Max</b>	167.06	180.73	203.43
<b>Coolant Pressure (kPa) - Range (Min-Max)</b>	0-0.8731	0-0.7754	0-0.6925
<b>Cooling Channel Reynolds Number (-) - Avg</b>	5456.515	6787.789	8287.003
<b>Coolant Temperature (°C) - Min</b>	15	25	35
<b>Warpage</b>			
<b>Total Displacement (mm) - Max</b>	0.764	0.78	0.801

## Simulation Results Data for Circular Cooling Channels

#	1	2	3	4	5	6	7	8	9
<b>Run</b>	Run 1	Run 2	Run 3	Run 4	Run 5	Run 6	Run 7	Run 8	Run 9
<b>Remark</b>	CL-2-15	CL-2-25	CL-2-35	CL-5-15	CL-5-25	CL-5-35	CL-10-15	CL-10-25	CL-10-35
<b>Note</b>	2L/m_15°C	2L/m_25°C	2L/m_35°C	5L/m_15°C	5L/m_25°C	5L/m_35°C	10L/m_15°C	10L/m_25°C	10L/m_35°C
<b>Material</b>									
<b>Polymer</b>	PP	PP	PP	PP	PP	PP	PP	PP	PP
<b>Melt Temperature Range (°C)</b>	190~250	190~250	190~250	190~250	190~250	190~250	190~250	190~250	190~250
<b>Mold Temperature (°C)</b>	40	40	40	40	40	40	40	40	40
<b>Ejection Temperature (°C)</b>	102.93	102.93	102.93	102.93	102.93	102.93	102.93	102.93	102.93
<b>Freeze Temperature (°C)</b>	122.93	122.93	122.93	122.93	122.93	122.93	122.93	122.93	122.93
<b>Process Condition</b>									
<b>Filling Time (sec)</b>	2.75	2.75	2.75	2.75	2.75	2.75	2.75	2.75	2.75
<b>Packing Time (sec)</b>	9.56	9.56	9.56	9.56	9.56	9.56	9.56	9.56	9.56
<b>Cooling Time (sec)</b>	30	30	30	30	30	30	30	30	30
<b>Cycle Time (sec)</b>	47.31	47.31	47.31	47.31	47.31	47.31	47.31	47.31	47.31
<b>Melt Temperature (°C)</b>	230	230	230	230	230	230	230	230	230
<b>Mold Temperature (°C)</b>	50	50	50	50	50	50	50	50	50
<b>Filling</b>									
<b>Melt Front Time (sec) - Max</b>	2.759	2.839	2.763	2.754	2.757	2.759	2.842	2.835	2.834
<b>Pressure (MPa) - Max</b>	20.617	20.246	19.754	21.621	20.961	20.311	21.162	20.525	19.936
<b>Packing</b>									
<b>Temperature (°C) - Max</b>	230	230	230.03	230	230	230.01	230	230	230.01
<b>Pressure (MPa) - Max</b>	10.552	10.369	10.106	11.042	10.729	10.396	10.828	10.493	10.208
<b>Cooling</b>									
<b>Average Temperature (°C) - Max</b>	128.701	132.233	135.448	123.457	127.405	131.531	121.552	125.856	130.268
<b>Average Temperature (°C) - Avg</b>	48.881	55.724	61.412	36.299	44.076	52.051	31.119	39.754	48.526
<b>Time to Reach Ejection Temperature (sec) - Max</b>	95.199	98.544	102.51	89.586	93.978	98.525	86.922	92.104	97.227
<b>Coolant Pressure (kPa) - Range (Min-Max)</b>	0-4	0-4	0-3	0-19	0-18	0-17	0-64	0-62	0-61
<b>Cooling Channel Reynolds Number (-) - Avg</b>	2955.952	3508.093	4075.821	6377.085	8015.47	9808.318	12490	15930	19550
<b>Coolant Temperature (°C) - Min</b>	15	25	35	15	25	35	15	25	35
<b>Warpage</b>									
<b>Total Displacement (mm) - Max</b>	0.743	0.76	0.773	0.716	0.735	0.754	0.71	0.73	0.749

## Simulation Results Data for Elliptical Cooling Channels

#	1	2	3	4	5	6	7	8	9
<b>Run</b>	<b>Run 1</b>	<b>Run 2</b>	<b>Run 3</b>	<b>Run 4</b>	<b>Run 5</b>	<b>Run 6</b>	<b>Run 7</b>	<b>Run 8</b>	<b>Run 9</b>
<b>Remark</b>	<b>EL-2-15</b>	<b>EL-2-25</b>	<b>EL-2-35</b>	<b>EL-5-15</b>	<b>EL-5-25</b>	<b>EL-5-35</b>	<b>EL-10-15</b>	<b>EL-10-25</b>	<b>EL-10-35</b>
<b>Note</b>	<b>2L/m_15°C</b>	<b>2L/m_25°C</b>	<b>2L/m_35°C</b>	<b>5L/m_15°C</b>	<b>5L/m_25°C</b>	<b>5L/m_35°C</b>	<b>10L/m_15°C</b>	<b>10L/m_25°C</b>	<b>10L/m_35°C</b>
<b>Material</b>									
<b>Polymer</b>	PP	PP	PP	PP	PP	PP	PP	PP	PP
<b>Melt Temperature Range (°C)</b>	190~250	190~250	190~250	190~250	190~250	190~250	190~250	190~250	190~250
<b>Mold Temperature (°C)</b>	40	40	40	40	40	40	40	40	40
<b>Ejection Temperature (°C)</b>	102.93	102.93	102.93	102.93	102.93	102.93	102.93	102.93	102.93
<b>Freeze Temperature (°C)</b>	122.93	122.93	122.93	122.93	122.93	122.93	122.93	122.93	122.93
<b>Process Condition</b>									
<b>Filling Time (sec)</b>	2.75	2.75	2.75	2.75	2.75	2.75	2.75	2.75	2.75
<b>Packing Time (sec)</b>	9.56	9.56	9.56	9.56	9.56	9.56	9.56	9.56	9.56
<b>Cooling Time (sec)</b>	30	30	30	30	30	30	30	30	30
<b>Cycle Time (sec)</b>	47.31	47.31	47.31	47.31	47.31	47.31	47.31	47.31	47.31
<b>Melt Temperature (°C)</b>	230	230	230	230	230	230	230	230	230
<b>Mold Temperature (°C)</b>	50	50	50	50	50	50	50	50	50
<b>Filling</b>									
<b>Melt Front Time (sec) - Max</b>	2.835	2.833	2.831	2.839	2.841	2.836	2.843	2.836	2.836
<b>Pressure (MPa) - Max</b>	20.026	19.584	19.144	20.839	20.222	19.679	21.127	20.496	19.874
<b>Packing</b>									
<b>Temperature (°C) - Max</b>	230	230.02	230.02	230	230	230.01	230	230	230.01
<b>Pressure (MPa) - Max</b>	10.263	10.025	9.809	10.683	10.362	10.076	10.806	10.484	10.175
<b>Cooling</b>									
<b>Average Temperature (°C) - Max</b>	128.008	131.376	134.765	123.263	127.336	131.334	121.405	125.745	130.013
<b>Average Temperature (°C) - Avg</b>	47.894	54.28	60.726	36.016	43.934	51.795	31.026	39.81	48.326
<b>Time to Reach Ejection Temperature (sec) - Max</b>	95.773	99.149	103.18	89.663	95.62	99.784	87.506	93.914	98.931
<b>Coolant Pressure (kPa) - Range (Min-Max)</b>	0-4	0-4	0-3	0-18	0-17	0-16	0-61	0-59	0-58
<b>Cooling Channel Reynolds Number (-) - Avg</b>	2748.41	3257.195	3799.826	6005.583	7523.249	9165.332	11740	14920	18240
<b>Coolant Temperature (°C) - Min</b>	15	25	35	15	25	35	15	25	35
<b>Warpage</b>									
<b>Total Displacement (mm) - Max</b>	0.741	0.756	0.772	0.717	0.736	0.754	0.709	0.728	0.748

## Simulation Results Data for Teardrop Cooling Channels

#	1	2	3	4	5	6	7	8	9
<b>Run</b>	<b>Run 1</b>	<b>Run 2</b>	<b>Run 3</b>	<b>Run 4</b>	<b>Run 5</b>	<b>Run 6</b>	<b>Run 7</b>	<b>Run 8</b>	<b>Run 9</b>
<b>Remark</b>	<b>TD-2-15</b>	<b>TD-2-25</b>	<b>TD-2-35</b>	<b>TD-5-15</b>	<b>TD-5-25</b>	<b>TD-5-35</b>	<b>TD-10-15</b>	<b>TD-10-25</b>	<b>TD-10-35</b>
<b>Note</b>	<b>2L/m_15°C</b>	<b>2L/m_25°C</b>	<b>2L/m_35°C</b>	<b>5L/m_15°C</b>	<b>5L/m_25°C</b>	<b>5L/m_35°C</b>	<b>10L/m_15°C</b>	<b>10L/m_25°C</b>	<b>10L/m_35°C</b>
<b>Material</b>									
<b>Polymer</b>	PP	PP	PP	PP	PP	PP	PP	PP	PP
<b>Melt Temperature Range (°C)</b>	190~250	190~250	190~250	190~250	190~250	190~250	190~250	190~250	190~250
<b>Mold Temperature (°C)</b>	40	40	40	40	40	40	40	40	40
<b>Ejection Temperature (°C)</b>	102.93	102.93	102.93	102.93	102.93	102.93	102.93	102.93	102.93
<b>Freeze Temperature (°C)</b>	122.93	122.93	122.93	122.93	122.93	122.93	122.93	122.93	122.93
<b>Process Condition</b>									
<b>Filling Time (sec)</b>	2.75	2.75	2.75	2.75	2.75	2.75	2.75	2.75	2.75
<b>Packing Time (sec)</b>	9.56	9.56	9.56	9.56	9.56	9.56	9.56	9.56	9.56
<b>Cooling Time (sec)</b>	30	30	30	30	30	30	30	30	30
<b>Cycle Time (sec)</b>	47.31	47.31	47.31	47.31	47.31	47.31	47.31	47.31	47.31
<b>Melt Temperature (°C)</b>	230	230	230	230	230	230	230	230	230
<b>Mold Temperature (°C)</b>	50	50	50	50	50	50	50	50	50
<b>Filling</b>									
<b>Melt Front Time (sec) - Max</b>	2.836	2.825	2.826	2.834	2.824	2.826	2.836	2.831	2.828
<b>Pressure (MPa) - Max</b>	20.633	19.476	18.976	20.778	20.203	19.66	21.047	20.411	19.832
<b>Packing</b>									
<b>Temperature (°C) - Max</b>	230	230.02	230.02	230	230	230.01	230	230	230.01
<b>Pressure (MPa) - Max</b>	10.558	9.965	9.723	10.621	10.314	10.053	10.779	10.45	10.132
<b>Cooling</b>									
<b>Average Temperature (°C) - Max</b>	120.788	124.416	128.201	115.626	120.224	124.793	113.717	118.605	123.514
<b>Average Temperature (°C) - Avg</b>	48.494	54.791	61.237	36.061	43.934	51.903	31.004	39.7	48.434
<b>Time to Reach Ejection Temperature (sec) - Max</b>	91.325	94.902	100.35	86.358	91.23	95.639	84.349	89.707	94.51
<b>Coolant Pressure (kPa) - Range (Min-Max)</b>	0-4	0-4	0-3	0-19	0-18	0-17	0-66	0-64	0-63
<b>Cooling Channel Reynolds Number (-) - Avg</b>	2645.312	3135.234	3656.934	5915.928	7179.421	8790.302	11260	14330	17540
<b>Coolant Temperature (°C) - Min</b>	15	25	35	15	25	35	15	25	35
<b>Warpage</b>									
<b>Total Displacement (mm) - Max</b>	0.75	0.765	0.781	0.725	0.744	0.762	0.715	0.735	0.755

## Appendix 5. JASP RSM Analysis Results for Circular Conformal Cooling Channel

Average Part Temperature -  $T_{avg}$  (.C)

### Model Summary

S	R <sup>2</sup>	Adjusted R <sup>2</sup>	Predictive R <sup>2</sup>
0.525	0.999	0.997	0.988

### ANOVA

Source	Sum of squares	df	Mean square	F	p
Model	777.5	5	155.5	563.5	< .001
Linear terms	715.4	2			
Tc (.C)	353.2	1	353.2	1280	< .001
Q (L/min)	362.2	1	362.2	1313	< .001
Squared terms	56.53	2			
Tc (.C) <sup>2</sup>	0.037	1	0.037	0.135	.737
Q (L/min) <sup>2</sup>	56.49	1	56.49	204.7	< .001
Interaction terms	5.515	1			
Tc (.C) * Q (L/min)	5.515	1	5.515	19.99	.021
Error	0.828	3	0.276		
Total	778.3	8			

Note. Type III sums of squares.

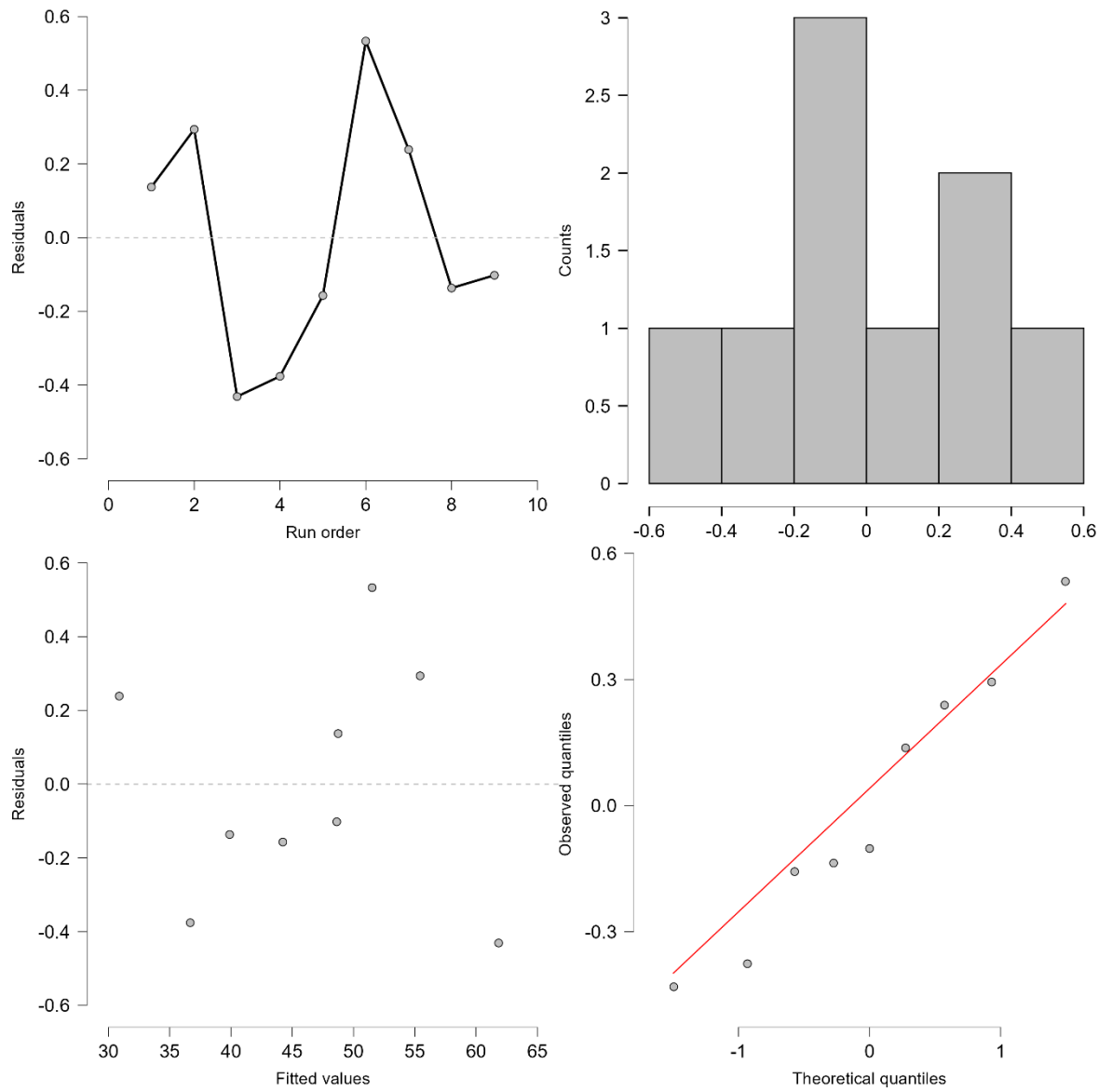
### Coded Coefficients

Alias	Term	Effect	Coefficient	Standard error	t	p	VIF
(Intercept)	(Intercept)		41.93	0.412	101.9	< .001	
A	Tc (.C)	15.42	7.712	0.216	35.78	< .001	1.010
B	Q (L/min)	-15.54	-7.770	0.214	-36.23	< .001	1.021
A <sup>2</sup>	Tc (.C) <sup>2</sup>	-0.273	-0.137	0.371	-0.368	.737	
B <sup>2</sup>	Q (L/min) <sup>2</sup>	11.46	5.728	0.400	14.31	< .001	
AB	Tc (.C) * Q (L/min)	2.324	1.162	0.260	4.471	.021	1.010

### Regression equation in Coded Units

$$T_{avg} (.C) = 41.933 + 7.712 A - 7.77 B - 0.137 A^2 + 5.728 B^2 + 1.162 AB$$

Matrix residual plot for  $T_{avg}$



## Maximum Part Temperature - $T_{max}$ (.C)

### Model Summary

S	R <sup>2</sup>	Adjusted R <sup>2</sup>	Predictive R <sup>2</sup>
0.214	0.999	0.998	0.990

### ANOVA

Source	Sum of squares	df	Mean square	F	p
Model	163.0	5	32.61	713.7	< .001
Linear terms	151.5	2			
Tc (.C)	93.23	1	93.23	2041	< .001
Q (L/min)	58.32	1	58.32	1277	< .001
Squared terms	10.59	2			
Tc (.C)^2	5.339×10 <sup>-5</sup>	1	5.339×10 <sup>-5</sup>	0.001	.975
Q (L/min)^2	10.59	1	10.59	231.8	< .001
Interaction terms	0.895	1			
Tc (.C) * Q (L/min)	0.895	1	0.895	19.60	.021
Error	0.137	3	0.046		
Total	163.2	8			

Note. Type III sums of squares.

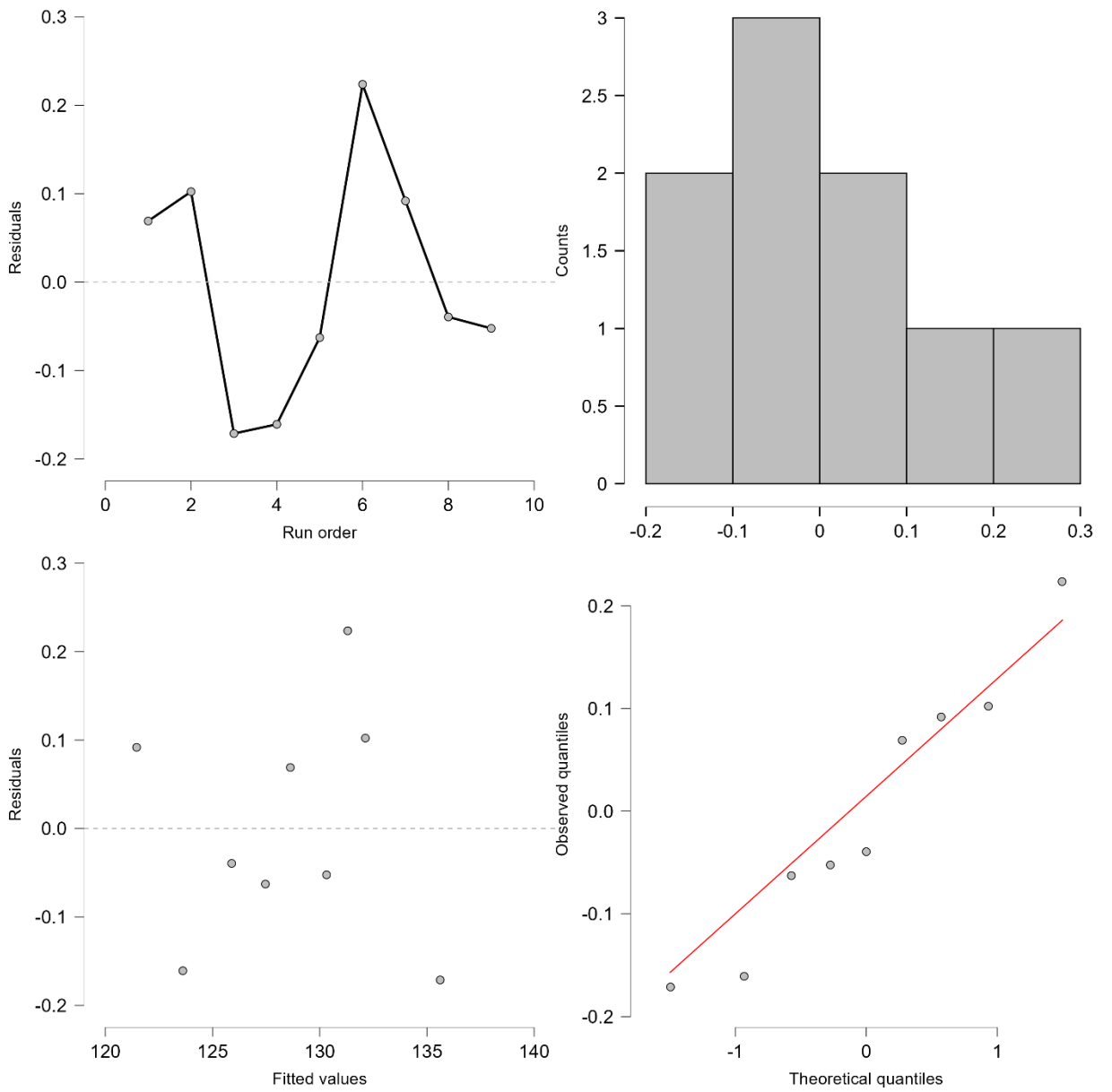
### Coded Coefficients

Alias	Term	Effect	Coefficient	Standard error	t	p	VIF
(Intercept)	(Intercept)		126.5	0.167	755.5	< .001	
A	Tc (.C)	7.924	3.962	0.088	45.17	< .001	1.010
B	Q (L/min)	-6.235	-3.118	0.087	-35.73	< .001	1.021
A^2	Tc (.C)^2	-0.010	-0.005	0.151	-0.034	.975	
B^2	Q (L/min)^2	4.959	2.480	0.163	15.22	< .001	
AB	Tc (.C)* Q (L/min)	0.936	0.468	0.106	4.427	.021	1.010

### Regression equation in Coded Units

$$T_{max} (.C) = 126.533 + 3.962 A - 3.118 B - 0.005 A^2 + 2.48 B^2 + 0.468 AB$$

# Matrix residual plot for $T_{max}$



## Time to Reach Ejection Temperature - $t_{cool}$ (s)

### Model Summary

S	R <sup>2</sup>	Adjusted R <sup>2</sup>	Predictive R <sup>2</sup>
0.203	0.999	0.998	0.992

### ANOVA

Source	Sum of squares	df	Mean square	F	p
Model	198.1	5	39.62	961.1	< .001
Linear terms	186.2	2			
Tc (.C)	119.6	1	119.6	2900	< .001
Q (L/min)	66.67	1	66.67	1617	< .001
Squared terms	9.696	2			
Tc (.C)^2	0.029	1	0.029	0.693	.466
Q (L/min)^2	9.667	1	9.667	234.5	< .001
Interaction terms	2.163	1			
Tc (.C) * Q (L/min)	2.163	1	2.163	52.49	.005
Error	0.124	3	0.041		
Total	198.2	8			

Note. Type III sums of squares.

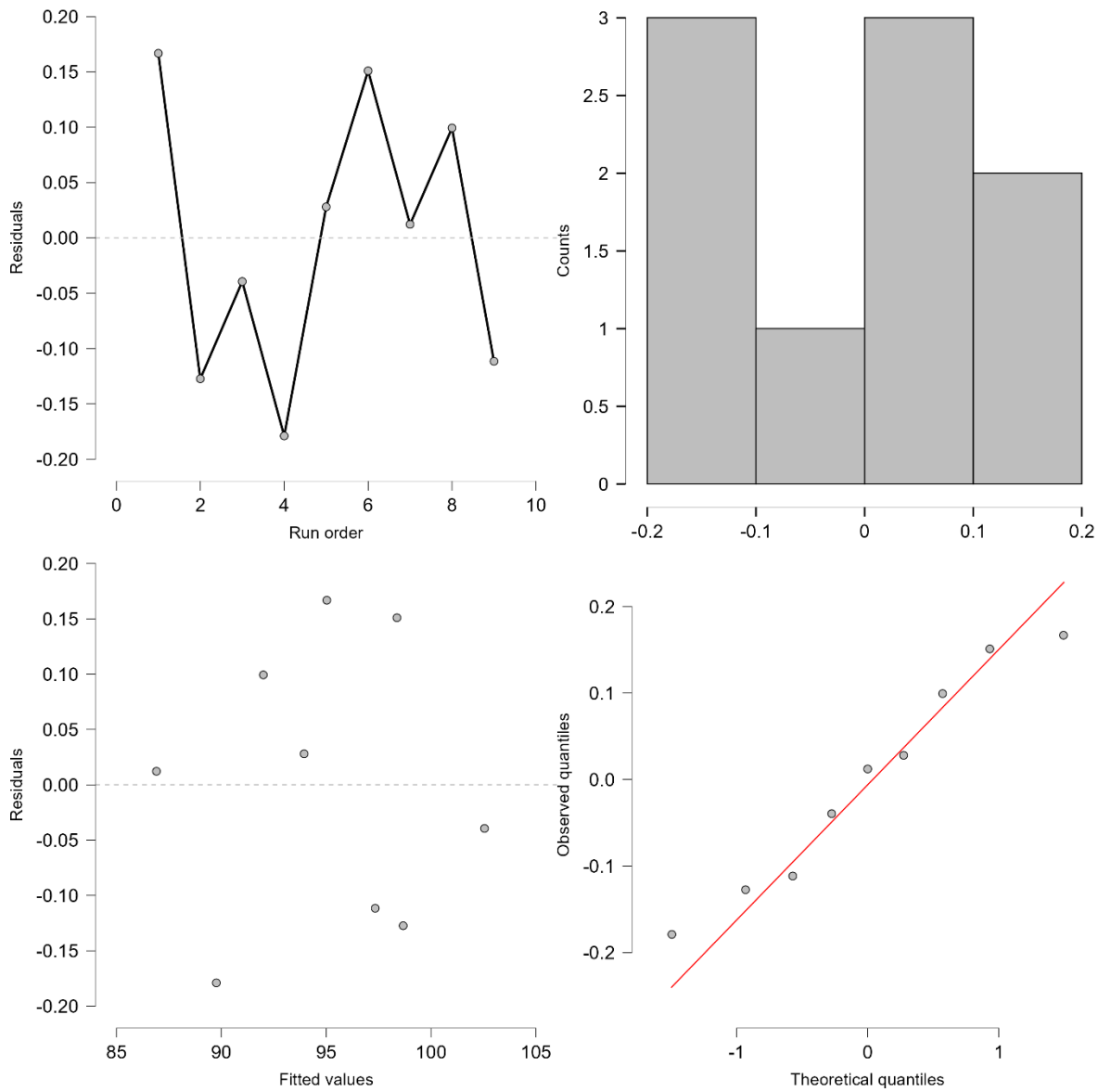
### Coded Coefficients

Alias	Term	Effect	Coefficient	Standard error	t	p	VIF
(Intercept)	(Intercept)		92.97	0.159	584.4	< .001	
A	Tc (.C)	8.973	4.486	0.083	53.86	< .001	1.010
B	Q (L/min)	-6.667	-3.333	0.083	-40.22	< .001	1.021
A^2	Tc (.C)^2	0.239	0.119	0.144	0.832	.466	
B^2	Q (L/min)^2	4.739	2.369	0.155	15.31	< .001	
AB	Tc (.C)* Q (L/min)	1.456	0.728	0.100	7.245	.005	1.010

### Regression equation in Coded Units

$$t_{cool} \text{ (s)} = 92.969 + 4.486 A - 3.333 B + 0.119 A^2 + 2.369 B^2 + 0.728 AB$$

# Matrix residual plot for $t_{cool}$



## Coolant Pressure Drop - dP (kPa)

### Model Summary

S	R <sup>2</sup>	Adjusted R <sup>2</sup>	Predictive R <sup>2</sup>
0.343	1.000	1.000	0.999

### ANOVA

Source	Sum of squares	df	Mean square	F	p
Model	5285	5	1057	8965	< .001
Linear terms	5169	2			
Tc (.C)	6.434	1	6.434	54.57	.005
Q (L/min)	5163	1	5163	43780	< .001
Squared terms	115.2	2			
Tc (.C)^2	0.000	1	0.000	0.000	1.000
Q (L/min)^2	115.2	1	115.2	976.6	< .001
Interaction terms	0.980	1			
Tc (.C) * Q (L/min)	0.980	1	0.980	8.308	.063
Error	0.354	3	0.118		
Total	5286	8			

Note. Type III sums of squares.

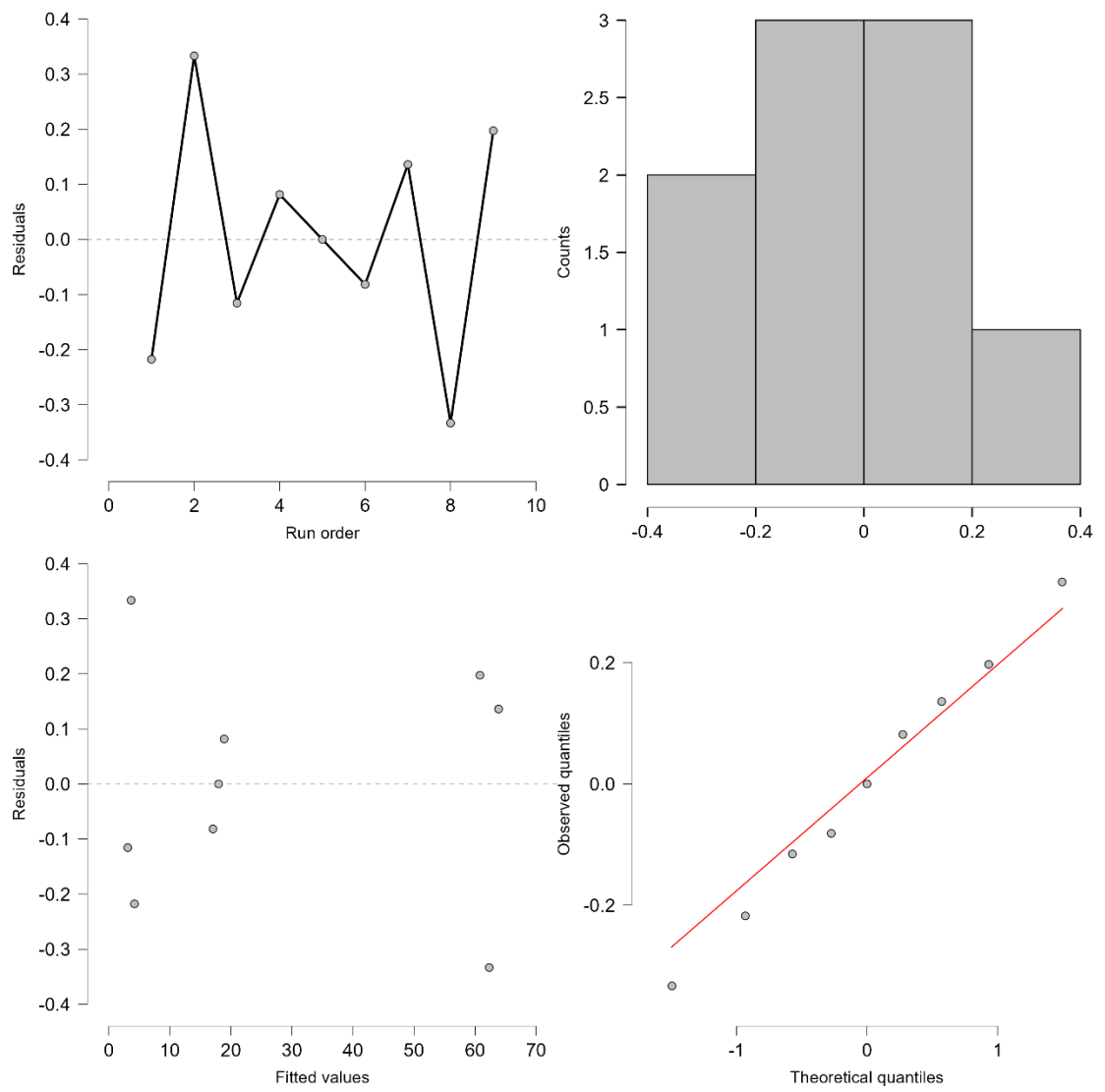
### Coded Coefficients

Alias	Term	Effect	Coefficient	Standard error	t	p	VIF
(Intercept)	(Intercept)		24.82	0.269	92.25	< .001	
A	Tc (.C)	-2.082	-1.041	0.141	-7.387	.005	1.010
B	Q (L/min)	58.67	29.33	0.140	209.2	< .001	1.021
A^2	Tc (.C)^2	-5.015×10 <sup>-15</sup>	-2.507×10 <sup>-15</sup>	0.243	-1.033×10 <sup>-14</sup>	1.000	
B^2	Q (L/min)^2	16.36	8.178	0.262	31.25	< .001	
AB	Tc (.C)* Q (L/min)	-0.980	-0.490	0.170	-2.882	.063	1.010

### Regression equation in Coded Units

$$dP \text{ (kPa)} = 24.822 - 1.041 A + 29.333 B - 0 A^2 + 8.178 B^2 - 0.49 AB$$

# Matrix residual plot for dP



## Average Reynolds Number - $Re_{avg}$

### Model Summary

S	R <sup>2</sup>	Adjusted R <sup>2</sup>	Predictive R <sup>2</sup>
40.43	1.000	1.000	1.000

### ANOVA

Source	Sum of squares	df	Mean square	F	p
Model	2.677×10 <sup>+8</sup>	5	5.354×10 <sup>+7</sup>	32750	< .001
Linear terms	2.587×10 <sup>+8</sup>	2			
Tc (.C)	2.517×10 <sup>+7</sup>	1	2.517×10 <sup>+7</sup>	15400	< .001
Q (L/min)	2.335×10 <sup>+8</sup>	1	2.335×10 <sup>+8</sup>	142900	< .001
Squared terms	37470	2			
Tc (.C) <sup>2</sup>	6808	1	6808	4.165	.134
Q (L/min) <sup>2</sup>	30660	1	30660	18.76	.023
Interaction terms	8.964×10 <sup>+6</sup>	1			
Tc (.C) * Q (L/min)	8.964×10 <sup>+6</sup>	1	8.964×10 <sup>+6</sup>	5484	< .001
Error	4903	3	1634		
Total	2.677×10 <sup>+8</sup>	8			

Note. Type III sums of squares.

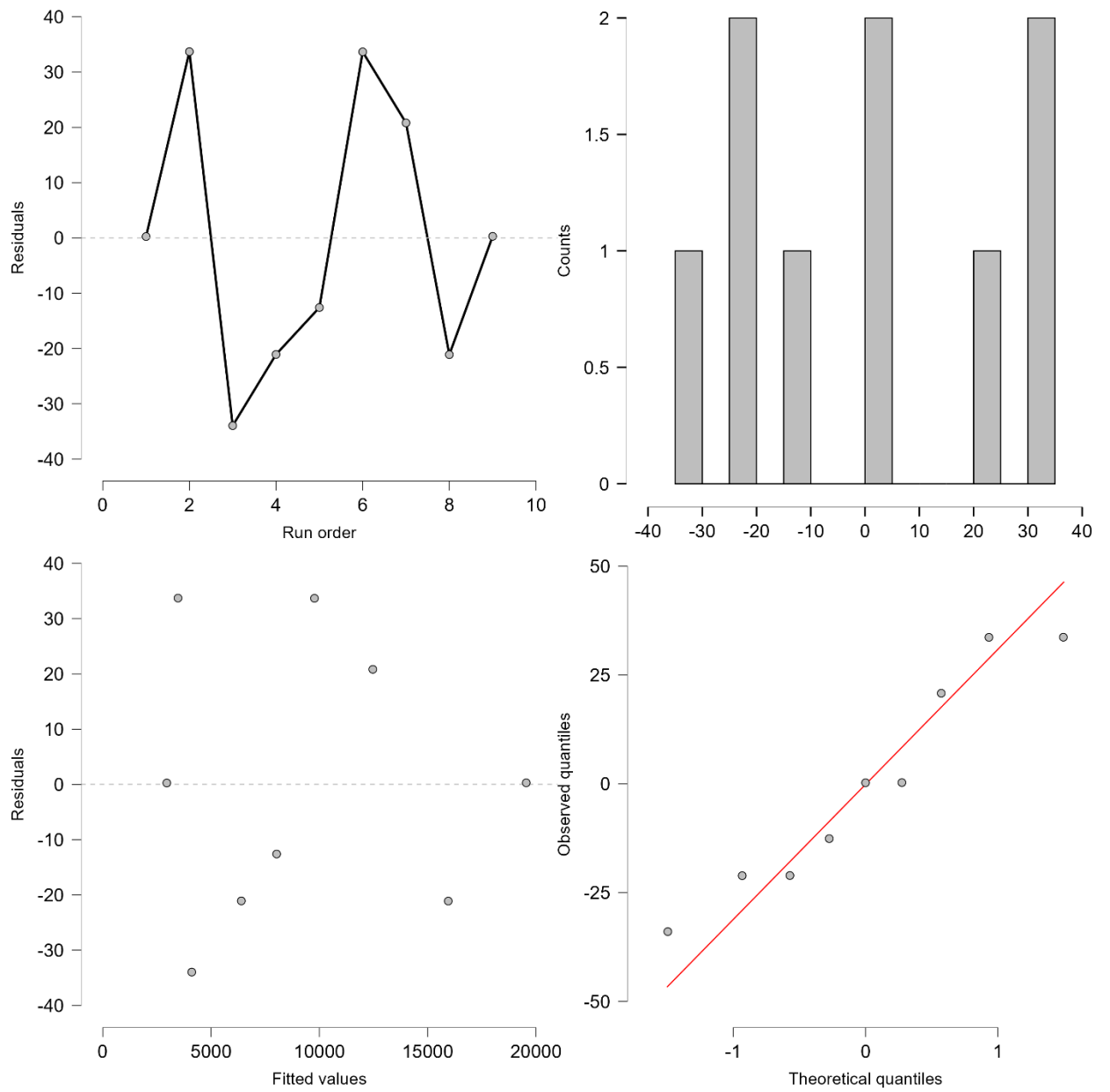
### Coded Coefficients

Alias	Term	Effect	Coefficient	Standard error	t	p	VIF
(Intercept)	(Intercept)		9579	31.68	302.4	< .001	
A	Tc (.C)	4117	2059	16.59	124.1	< .001	1.010
B	Q (L/min)	12480	6238	16.50	378.0	< .001	1.021
A <sup>2</sup>	Tc (.C) <sup>2</sup>	116.7	58.34	28.59	2.041	.134	
B <sup>2</sup>	Q (L/min) <sup>2</sup>	266.9	133.4	30.81	4.331	.023	
AB	Tc (.C) * Q (L/min)	2963	1482	20.01	74.06	< .001	1.010

### Regression equation in Coded Units

$$Re_{avg} = 9579.312 + 2058.651 A + 6238.356 B + 58.342 A^2 + 133.438 B^2 + 1481.612 AB$$

# Matrix residual plot for $Re_{avg}$



## Warpage Displacement - *Warp* (mm)

### Model Summary

S	R <sup>2</sup>	Adjusted R <sup>2</sup>	Predictive R <sup>2</sup>
0.002	0.997	0.993	0.972

### ANOVA

Source	Sum of squares	df	Mean square	F	p
Model	0.004	5	7.053×10 <sup>-4</sup>	251.0	< .001
Linear terms	0.003	2			
Tc (.C)	0.002	1	0.002	685.3	< .001
Q (L/min)	0.001	1	0.001	449.0	< .001
Squared terms	3.220×10 <sup>-4</sup>	2			
Tc (.C)^2	1.389×10 <sup>-6</sup>	1	1.389×10 <sup>-6</sup>	0.494	.533
Q (L/min)^2	3.206×10 <sup>-4</sup>	1	3.206×10 <sup>-4</sup>	114.1	.002
Interaction terms	1.735×10 <sup>-5</sup>	1			
Tc (.C) * Q (L/min)	1.735×10 <sup>-5</sup>	1	1.735×10 <sup>-5</sup>	6.175	.089
Error	8.429×10 <sup>-6</sup>	3	2.810×10 <sup>-6</sup>		
Total	0.004	8			

Note. Type III sums of squares.

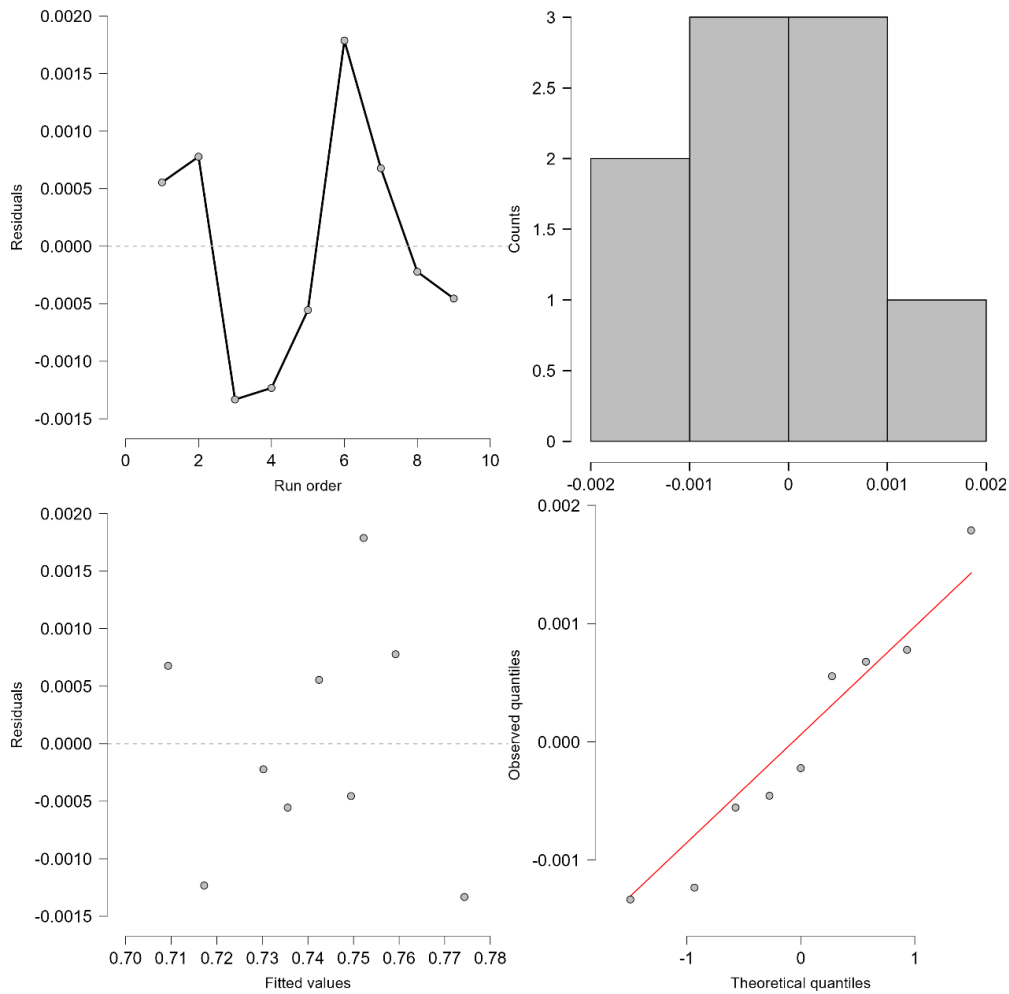
### Coded Coefficients

Alias	Term	Effect	Coefficient	Standard error	t	p	VIF
(Intercept)	(Intercept)		0.731	0.001	556.6	< .001	
A	Tc (.C)	0.036	0.018	6.878×10 <sup>-4</sup>	26.18	< .001	1.010
B	Q (L/min)	-0.029	-0.014	6.843×10 <sup>-4</sup>	-21.19	< .001	1.021
A^2	Tc (.C)^2	-0.002	-8.333×10 <sup>-4</sup>	0.001	-0.703	.533	
B^2	Q (L/min)^2	0.027	0.014	0.001	10.68	.002	
AB	Tc (.C)* Q (L/min)	0.004	0.002	8.295×10 <sup>-4</sup>	2.485	.089	1.010

### Regression equation in Coded Units

$$\text{Warp (mm)} = 0.731 + 0.018 A - 0.014 B - 0.001 A^2 + 0.014 B^2 + 0.002 AB$$

## Matrix residual plot for *Warp*



## Circular Profile - Response Optimiser output

### Response Optimizer Settings

Response	Goal	Lower	Target	Upper	Weight	Importance
Tavg (.C)	Minimize		31.12	61.41	1.000	1.000
Tmax (.C)	Minimize		121.6	135.4	1.000	1.000
tcool (s)	Minimize		86.92	102.5	1.000	1.000
dP (kPa)	Minimize		3.000	64.00	1.000	1.000
Warp (mm)	Minimize		0.710	0.773	1.000	1.000

*Note.* The lower and upper bounds and target are estimated from data.

### Response Optimizer Solution

Composite desirability	Tc (.C)	Q (L/min)	Tavg (.C) fit	Tmax (.C) fit	tcool (s) fit	dP (kPa) fit	Warp (mm) fit
0.989	15.611	4.73	30.646	120.89	86.922	6.24	0.704

## Appendix 6. JASP RSM Analysis Results for Elliptical Conformal Cooling Channel

Average Part Temperature -  $T_{avg}$  (.C)

### Model Summary

S	R <sup>2</sup>	Adjusted R <sup>2</sup>	Predictive R <sup>2</sup>
0.423	0.999	0.998	0.991

### ANOVA

Source	Sum of squares	df	Mean square	F	p
Model	726.7	5	145.3	811.8	< .001
Linear terms	674.7	2			
Tc (.C)	355.9	1	355.9	1988	< .001
Q (L/min)	318.8	1	318.8	1781	< .001
Squared terms	47.39	2			
Tc (.C) <sup>2</sup>	0.004	1	0.004	0.022	.892
Q (L/min) <sup>2</sup>	47.38	1	47.38	264.6	< .001
Interaction terms	4.632	1			
Tc (.C) * Q (L/min)	4.632	1	4.632	25.87	.015
Error	0.537	3	0.179		
Total	727.3	8			

Note. Type III sums of squares.

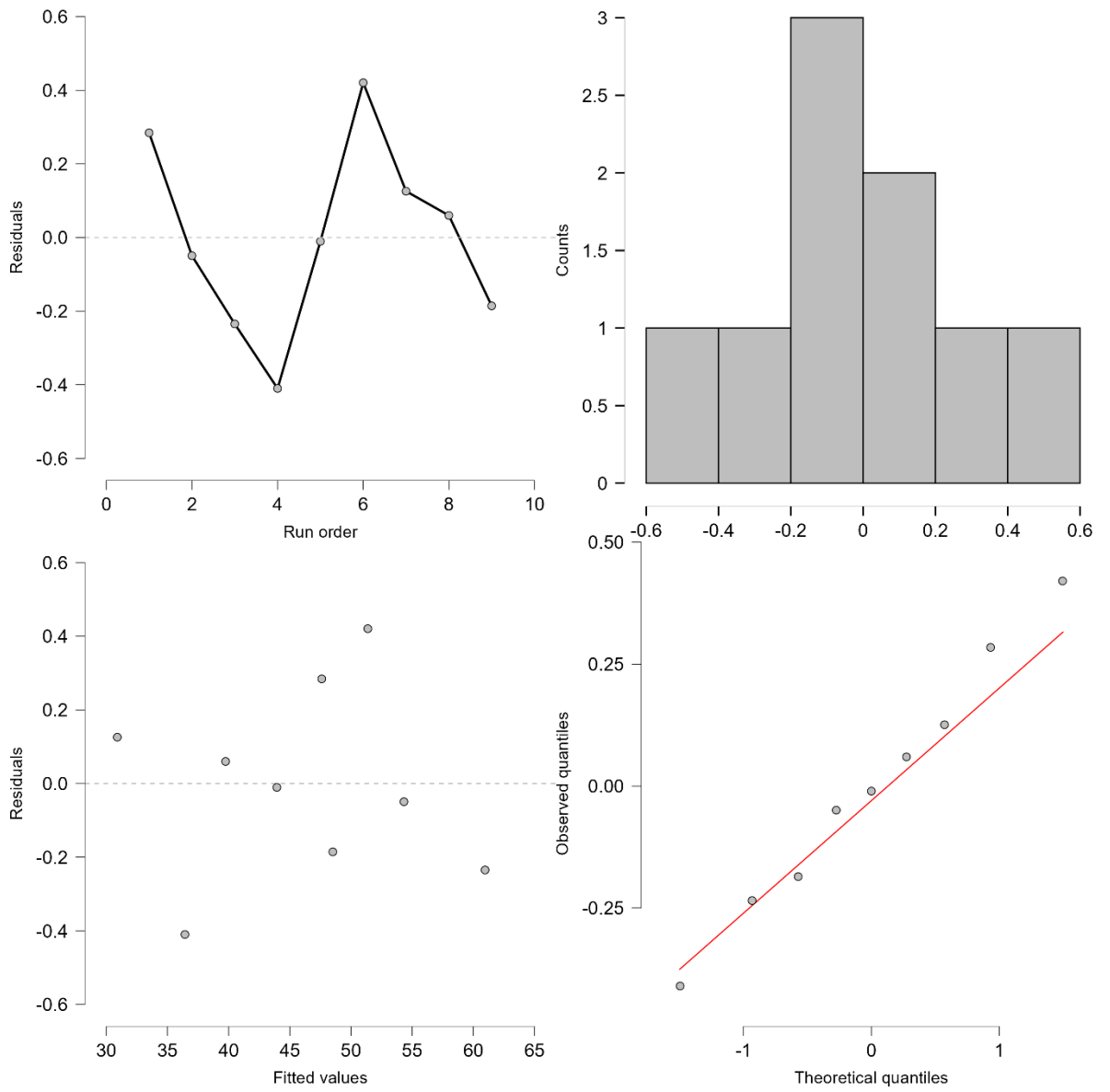
### Coded Coefficients

Alias	Term	Effect	Coefficient	Standard error	t	p	VIF
(Intercept)	(Intercept)		41.79	0.332	126.0	< .001	
A	Tc (.C)	15.48	7.741	0.174	44.58	< .001	1.010
B	Q (L/min)	-14.58	-7.290	0.173	-42.20	< .001	1.021
A <sup>2</sup>	Tc (.C) <sup>2</sup>	-0.088	-0.044	0.299	-0.148	.892	
B <sup>2</sup>	Q (L/min) <sup>2</sup>	10.49	5.246	0.322	16.27	< .001	
AB	Tc (.C) * Q (L/min)	2.130	1.065	0.209	5.087	.015	1.010

### Regression equation in Coded Units

$$T_{avg} (.C) = 41.794 + 7.741 A - 7.29 B - 0.044 A^2 + 5.246 B^2 + 1.065 AB$$

# Matrix residual plot for $T_{avg}$



## Maximum Part Temperature - $T_{max}$ (.C)

### Model Summary

S	R <sup>2</sup>	Adjusted R <sup>2</sup>	Predictive R <sup>2</sup>
0.205	0.999	0.998	0.990

### ANOVA

Source	Sum of squares	df	Mean square	F	p
Model	148.6	5	29.73	705.2	< .001
Linear terms	140.4	2			
Tc (.C)	92.32	1	92.32	2190	< .001
Q (L/min)	48.09	1	48.09	1141	< .001
Squared terms	7.441	2			
Tc (.C)^2	8.820×10 <sup>-4</sup>	1	8.820×10 <sup>-4</sup>	0.021	.894
Q (L/min)^2	7.440	1	7.440	176.5	< .001
Interaction terms	0.781	1			
Tc (.C) * Q (L/min)	0.781	1	0.781	18.54	.023
Error	0.126	3	0.042		
Total	148.8	8			

Note. Type III sums of squares.

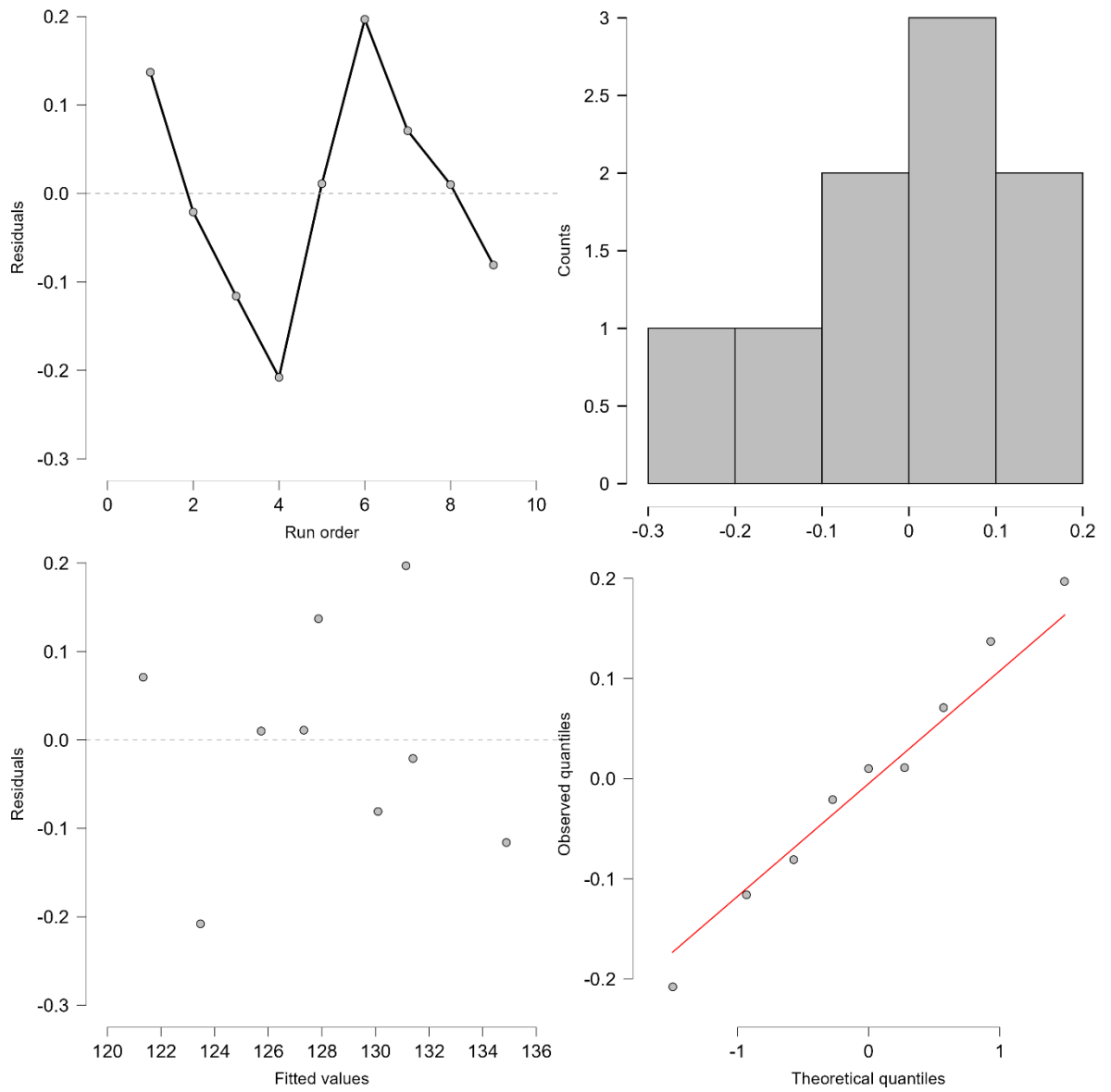
### Coded Coefficients

Alias	Term	Effect	Coefficient	Standard error	t	p	VIF
(Intercept)	(Intercept)		126.5	0.161	786.2	< .001	
A	Tc (.C)	7.885	3.942	0.084	46.80	< .001	1.010
B	Q (L/min)	-5.662	-2.831	0.084	-33.78	< .001	1.021
A^2	Tc (.C)^2	-0.042	-0.021	0.145	-0.145	.894	
B^2	Q (L/min)^2	4.157	2.079	0.156	13.29	< .001	
AB	Tc (.C)* Q (L/min)	0.875	0.437	0.102	4.305	.023	1.010

### Regression equation in Coded Units

$$T_{max} (.C) = 126.487 + 3.942 A - 2.831 B - 0.021 A^2 + 2.079 B^2 + 0.437 AB$$

Matrix residual plot for  $T_{max}$



## Time to reach Ejection Temperature - $t_{cool}$ (s)

### Model Summary

S	R <sup>2</sup>	Adjusted R <sup>2</sup>	Predictive R <sup>2</sup>
0.592	0.995	0.986	0.947

### ANOVA

Source	Sum of squares	df	Mean square	F	p
Model	208.4	5	41.67	119.0	.001
Linear terms	195.4	2			
Tc (.C)	142.9	1	142.9	408.1	< .001
Q (L/min)	52.52	1	52.52	150.0	.001
Squared terms	9.212	2			
Tc (.C)^2	0.355	1	0.355	1.015	.388
Q (L/min)^2	8.856	1	8.856	25.29	.015
Interaction terms	3.726	1			
Tc (.C) * Q (L/min)	3.726	1	3.726	10.64	.047
Error	1.050	3	0.350		
Total	209.4	8			

Note. Type III sums of squares.

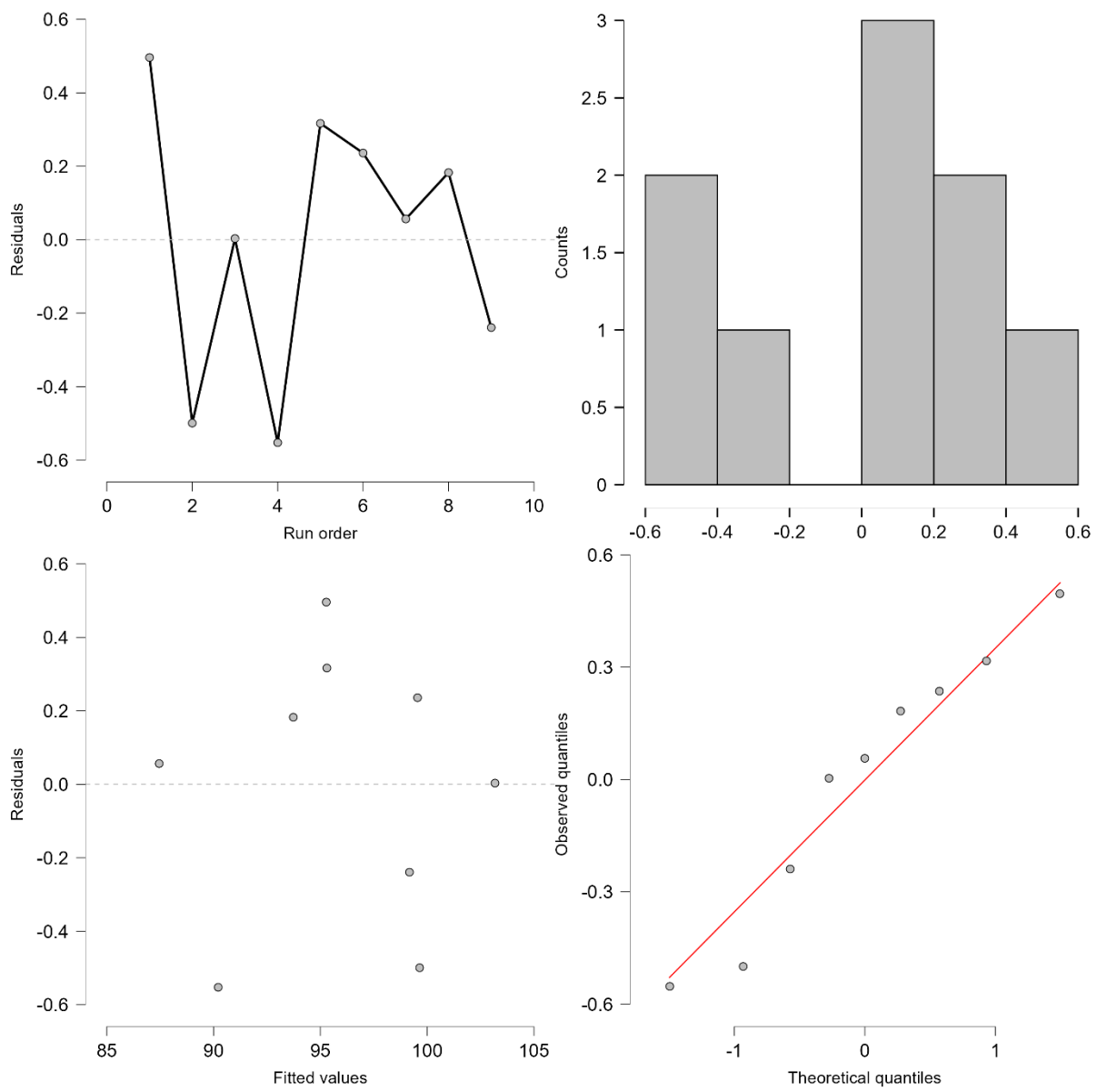
### Coded Coefficients

Alias	Term	Effect	Coefficient	Standard error	t	p	VIF
(Intercept)	(Intercept)		94.42	0.464	203.6	< .001	
A	Tc (.C)	9.810	4.905	0.243	20.20	< .001	1.010
B	Q (L/min)	-5.917	-2.958	0.242	-12.25	.001	1.021
A^2	Tc (.C)^2	-0.843	-0.422	0.418	-1.007	.388	
B^2	Q (L/min)^2	4.536	2.268	0.451	5.029	.015	
AB	Tc (.C)* Q (L/min)	1.910	0.955	0.293	3.262	.047	1.010

### Regression equation in Coded Units

$$t_{cool} \text{ (s)} = 94.422 + 4.905 A - 2.958 B - 0.422 A^2 + 2.268 B^2 + 0.955 AB$$

# Matrix residual plot for $t_{cool}$



## Coolant Pressure Drop - dP (kPa)

### Model Summary

S	R <sup>2</sup>	Adjusted R <sup>2</sup>	Predictive R <sup>2</sup>
0.343	1.000	1.000	0.999

### ANOVA

Source	Sum of squares	df	Mean square	F	p
Model	4767	5	953.4	8086	< .001
Linear terms	4655	2			
Tc (.C)	6.434	1	6.434	54.57	.005
Q (L/min)	4648	1	4648	39420	< .001
Squared terms	111.4	2			
Tc (.C)^2	0.000	1	0.000	0.000	1.000
Q (L/min)^2	111.4	1	111.4	945.0	< .001
Interaction terms	0.980	1			
Tc (.C) * Q (L/min)	0.980	1	0.980	8.308	.063
Error	0.354	3	0.118		
Total	4767	8			

Note. Type III sums of squares.

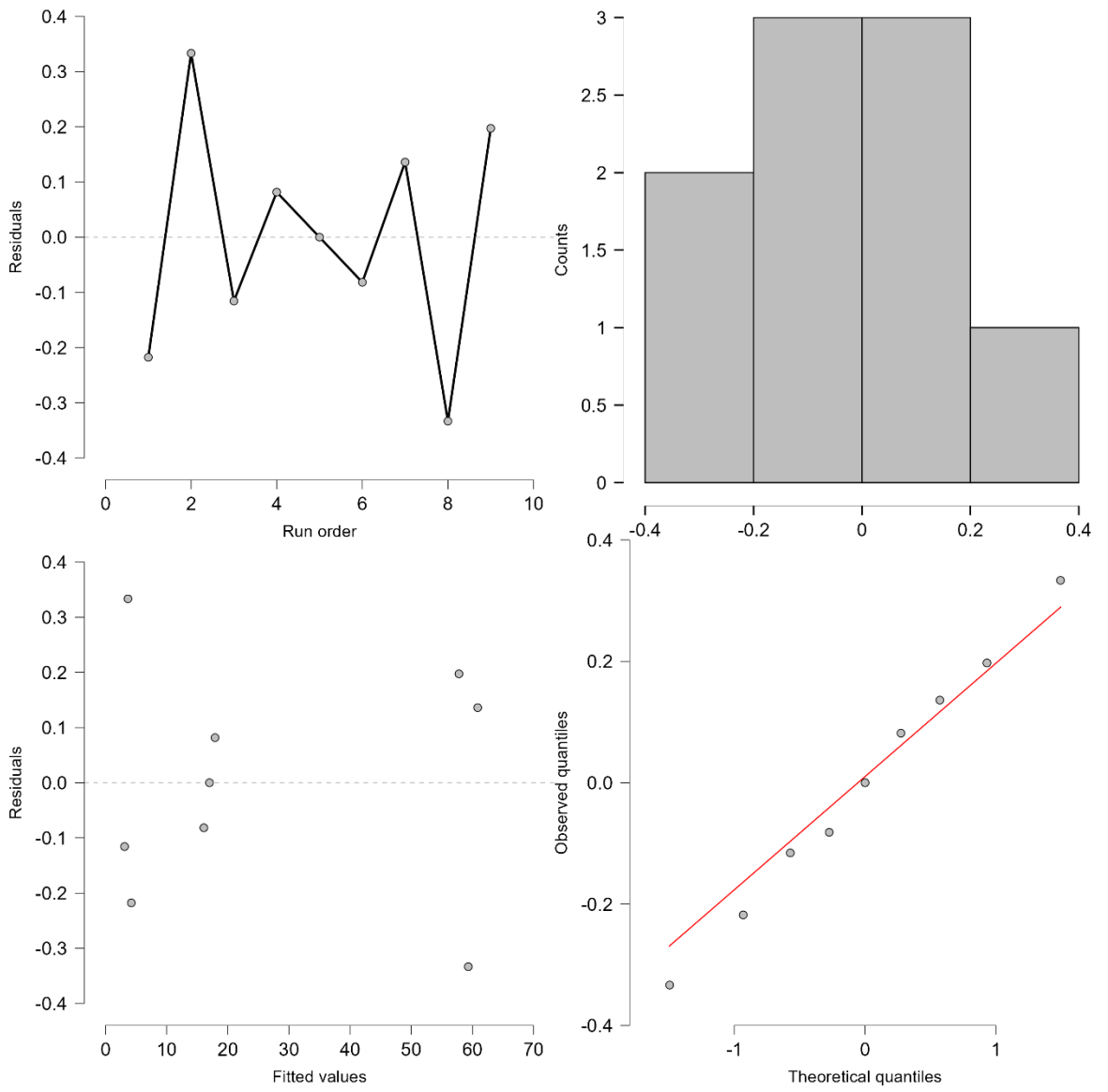
### Coded Coefficients

Alias	Term	Effect	Coefficient	Standard error	t	p	VIF
(Intercept)	(Intercept)		23.46	0.269	87.17	< .001	
A	Tc (.C)	-2.082	-1.041	0.141	-7.387	.005	1.010
B	Q (L/min)	55.67	27.83	0.140	198.5	< .001	1.021
A^2	Tc (.C)^2	-6.271×10 <sup>-15</sup>	-3.135×10 <sup>-15</sup>	0.243	-1.291×10 <sup>-14</sup>	1.000	
B^2	Q (L/min)^2	16.09	8.044	0.262	30.74	< .001	
AB	Tc (.C)* Q (L/min)	-0.980	-0.490	0.170	-2.882	.063	1.010

### Regression equation in Coded Units

$$dP \text{ (kPa)} = 23.456 - 1.041 A + 27.833 B - 0 A^2 + 8.044 B^2 - 0.49 AB$$

# Matrix residual plot for dP



## Average Reynolds Number - $Re_{avg}$

### Model Summary

S	R <sup>2</sup>	Adjusted R <sup>2</sup>	Predictive R <sup>2</sup>
28.75	1.000	1.000	1.000

### ANOVA

Source	Sum of squares	df	Mean square	F	p
Model	2.342×10 <sup>+8</sup>	5	4.685×10 <sup>+7</sup>	56680	< .001
Linear terms	2.267×10 <sup>+8</sup>	2			
Tc (.C)	2.141×10 <sup>+7</sup>	1	2.141×10 <sup>+7</sup>	25900	< .001
Q (L/min)	2.053×10 <sup>+8</sup>	1	2.053×10 <sup>+8</sup>	248300	< .001
Squared terms	21020	2			
Tc (.C) <sup>2</sup>	4942	1	4942	5.979	.092
Q (L/min) <sup>2</sup>	16070	1	16070	19.45	.022
Interaction terms	7.547×10 <sup>+6</sup>	1			
Tc (.C) * Q (L/min)	7.547×10 <sup>+6</sup>	1	7.547×10 <sup>+6</sup>	9130	< .001
Error	2480	3	826.6		
Total	2.342×10 <sup>+8</sup>	8			

Note. Type III sums of squares.

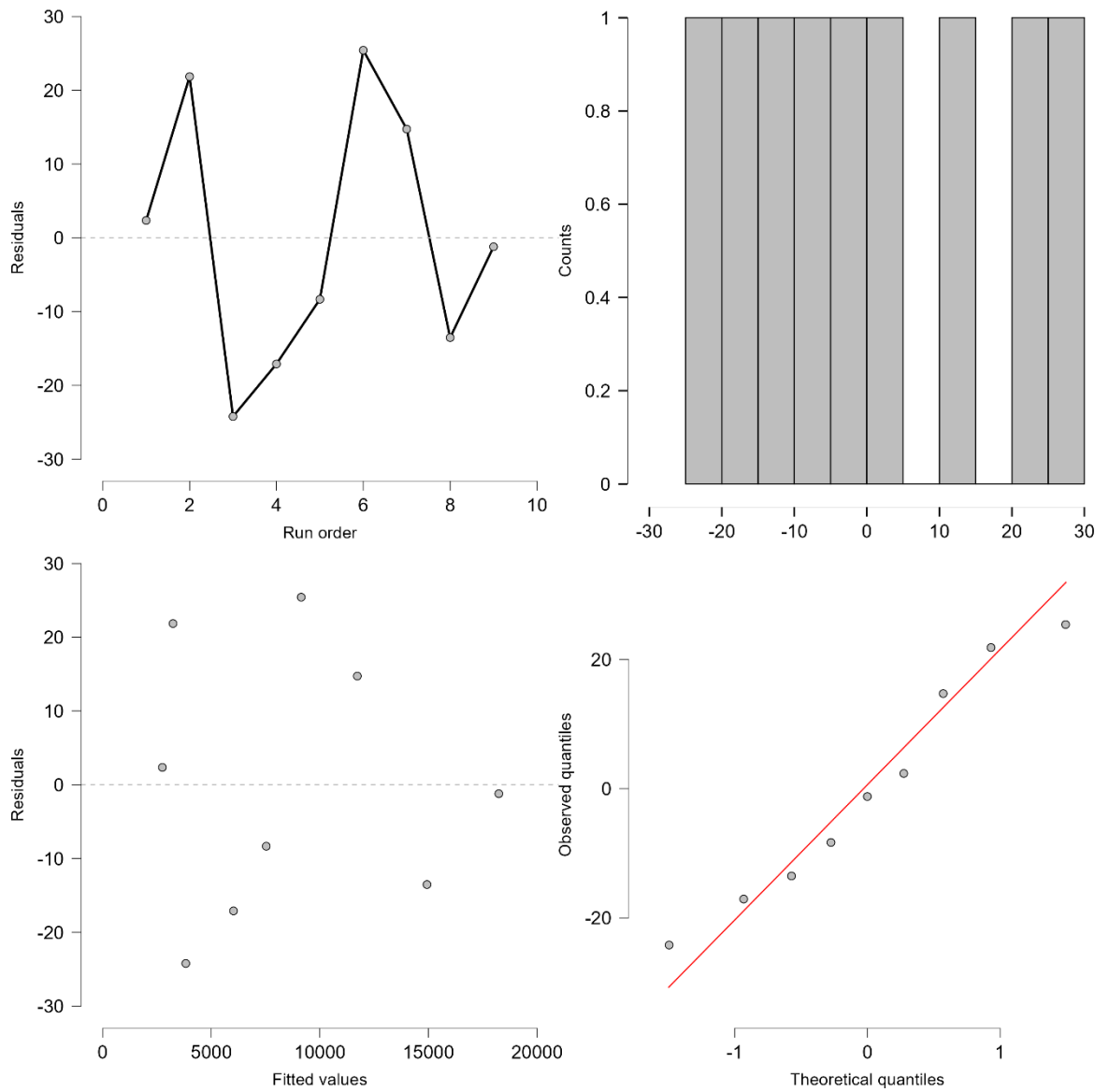
### Coded Coefficients

Alias	Term	Effect	Coefficient	Standard error	t	p	VIF
(Intercept)	(Intercept)		8988	22.53	398.9	< .001	
A	Tc (.C)	3797	1898	11.80	160.9	< .001	1.010
B	Q (L/min)	11700	5849	11.74	498.3	< .001	1.021
A <sup>2</sup>	Tc (.C) <sup>2</sup>	99.42	49.71	20.33	2.445	.092	
B <sup>2</sup>	Q (L/min) <sup>2</sup>	193.2	96.62	21.91	4.410	.022	
AB	Tc (.C) * Q (L/min)	2719	1359	14.23	95.55	< .001	1.010

### Regression equation in Coded Units

$$Re_{avg} = 8987.816 + 1898.485 A + 5849.095 B + 49.71 A^2 + 96.615 B^2 + 1359.488 AB$$

# Matrix residual plot for $Re_{avg}$



## Warpage Displacement - *Warp* (mm)

### Model Summary

S	R <sup>2</sup>	Adjusted R <sup>2</sup>	Predictive R <sup>2</sup>
0.001	0.999	0.997	0.988

### ANOVA

Source	Sum of squares	df	Mean square	F	p
Model	0.003	5	6.630×10 <sup>-4</sup>	587.9	< .001
Linear terms	0.003	2			
Tc (.C)	0.002	1	0.002	1704	< .001
Q (L/min)	0.001	1	0.001	1043	< .001
Squared terms	2.026×10 <sup>-4</sup>	2			
Tc (.C)^2	5.556×10 <sup>-8</sup>	1	5.556×10 <sup>-8</sup>	0.049	.839
Q (L/min)^2	2.025×10 <sup>-4</sup>	1	2.025×10 <sup>-4</sup>	179.6	< .001
Interaction terms	1.439×10 <sup>-5</sup>	1			
Tc (.C) * Q (L/min)	1.439×10 <sup>-5</sup>	1	1.439×10 <sup>-5</sup>	12.76	.037
Error	3.383×10 <sup>-6</sup>	3	1.128×10 <sup>-6</sup>		
Total	0.003	8			

Note. Type III sums of squares.

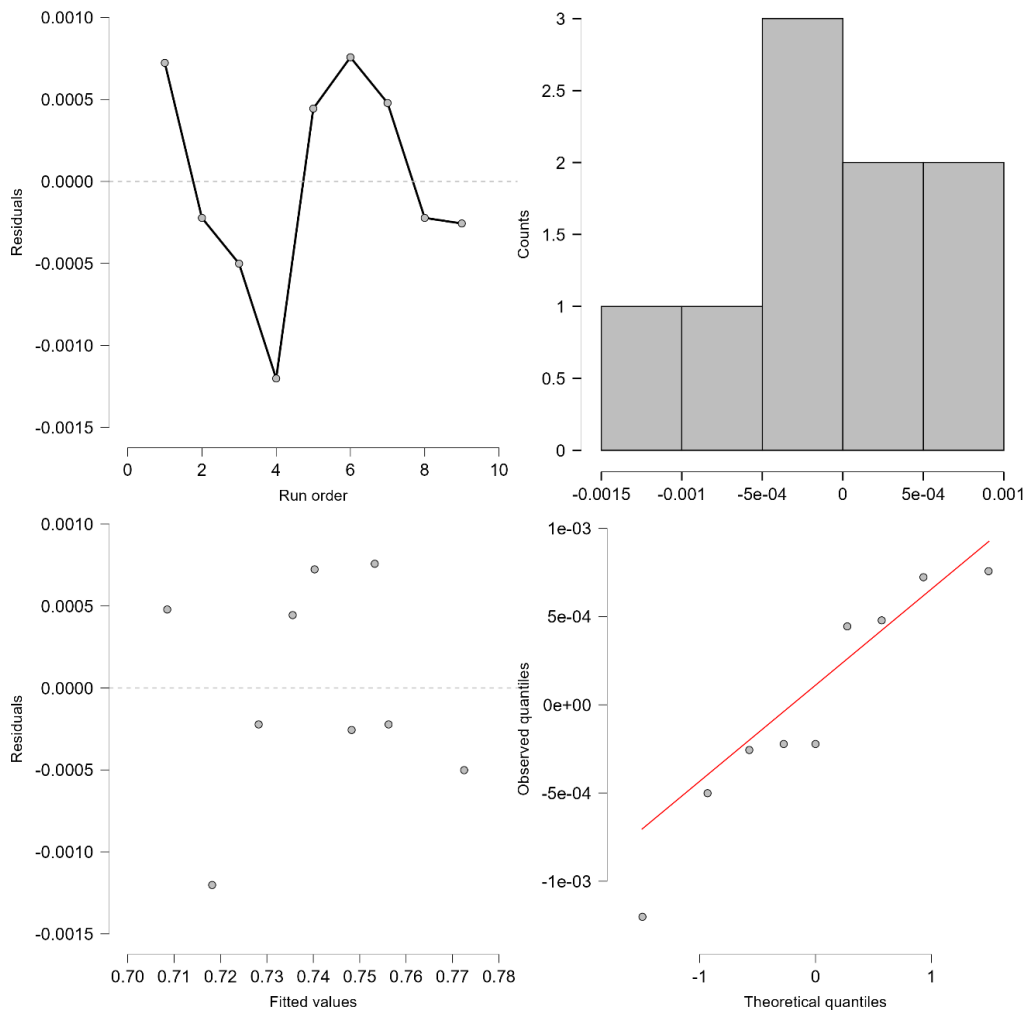
### Coded Coefficients

Alias	Term	Effect	Coefficient	Standard error	t	p	VIF
(Intercept)	(Intercept)		0.731	8.322×10 <sup>-4</sup>	878.9	< .001	
A	Tc (.C)	0.036	0.018	4.357×10 <sup>-4</sup>	41.29	< .001	1.010
B	Q (L/min)	-0.028	-0.014	4.335×10 <sup>-4</sup>	-32.29	< .001	1.021
A^2	Tc (.C)^2	3.333×10 <sup>-4</sup>	1.667×10 <sup>-4</sup>	7.509×10 <sup>-4</sup>	0.222	.839	
B^2	Q (L/min)^2	0.022	0.011	8.093×10 <sup>-4</sup>	13.40	< .001	
AB	Tc (.C)* Q (L/min)	0.004	0.002	5.255×10 <sup>-4</sup>	3.573	.037	1.010

### Regression equation in Coded Units

$$\text{Warp (mm)} = 0.731 + 0.018 A - 0.014 B + 0 A^2 + 0.011 B^2 + 0.002 AB$$

## Matrix residual plot for *Warp*



## Elliptical Profile – Response Optimiser Output

### Response Optimizer Settings

Response	Goal	Lower	Target	Upper	Weight	Importance
Tavg (.C)	Minimize		31.03	60.73	1.000	1.000
Tmax (.C)	Minimize		121.4	134.8	1.000	1.000
tcool (s)	Minimize		87.51	103.2	1.000	1.000
dP (kPa)	Minimize		3.000	61.00	1.000	1.000
Warp (mm)	Minimize		0.709	0.772	1.000	1.000

*Note.* The lower and upper bounds and target are estimated from data.

### Response Optimizer Solution

Composite desirability	Tc (.C)	Q (L/min)	Tavg (.C) fit	Tmax (.C) fit	tcool (s) fit	dP (kPa) fit	Warp (mm) fit
0.989	15.701	5.273	27.557	120.029	87.506	6.071	0.699

## Appendix 7. JASP RSM Analysis Results for Teardrop Conformal Cooling Channel

Average Part Temperature -  $T_{avg}$  (.C)

### Model Summary

S	R <sup>2</sup>	Adjusted R <sup>2</sup>	Predictive R <sup>2</sup>
0.443	0.999	0.998	0.991

### ANOVA

Source	Sum of squares	df	Mean square	F	p
Model	759.3	5	151.9	774.0	< .001
Linear terms	701.1	2			
Tc (.C)	357.9	1	357.9	1824	< .001
Q (L/min)	343.3	1	343.3	1750	< .001
Squared terms	53.01	2			
Tc (.C) <sup>2</sup>	0.004	1	0.004	0.023	.890
Q (L/min) <sup>2</sup>	53.01	1	53.01	270.2	< .001
Interaction terms	5.095	1			
Tc (.C) * Q (L/min)	5.095	1	5.095	25.97	.015
Error	0.589	3	0.196		
Total	759.8	8			

Note. Type III sums of squares.

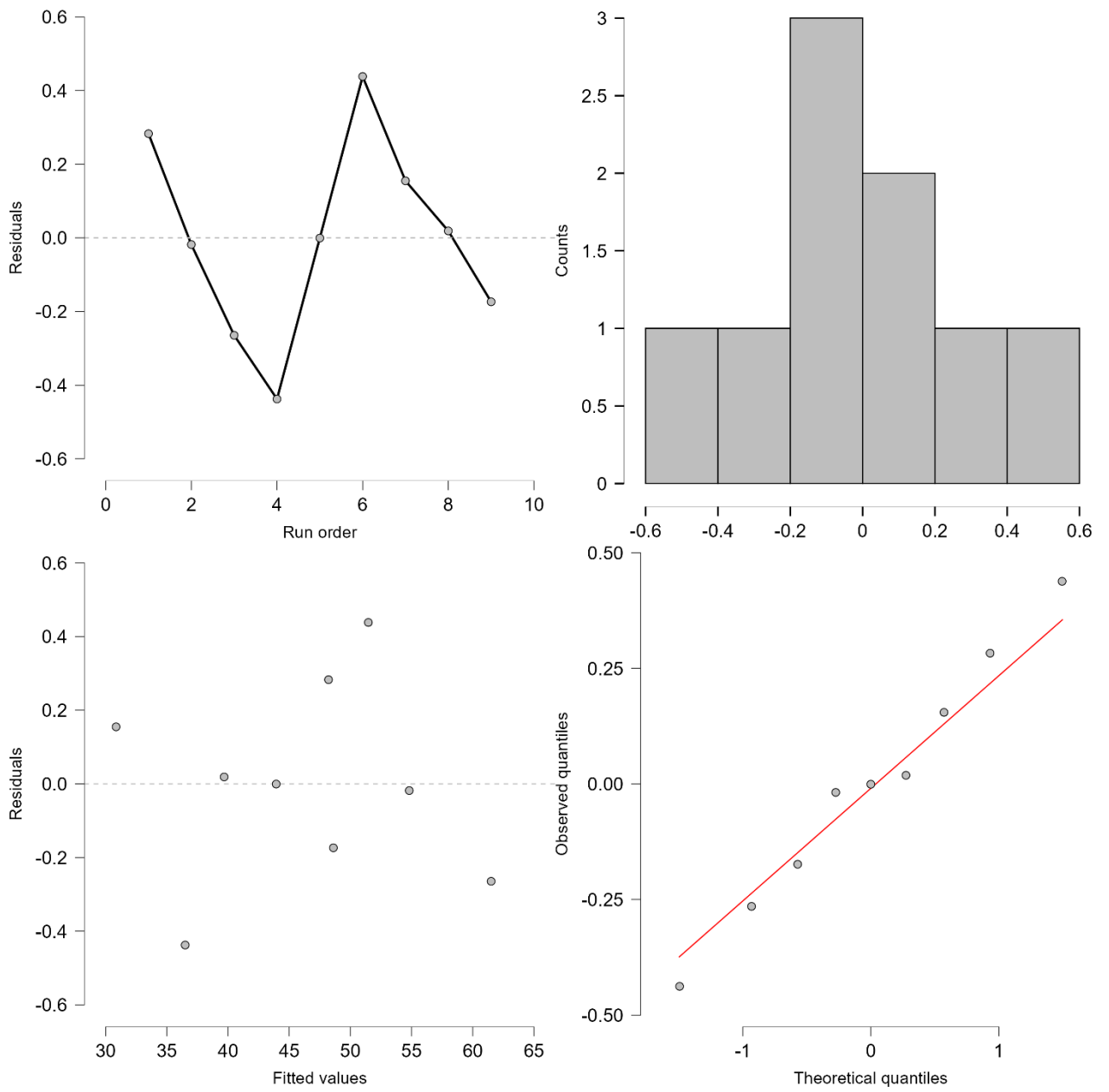
### Coded Coefficients

Alias	Term	Effect	Coefficient	Standard error	t	p	VIF
(Intercept)	(Intercept)		41.70	0.347	120.1	< .001	
A	Tc (.C)	15.52	7.762	0.182	42.71	< .001	1.010
B	Q (L/min)	-15.13	-7.564	0.181	-41.83	< .001	1.021
A <sup>2</sup>	Tc (.C) <sup>2</sup>	0.094	0.047	0.313	0.151	.890	
B <sup>2</sup>	Q (L/min) <sup>2</sup>	11.10	5.548	0.338	16.44	< .001	
AB	Tc (.C) * Q (L/min)	2.234	1.117	0.219	5.096	.015	1.010

### Regression equation in Coded Units

$$T_{avg} (.C) = 41.697 + 7.762 A - 7.564 B + 0.047 A^2 + 5.548 B^2 + 1.117 AB$$

Matrix residual plot for  $T_{avg}$



## Maximum Part Temperature - $T_{max}$ (.C)

### Model Summary

S	R <sup>2</sup>	Adjusted R <sup>2</sup>	Predictive R <sup>2</sup>
0.286	0.999	0.996	0.984

### ANOVA

Source	Sum of squares	df	Mean square	F	p
Model	178.3	5	35.65	437.3	< .001
Linear terms	168.7	2			
Tc (.C)	117.2	1	117.2	1438	< .001
Q (L/min)	51.44	1	51.44	631.0	< .001
Squared terms	8.298	2			
Tc (.C)^2	0.001	1	0.001	0.015	.910
Q (L/min)^2	8.297	1	8.297	101.8	.002
Interaction terms	1.285	1			
Tc (.C) * Q (L/min)	1.285	1	1.285	15.76	.029
Error	0.245	3	0.082		
Total	178.5	8			

Note. Type III sums of squares.

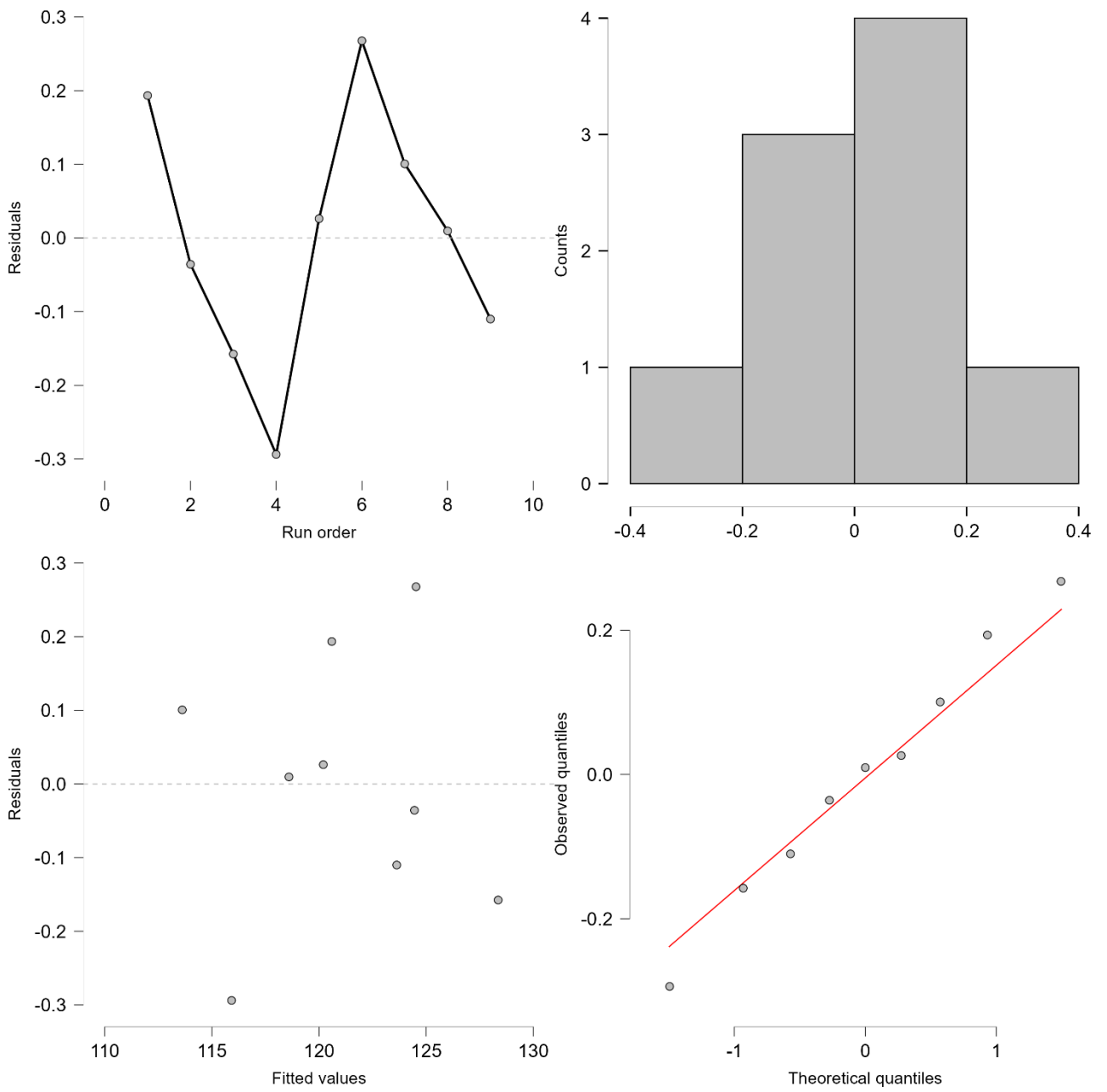
### Coded Coefficients

Alias	Term	Effect	Coefficient	Standard error	t	p	VIF
(Intercept)	(Intercept)		119.3	0.224	533.3	< .001	
A	Tc (.C)	8.886	4.443	0.117	37.92	< .001	1.010
B	Q (L/min)	-5.856	-2.928	0.117	-25.12	< .001	1.021
A^2	Tc (.C)^2	0.050	0.025	0.202	0.123	.910	
B^2	Q (L/min)^2	4.390	2.195	0.218	10.09	.002	
AB	Tc (.C)* Q (L/min)	1.122	0.561	0.141	3.969	.029	1.010

### Regression equation in Coded Units

$$T_{max} (.C) = 119.329 + 4.443 A - 2.928 B + 0.025 A^2 + 2.195 B^2 + 0.561 AB$$

### Matrix residual plot for $T_{max}$



## Time to Reach Ejection Temperature - $t_{cool}$ (s)

### Model Summary

S	R <sup>2</sup>	Adjusted R <sup>2</sup>	Predictive R <sup>2</sup>
0.462	0.997	0.991	0.967

### ANOVA

Source	Sum of squares	df	Mean square	F	p
Model	199.0	5	39.80	186.7	< .001
Linear terms	189.1	2			
Tc (.C)	135.1	1	135.1	633.6	< .001
Q (L/min)	54.07	1	54.07	253.6	< .001
Squared terms	9.511	2			
Tc (.C)^2	0.040	1	0.040	0.190	.693
Q (L/min)^2	9.471	1	9.471	44.43	.007
Interaction terms	0.346	1			
Tc (.C) * Q (L/min)	0.346	1	0.346	1.621	.293
Error	0.640	3	0.213		
Total	199.6	8			

Note. Type III sums of squares.

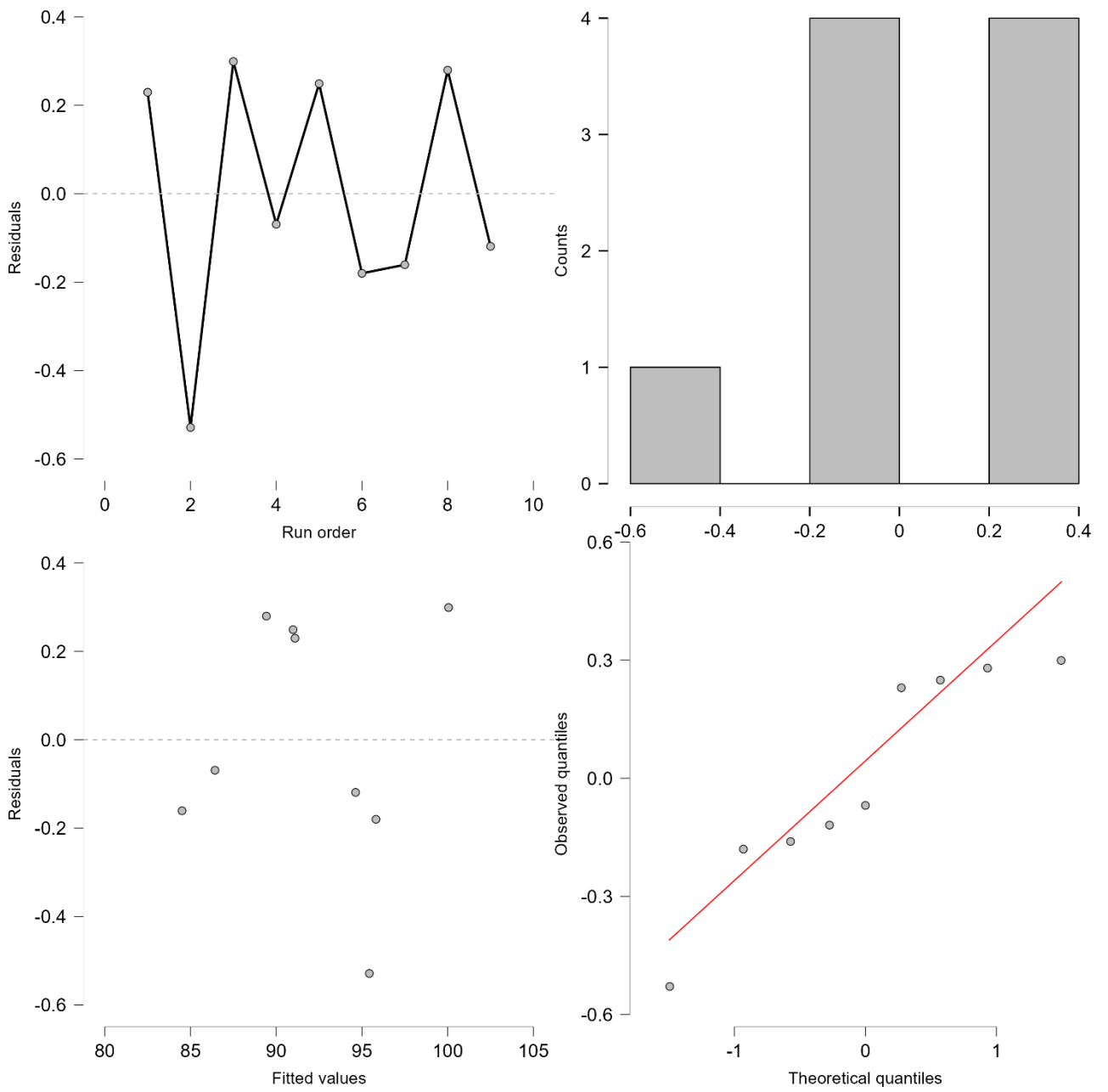
### Coded Coefficients

Alias	Term	Effect	Coefficient	Standard error	t	p	VIF
(Intercept)	(Intercept)		90.08	0.362	249.0	< .001	
A	Tc (.C)	9.537	4.769	0.189	25.17	< .001	1.010
B	Q (L/min)	-6.004	-3.002	0.188	-15.93	< .001	1.021
A^2	Tc (.C)^2	0.284	0.142	0.326	0.435	.693	
B^2	Q (L/min)^2	4.690	2.345	0.352	6.665	.007	
AB	Tc (.C)* Q (L/min)	0.582	0.291	0.228	1.273	.293	1.010

### Regression equation in Coded Units

$$t_{cool} \text{ (s)} = 90.084 + 4.769 A - 3.002 B + 0.142 A^2 + 2.345 B^2 + 0.291 AB$$

# Matrix residual plot for $t_{cool}$



## Coolant Pressure Drop - dP (kPa)

### Model Summary

S	R <sup>2</sup>	Adjusted R <sup>2</sup>	Predictive R <sup>2</sup>
0.343	1.000	1.000	0.999

### ANOVA

Source	Sum of squares	df	Mean square	F	p
Model	5667	5	1133	9612	< .001
Linear terms	5527	2			
Tc (.C)	6.434	1	6.434	54.57	.005
Q (L/min)	5521	1	5521	46820	< .001
Squared terms	138.8	2			
Tc (.C)^2	0.000	1	0.000	0.000	1.000
Q (L/min)^2	138.8	1	138.8	1177	< .001
Interaction terms	0.980	1			
Tc (.C) * Q (L/min)	0.980	1	0.980	8.308	.063
Error	0.354	3	0.118		
Total	5667	8			

Note. Type III sums of squares.

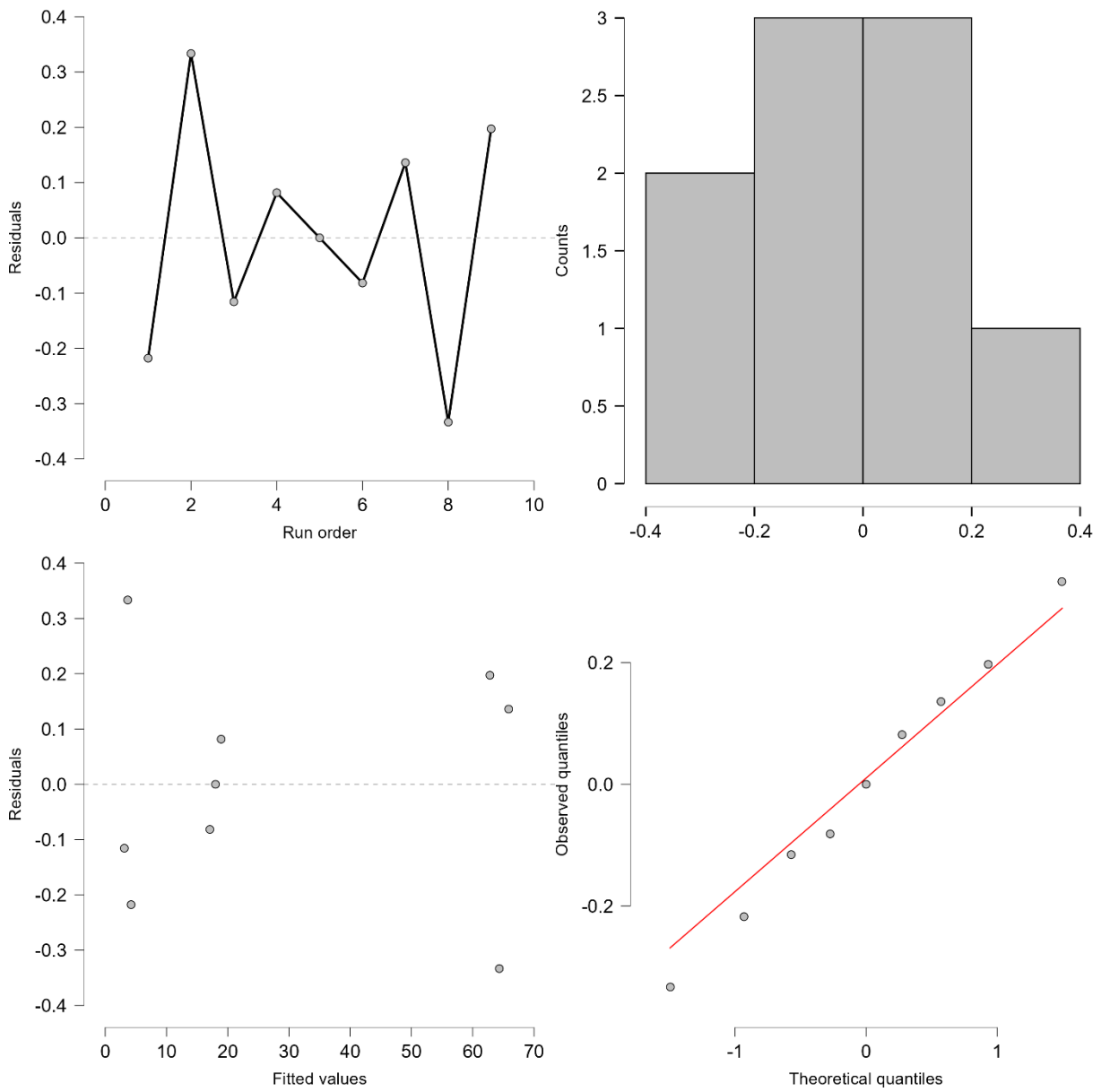
### Coded Coefficients

Alias	Term	Effect	Coefficient	Standard error	t	p	VIF
(Intercept)	(Intercept)		25.02	0.269	92.99	< .001	
A	Tc (.C)	-2.082	-1.041	0.141	-7.387	.005	1.010
B	Q (L/min)	60.67	30.33	0.140	216.4	< .001	1.021
A^2	Tc (.C)^2	$2.522 \times 10^{-15}$	$1.261 \times 10^{-15}$	0.243	$5.193 \times 10^{-15}$	1.000	
B^2	Q (L/min)^2	17.96	8.978	0.262	34.31	< .001	
AB	Tc (.C) * Q (L/min)	-0.980	-0.490	0.170	-2.882	.063	1.010

### Regression equation in Coded Units

$$dP \text{ (kPa)} = 25.022 - 1.041 A + 30.333 B + 0 A^2 + 8.978 B^2 - 0.49 AB$$

# Matrix residual plot for dP



## Average Reynolds Number - $Re_{avg}$

### Model Summary

S	R <sup>2</sup>	Adjusted R <sup>2</sup>	Predictive R <sup>2</sup>
65.15	1.000	1.000	1.000

### ANOVA

Source	Sum of squares	df	Mean square	F	p
Model	2.157×10 <sup>+8</sup>	5	4.314×10 <sup>+7</sup>	10160	< .001
Linear terms	2.085×10 <sup>+8</sup>	2			
Tc (.C)	1.934×10 <sup>+7</sup>	1	1.934×10 <sup>+7</sup>	4556	< .001
Q (L/min)	1.892×10 <sup>+8</sup>	1	1.892×10 <sup>+8</sup>	44570	< .001
Squared terms	22550	2			
Tc (.C) <sup>2</sup>	14970	1	14970	3.527	.157
Q (L/min) <sup>2</sup>	7574	1	7574	1.784	.274
Interaction terms	7.133×10 <sup>+6</sup>	1			
Tc (.C) * Q (L/min)	7.133×10 <sup>+6</sup>	1	7.133×10 <sup>+6</sup>	1680	< .001
Error	12740	3	4245		
Total	2.157×10 <sup>+8</sup>	8			

Note. Type III sums of squares.

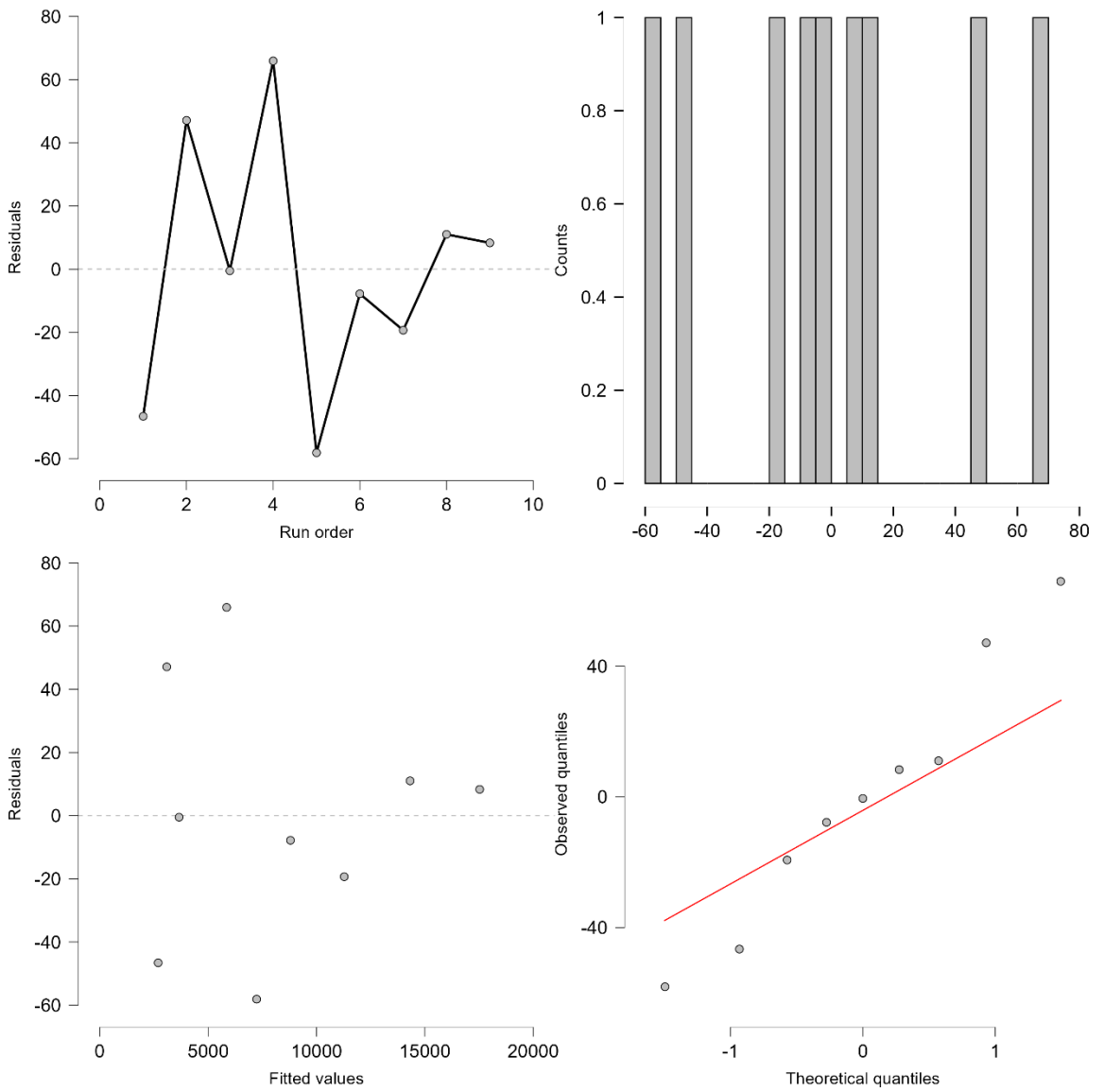
### Coded Coefficients

Alias	Term	Effect	Coefficient	Standard error	t	p	VIF
(Intercept)	(Intercept)		8637	51.06	169.2	< .001	
A	Tc (.C)	3609	1804	26.73	67.50	< .001	1.010
B	Q (L/min)	11230	5615	26.60	211.1	< .001	1.021
A <sup>2</sup>	Tc (.C) <sup>2</sup>	173.1	86.53	46.07	1.878	.157	
B <sup>2</sup>	Q (L/min) <sup>2</sup>	132.6	66.32	49.65	1.336	.274	
AB	Tc (.C)* Q (L/min)	2643	1322	32.24	40.99	< .001	1.010

### Regression equation in Coded Units

$$Re_{avg} = 8637.242 + 1804.475 A + 5615.42 B + 86.528 A^2 + 66.32 B^2 + 1321.702 AB$$

# Matrix residual plot for $Re_{avg}$



## Warpage Displacement - *Warp* (mm)

### Model Summary

S	R <sup>2</sup>	Adjusted R <sup>2</sup>	Predictive R <sup>2</sup>
9.280×10 <sup>-4</sup>	0.999	0.998	0.992

### ANOVA

Source	Sum of squares	df	Mean square	F	p
Model	0.004	5	7.138×10 <sup>-4</sup>	829.0	< .001
Linear terms	0.003	2			
Tc (.C)	0.002	1	0.002	2279	< .001
Q (L/min)	0.001	1	0.001	1603	< .001
Squared terms	2.075×10 <sup>-4</sup>	2			
Tc (.C) <sup>2</sup>	0.000	1	0.000	0.000	1.000
Q (L/min) <sup>2</sup>	2.075×10 <sup>-4</sup>	1	2.075×10 <sup>-4</sup>	241.0	< .001
Interaction terms	1.875×10 <sup>-5</sup>	1			
Tc (.C) * Q (L/min)	1.875×10 <sup>-5</sup>	1	1.875×10 <sup>-5</sup>	21.77	.019
Error	2.583×10 <sup>-6</sup>	3	8.611×10 <sup>-7</sup>		
Total	0.004	8			

Note. Type III sums of squares.

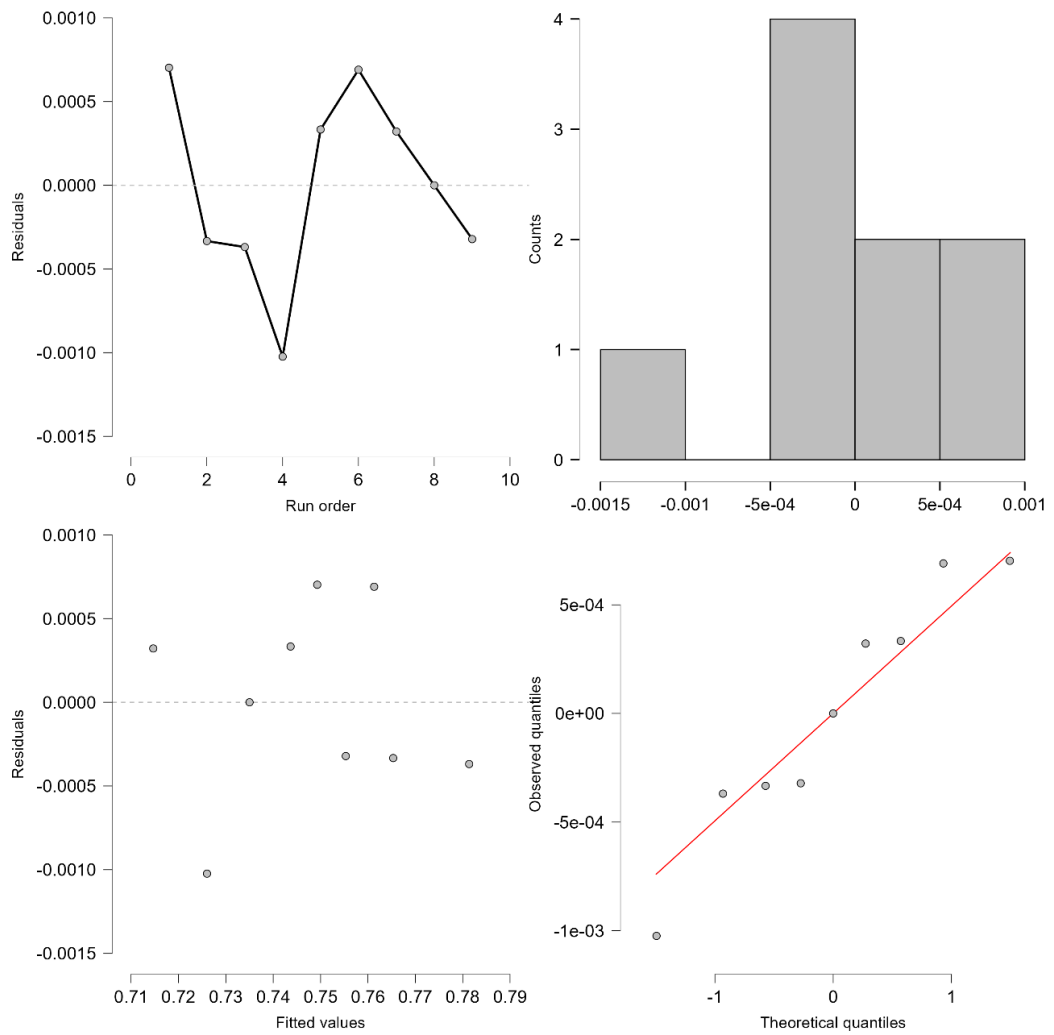
### Coded Coefficients

Alias	Term	Effect	Coefficient	Standard error	t	p	VIF
(Intercept)	(Intercept)		0.739	7.272×10 <sup>-4</sup>	1017	< .001	
A	Tc (.C)	0.036	0.018	3.808×10 <sup>-4</sup>	47.74	< .001	1.010
B	Q (L/min)	-0.030	-0.015	3.788×10 <sup>-4</sup>	-40.03	< .001	1.021
A <sup>2</sup>	Tc (.C) <sup>2</sup>	-6.873×10 <sup>-17</sup>	-3.437×10 <sup>-17</sup>	6.562×10 <sup>-4</sup>	-5.238×10 <sup>-14</sup>	1.000	
B <sup>2</sup>	Q (L/min) <sup>2</sup>	0.022	0.011	7.072×10 <sup>-4</sup>	15.52	< .001	
AB	Tc (.C)* Q (L/min)	0.004	0.002	4.592×10 <sup>-4</sup>	4.666	.019	1.010

### Regression equation in Coded Units

$$\text{Warp (mm)} = 0.739 + 0.018 A - 0.015 B - 0 A^2 + 0.011 B^2 + 0.002 AB$$

## Matrix residual plot for *Warp*



## Teardrop Profile – Response Optimiser Output

### Response Optimizer Settings

Response	Goal	Lower	Target	Upper	Weight	Importance
Tavg (.C)	Minimize		31.00	61.24	1.000	1.000
Tmax (.C)	Minimize		113.7	128.2	1.000	1.000
tcool (s)	Minimize		84.35	100.4	1.000	1.000
dP (kPa)	Minimize		3.000	66.00	1.000	1.000
Warp (mm)	Minimize		0.715	0.781	1.000	1.000

*Note.* The lower and upper bounds and target are estimated from data.

### Response Optimizer Solution

Composite desirability	Tc (.C)	Q (L/min)	Tavg (.C) fit	Tmax (.C) fit	tcool (s) fit	dP (kPa) fit	Warp (mm) fit
0.993	16.023	4.713	30.618	113.717	83.736	5.083	0.715